Developing a Porcine Model to Study the Glymphatic System

Bechet, Nicholas

2022

Document Version:
Publisher's PDF, also known as Version of record

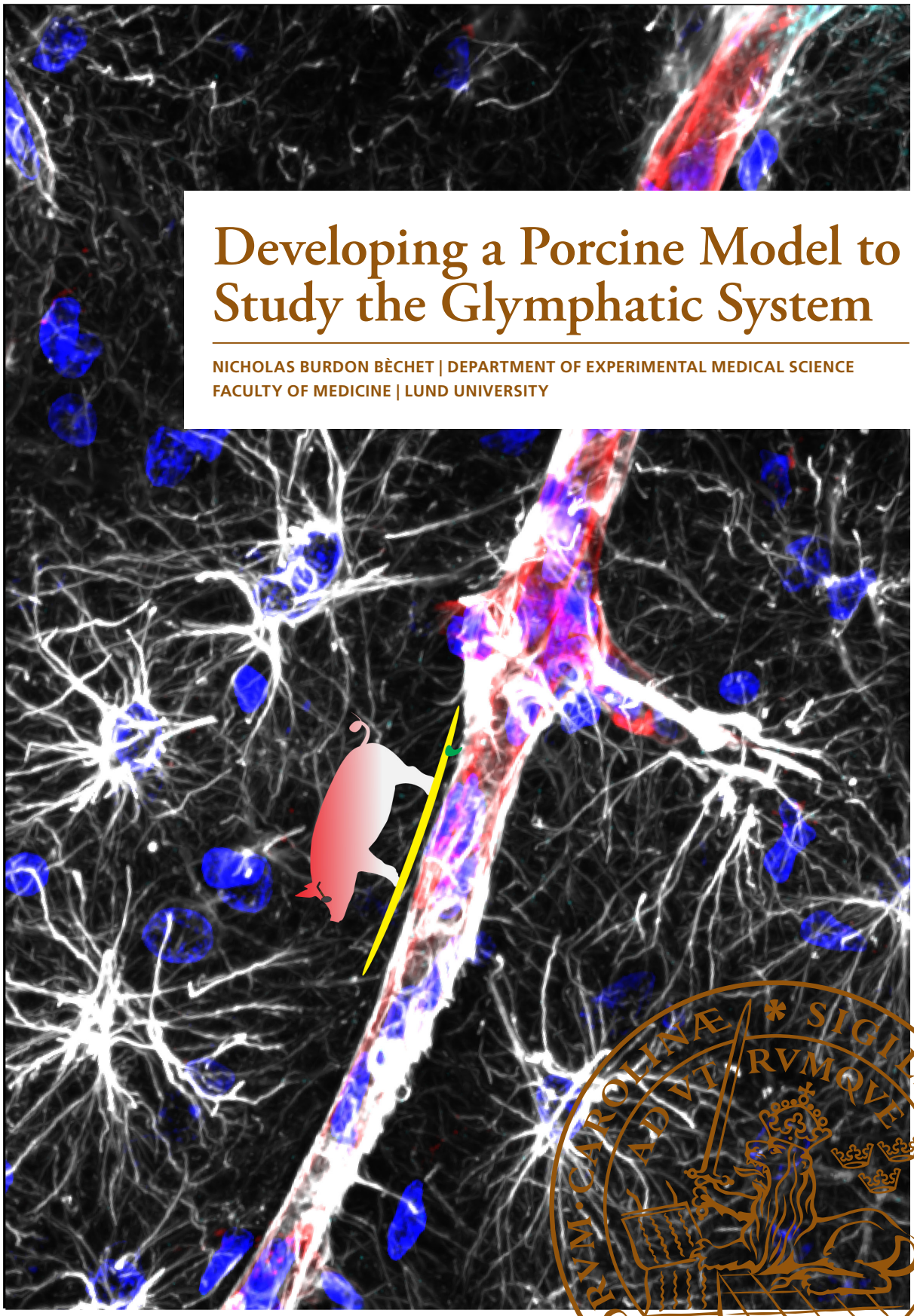

Developing a Porcine Model to Study the Glymphatic System

NICHOLAS BURDON BÈCHET | DEPARTMENT OF EXPERIMENTAL MEDICAL SCIENCE
FACULTY OF MEDICINE | LUND UNIVERSITY

Developing a Porcine Model to Study the Glymphatic System

Nicholas Burdon Bèchet

LUND
UNIVERSITY

DOCTORAL DISSERTATION

Doctoral dissertation for the degree of Doctor of Philosophy (PhD) at the Faculty of Medicine at Lund University to be publicly defended at Segerfalksen, Wallenberg Neuroscience Centre, Lund, on 17th of June at 13:15.

Faculty opponent

Per Kristian Eide

Professor of Neurosurgery

Oslo University Hospital, Neuroscience Research Unit

Organization: LUND UNIVERSITY Glia-Immune Interactions Department of Experimental Medical Science Faculty of Medicine	**Document name:** DOCTORAL DISSERTATION **Date of issue:** 17 June 2022
Author: Nicholas B. Bèchet	Sponsoring organization

Title:
Developing a Porcine Model to Study the Glymphatic System

Abstract:
The glymphatic system is a brain-wide solute clearance system that has developed in the brain to clear metabolic waste during sleep. This clearance is mediated by advective fluxes of cerebrospinal fluid (CSF) along perivascular spaces (PVS) and through the brain. The movement of CSF from the PVS and through the brain is dependent on the polarised expression of aquaporin-4 (AQP4) at astrocyte endfeet, that project to form the outer PVS boundary. The capacity of the glymphatic system to clear proteins like amyloid-beta (Aß) and tau has generated great interest in exploiting this system therapeutically in the context of Alzheimer's disease (AD). However, much of the knowledge on the glymphatic system, more specifically, the microscopic machinery and processes, have been studied and described exclusively in rodents. To this end, apart from several magnetic resonance imaging studies confirming the existence of macroscopic glymphatic phenomena in humans i.e. advective movement of gadobutrol from the CSF into the brain, the microscopic aspects of the glymphatic system remain largely unexplored in the large gyrencephalic brain. Thus, the aims of this thesis were to develop a large animal model to study the glymphatic system and further use this model to study the glymphatic system in the context of neuropathology, which in this case took the form of sub-dural haematoma, and amyloid-beta (re)-circulation in the context of AD. To achieve this, a cisterna magna (CM) cannulation surgery was translated from rodents to pigs, such that it would be possible to introduce fluorescent tracers into the porcine CSF in vivo and explore the glymphatic pathways. Initially, to characterise these pathways whole brains were extracted intact after fluorescent tracer circulation and processed using several advanced imaging readouts, including macroscopy, along with confocal, light sheet and electron microscopy. Imaging data revealed: 1) The folded architecture of the gyrencephalic brain helped direct upstream CSF distribution, 2) PVS-mediated CSF influx into the brain is steadfast in the pig brain, as in rodents, and could be traced in deep sub-cortical structures and down to a capillary level, 3) PVS influx sites are 4-fold more extensive in pigs than in rodents. Taken together these data indicate not only a conservation of the glymphatic system and its machinery from rodents to pigs but a more developed system in the large mammal. In the context of suspected sub-acute subdural haematoma (SDH) a brain-wide impairment in glymphatic influx amounted, raising important questions concerning the consequence of undiagnosed SDH for glymphatic function and brain clearance. In the context of AD the acute introduction of Aß1-42 into the CSF was found to impair glymphatic function, highlighting the consequences of Aß recirculation for brain clearance. Interestingly, upon closer examination it was found that Aß did not penetrate into the brain as was the case with inert protein tracers, but instead remained localised to pial and penetrating arteries. This localisation was elastin specific and only occured with Aß (1-40/1-42) but not dextran or bovine serum albumin. This outcome appears to reflect an Aß entrapment system that prevents the recirculation of Aß into the brain, but further work is necessary to unravel its potential as a clearance pathway for Aß from the CSF to protein transporters at the endothelial cell layer. In an attempt to study this in vivo a porcine cranial window model was generated in order to image PVS transport in the large gyrencephalic brain. While low resolution imaging was indeed possible, brain motion proved a challenge not yet overcome. We hope that in the future, through mitigating brain motion, it will be possible to study PVS transport, the glymphatic system, and this potential Aß entrapment pathway, in the brain of a large mammal in vivo.

Key words: Cerebrospinal fluid, glymphatic system, porcine model, amyloid-beta, in vivo imaging, subdural haematoma, Alzheimer's disease

Classification system and/or index terms (if any)

Supplementary bibliographical information		**Language:** English
ISSN and key title: 1652-8220		**ISBN:** 978-91-8021-261-8
Recipient's notes	**Number of pages 90**	Price
	Security classification	

Signature 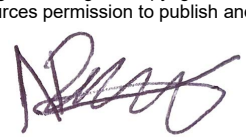 Date 2022-05-11

Developing a Porcine Model to Study the Glymphatic System

Nicholas Burdon Bèchet

Glia-Immune Interactions
Department of Experimental Medical Science
Faculty of Medicine

Cover photo by Nicholas B. Bèchet

Back cover: Brain slice from the first porcine glymphatic experiment

Sci-artwork between sections by Nicholas B. Bèchet

Faculty of Medicine
Department of Experimental Medical Science

ISBN 978-91-8021-261-8
ISSN 1652-8220
Lund University, Faculty of Medicine Doctoral Dissertation Series 2022: 100

Printed in Sweden by Media-Tryck, Lund University
Lund 2022

To Harry, Charles, and all my family

The creatures outside looked from pig to man, and from man to pig, and from pig to man again; but already it was impossible to say which was which.

-E. A. B.

Table of Contents

labyrinth of dreams

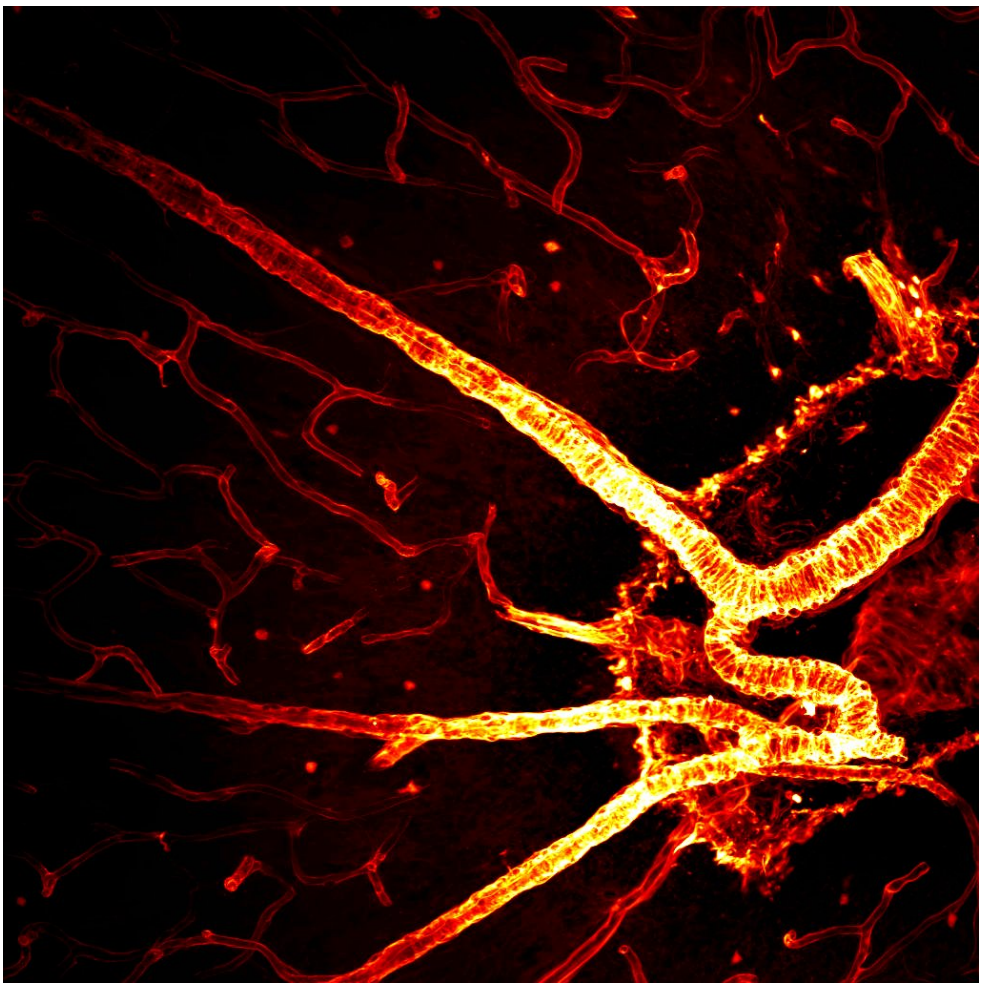

Original Papers and Manuscripts Included in the Thesis

I. **Bèchet NB**, Shanbhag NC, Lundgaard I. Direct cannula implantation in the cisterna magna of pigs. *Journal of Visualized Experiments*. 2021 Jun 9;172(172):e62641.

II. **Bèchet NB**, Shanbhag NC, Lundgaard I. Glymphatic pathways in the gyrencephalic brain. *Journal of Cerebral Blood Flow & Metabolism*. 2021 Sept;41(9):p2264-2279.

III. *Shanbhag NC, ***Bèchet NB**, Kritsilis M. and Lundgaard I. 2021. Impaired cerebrospinal fluid transport due to idiopathic subdural hematoma in pig: an unusual case. *BMC Veterinary Research*, 17(1), p1-8.

IV. **Bèchet NB**, Shanbhag NC, Kritsilis M, Liu C, Leon F, Meissner A and Lundgaard I. An arterial transmural entrapment system prevents amyloid recirculation into the brain. *Manuscript*.

V. **Bèchet NB**, Shanbhag NC and Lundgaard I. Live imaging of perivascular transport through a porcine cranial window. *Manuscript*.

Porcine Glymphatic Pathways • *JCBFM* Cover, September 2021

Published Papers, Chapters and Manuscripts Outside of the Thesis

I. *Ramos R, ***Bèchet NB**, Battistella R, Pavan C, Xavier ALR, Nedergaard M, Lundgaard I. (2018) Cisterna Magna Injection in Rats to Study Glymphatic Function. *Methods in Molecular Biology.*

II. Munk AS, Wang W, **Bèchet NB**, Eltanahy AM, Cheng AX, Sigurdsson B, Benraiss A, Mäe MA, Kress BT, Kelley DH, Betsholtz C. PDGF-B is required for development of the glymphatic system. *Cell reports*. 2019 Mar 12;26(11):p2955-69.

III. **Bèchet NB**, Kylkilahti TM, Mattsson B, Petrasova M, Shanbhag NC, Lundgaard I. Light sheet fluorescence microscopy of optically cleared brains for studying the glymphatic system. *Journal of Cerebral Blood Flow & Metabolism.* 2020 Oct;40(10):p1975-86.

IV. Vallianatou T, Lin W, **Bèchet NB**, Correia MS, Shanbhag NC, Lundgaard I, Globisch D. Differential regulation of oxidative stress, microbiota-derived, and energy metabolites in the mouse brain during sleep. *Journal of Cerebral Blood Flow & Metabolism.* 2021 Jul 22:0271678X211033358.

V. Vallianatou T, **Bèchet NB**, Correia MS, Lundgaard I, Globisch D. 2022. Regional Brain Analysis of Modified Amino Acids and Dipeptides during the Sleep/Wake Cycle. *Metabolites*, *12*(1), p.21.

VI. *Vallianatou T, *Lin W, ***Bèchet NB**, Shanbhag NC, Lundgaard I, Globisch D. Comprehensive mass spectrometric analysis of the gyrencephalic brain reveals unique clearance pathways of neurotoxic metabolites. Manuscript.

VII. Shanbhag NC, Kritsilis M, Li C, **Bèchet NB**, Lundgaard I. Species-specific CSF egress pathways across the cribriform plate. *Manuscript*.

comet and stars

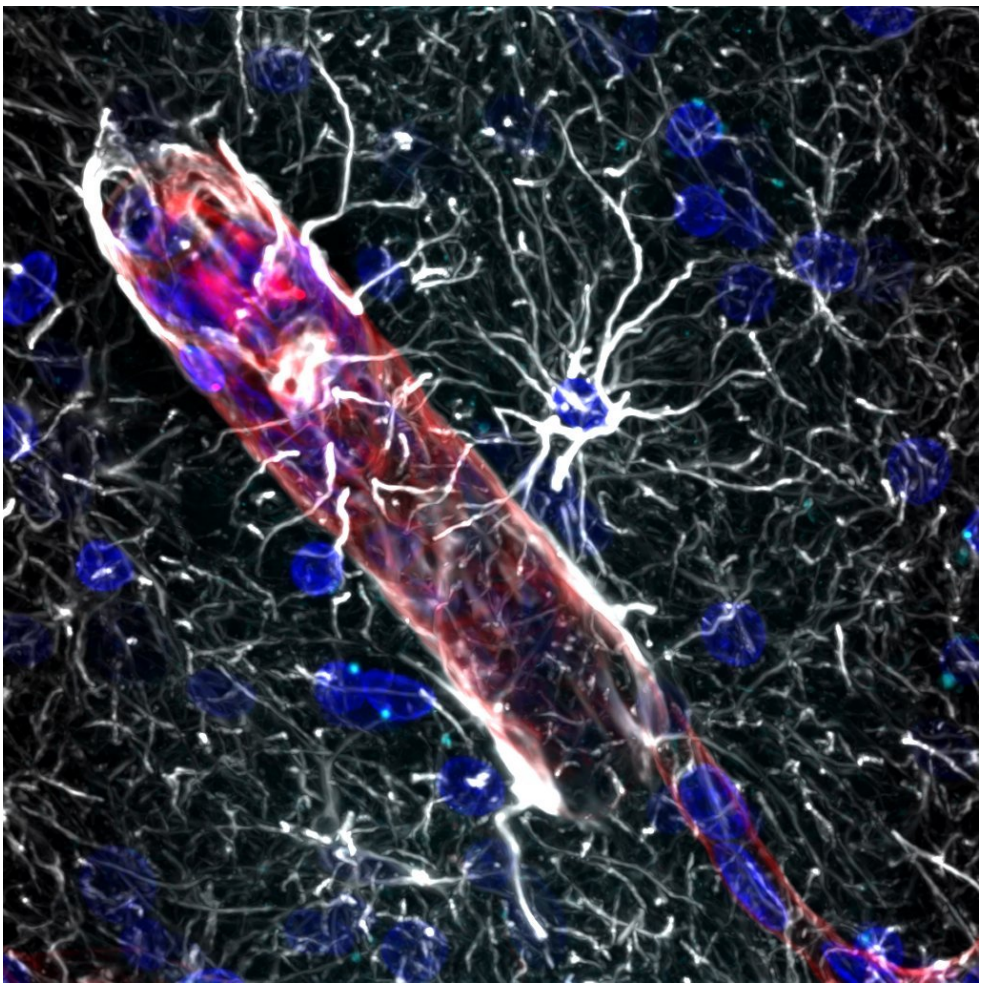

Popular Summary

Sleep is a highly conserved, fundamental part of life, with most people spending around one third of their time engaged in this activity. Recent work has shown that one of the important roles of sleep, is that it is a time when the brain actively cleans itself. During the day, sustained periods of activity from the billions of cells in the brain lead to the production of waste, which at some point, needs to be removed. If you have ever experienced a night of poor sleep, or perhaps too little sleep after a good night out, you will very well understand the consequences of not allowing time for this waste to be cleared.

The system that clears waste from the brain whilst we sleep is called the glymphatic system. This system was only discovered in 2012, so it is still a very new idea in the greater field of neuroscience. The way it operates, is, while we sleep, the space between all the cells in the brain increases ever so slightly. This increase in space allows a special fluid only found in the brain, called cerebrospinal fluid, to wash through the brain and remove the waste along with it as it passes through the tissue. The glymphatic system is of great interest in the context of Alzheimer's disease, which has been linked with the impaired clearance of a specific type of protein by-product called amyloid-beta. Thus, it is our hope that the glymphatic system cleaning could one day be enhanced and used to help with the clearance of this protein, as an aid to try and extend the onset of Alzheimer's disease.

However, one problem, is that the glymphatic system, and its clearance of amyloid-beta, has only been studied in rodents, which have very different brain size and structure to humans. In order to understand this system in the context of humans it becomes important to explore it in larger mammals with brains more similar to humans. To achieve this we set out to develop a pig model to study the glymphatic system. Using this model we characterized the system in a larger brain more similar to humans and found that it is even more developed than in rodents, hinting at what likely exists in humans. Through this pig model we have also been able to better understand amyloid-beta circulation in the brain and how it impacts the glymphatic system, taking us closer to understanding this process in humans and how it might be exploited therapeutically in diseases like Alzheimer's.

Populärvetenskaplig Sammanfattning

Sömn är en högst bevarad och fundamental del av livet, och är en aktivitet som de flesta människor tillbringar ungefär en tredjedel av sin tid till. Nya rön har visat att en av sömnens viktiga roller är att det är en period som hjärnan rensar sig själv. Under dagen leder aktivitet i flera miljarder celler i hjärnan till produktion av avfall som vid något tillfälle måste avlägsnas. Om du någonsin har upplevt en natt med dålig sömn, alternativt för lite sömn efter en trevlig utekväll, så kommer du ha god förståelse för konsekvenserna av att inte avsätta tillräckligt med tid för att detta avfall ska rensas.

Systemet som rensar avfall från hjärnan medan vi sover kallas för det glymfatiska systemet. Detta system upptäcktes först 2012, och är därmed fortfarande väldig ny kunskap inom det neurovetenskapliga forskningsområdet. Systemet fungerar som så, att medan vi sover inträffar en mycket liten utvidgning av utrymmet mellan cellerna i hjärnan. Denna utvidgning leder till att en särskild vätska som endast finns i hjärnan, kallad för cerebrospinalvätska, kan skölja igenom hjärnan och föra med sig avfall när den passerar vävnaderna. Det glymfatiska systemet är av mycket stort intresse i samband med Alzheimers sjukdom, vars orsak kopplats till försämrad rensning av en specifik typ av proteinbiprodukt som kallas amyloid-beta. Det är vår förhoppning att det glymfatiska systemets rengöring i framtiden kan förstärkas för att förbättra rensningen av detta protein. Det skulle då kunna vara ett verktyg för att fördröja uppkomsten av Alzheimers sjukdom.

Ett problem är att det glymfatiska systemet, och dess rensning av amyloid-beta, endast har studerats i gnagare, vars hjärnstruktur och storlek skiljer sig väsentligt från människans. För att förstå detta system i ett mänskligt sammanhang är det viktigt att utforska det i större däggdjur vars hjärnor mer liknar människans. För att möjliggöra detta utvecklade vi en grismodell för att studera det glymfatiska systemet. Med denna modell har vi karakteriserat systemet i en större och mer människolik hjärna, och har funnit att systemet i grisar är ännu mer utvecklat än hos gnagare, en indikation om vad som sannolikt finns hos människor. Genom denna grismodell har vi även fått bättre förståelse för cirkulationen av amyloid-beta i hjärnan och hur den påverkar det glymfatiska systemet. Denna insikt tar oss närmare en förståelse för processen i människor och hur den kan användas terapeutiskt vid sjukdomar som Alzheimers.

Santrauka lietuviškai

Miegas yra itin svarbi gyvenimo dalis, nes dauguma žmonių praleidžia apytiksliai trečdalį gyvenimo miegodami. Naujausi moksliniai tyrimai atskleidė, kad miego metu smegenys vykdo aktyvų valymasi. Dienos metu dėl nuolatinio milijardų smegenų ląstelių aktyvumo susidaro atliekos, kurios tam tikru momentu turi būti pašalintos. Jei kada nors prastai miegojote arba linksminotės visą naktį, tai labai gerai galite suprasti netinkamo atliekų išvalymo pasėkmes savo savijautai. Sistema, kuri yra atsakinga už atliekų pašalinimą mums miegant, vadinama glimfatine sistema.

Ši sistema buvo atrasta tik 2012 metais, todėl tai yra vis dar labai didelė naujovė neuromokslų srityje. Glimfatinė sistema veikia šiuo principu: miegant tarpai tarp smegenų ląstelių šiek tiek padidėja, todėl smegenų skystis gali prasiskverbti per smegenis ir išplauti susikaupusias atliekas. Manoma, kad sergant Alzhaimerio liga, glimfatinė sistema nesugeba efektyviai pašalinti tam tikros rūšies baltymų šalutinio produkto, vadinamo amiloidu-beta. Viliamasi, kad glimfatinės sistemos tyrimai galėtų būti naudingi šio baltymo pašalinimui iš smegenų, ir tai galėtų nutolinti Alzhaimerio ligos pradžią.

Viena problemų yra tai, kad glimfatinė sistema ir amiloido-beta pašalinimas buvo tirtas tik graužikuose, kurių smegenų dydis ir struktūra labai skiriasi nuo žmogaus. Norint suprasti kaip ši sistema veikia žmoguje, yra svarbu ją tirti didesniuose žinduoliuose, kurių smegenys yra panašesnės į žmonių. Norėdami tai padaryti, mes sukūrėme kiaulių modelį, kuris leido apibūdinti sistemą didesnėse ir artimesnėse žmogui smegenyse. Naudodamiesi šiuo kiaulių modeliu, mes taip pat galėjome geriau suprasti amiloido-beta cirkuliaciją smegenyse ir kaip tai veikia glimfatinę sistemą. Visa tai padeda geriau suvokti šį procesą žmogaus smegenyse ir ateityje, kuriant įvairių ligų, pavyzdžiui, Alzhaimerio gydymą.

a flaming nova 1

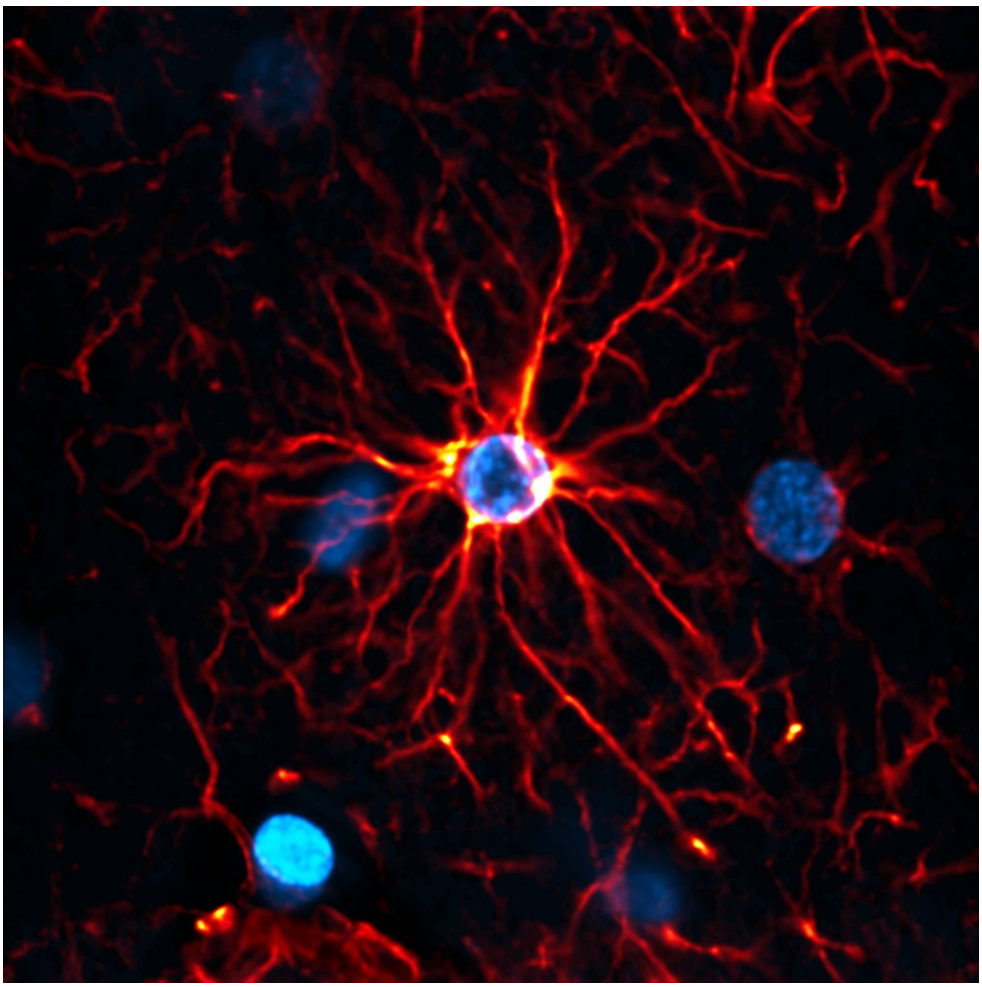

Abbreviations

Aß	Amyloid beta
AD	Alzheimers disease
AQP4	Aquaporin-4
APP	Amyloid precursor protein
CM	Cisterna magna
CP	Choroid plexus
CAA	Cerebral amyloid angiopathy
CSF	Cerebrospinal fluid
CVS	Cardiovascular system
CNS	Central nervous system
DAPC	Dystroglycan associated protein complex
Dex	Dexomedetomidine
EEG	Electroencephalogram
GFAP	Glial-fibrillary acidic protein
Hz	Hertz
ICP	Intracranial pressure
iNHP	Idiopathic normal pressure hydrocephalus
IS	Interstitial space
ISO	Isoflurane
KO	Knockout
KX	Ketamine-xylazine
LRP-1	Lipoprotein receptor-related protein 1
LS	Lymphatic system
LYVE-1	Lymphatic vessel endothelial hyaluronan receptor 1

MR	Magnetic resonance
MRI	Magnetic resonance imaging
NDD	Neurodegenerative disease
NFT	Neurofibrillary tangle
NHP	Non-human primate
NE	Noradrenergic
OAP	Orthogonal array of particles
PD	Parkinson's disease
PROX-1	Prospero homeobox 1
PS1	Presenilin 1
PVS	Perivascular space
SAH	Sub-arachnoid haemorrhage
SAS	Subarachnoid space
SMA	Smooth muscle actin
T	Tesla
TBI	Traumatic brain injury
TMA	Tetramethylammonium

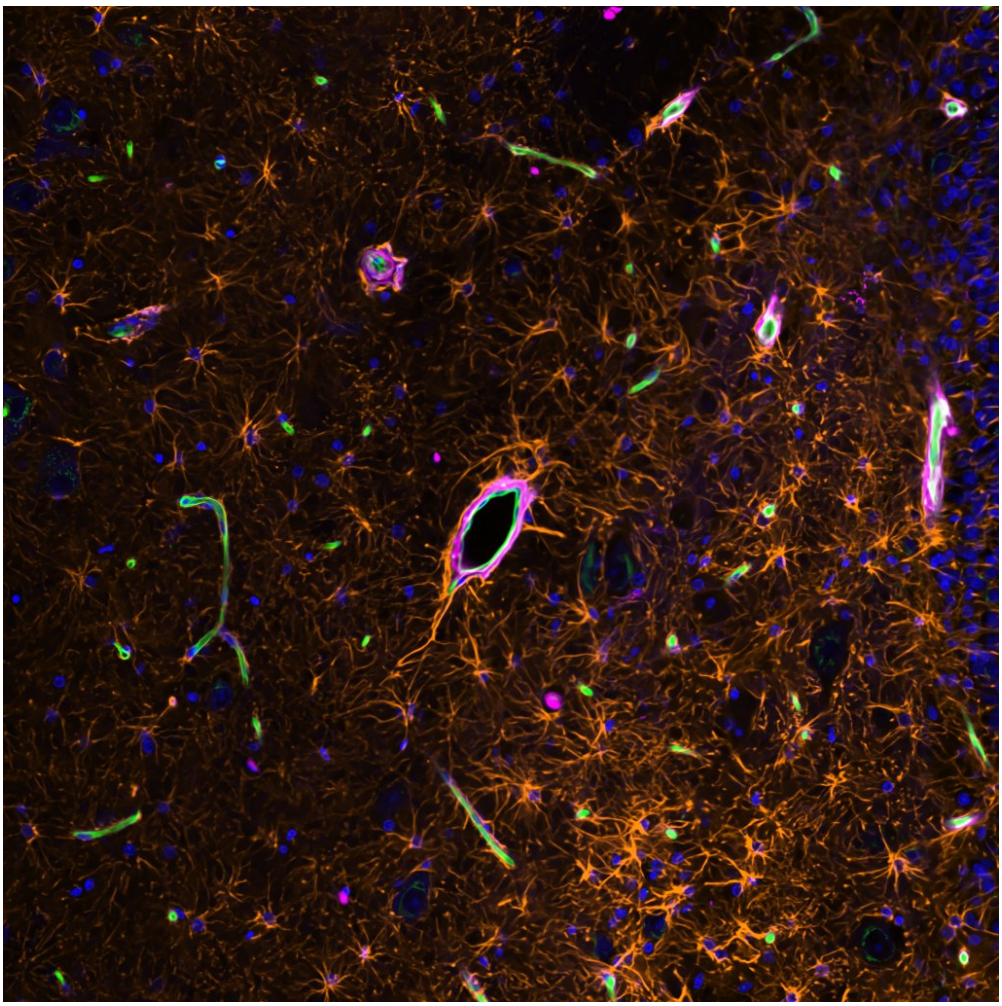

Introduction

The Glymphatic System

An Overview

As with all systems, mechanical or biological, the production of waste is an inevitable part of the process. The brain is no different in this regard, but where the brain does differ, especially when compared to other organ systems, is that it lacks some of the conventional machinery to remove said waste[1,2]. In the rest of the body exists a circulatory system secondary to the cardiovascular system (CVS), the lymphatic system (LS)[3,4]. As various cells, tissues and organs go about their normal physiological processes they produce metabolic waste. Much of this waste is rapidly carried away by the CVS, but some of it is left abandoned to the space that exists between cells, the interstitial space (IS)[1]. The LS acts to collect any waste left behind in the IS[3,4]. Once captured within the bounds of the LS the waste is transported as part of the lymphatic fluid, lymph, which is driven through a catacomb of vessels by surrounding skeletal muscle contractions, respiratory motion and the contraction of smooth muscle cells[3–5]. As lymph passes through the LS sentinel sampling of the lymph contents take place to detect the presence of any foreign pathogens or proteins which might require an immune response[3–5]. Finally, that which remains is returned to the CVS via large lymphatic ducts which empty their contents into the subclavian veins. Throughout the day this process accounts for the collection, surveillance, and return of around 3 litres of fluid[3–6].

Interestingly, or rather, peculiarly, the brain itself does not contain any lymphatic vessels, and despite the recent re-characterisation of lymphatic vessels in the outer membrane that surrounds the brain, the dura mater, this phenomenon still holds true[7,8]. The consensus as to why this may be lies in the immune surveillance aspect of the lymphatic system and subsequent immune response. The brain is considered an immune privileged site as a consequence of the irreparable neural damage that would and can amount in the case of an immune reaction, and is thus thought to lack conventional lymphatics for this very reason[9,10]. However, recent work has shown that the brain might not be as immune privileged as previously thought, with the identification of a skull bone marrow niche capable of mounting an immune

response through cues in the cerebrospinal fluid (CSF), mediated through ossified vascular channels[11].

Regardless of the intricacies of the neuroimmune landscape, some facts still hold true: 1) There are no lymphatic vessels in the brain itself, hereafter, neuropil[7,8,12], 2) The brain, which only makes up 2% of bodyweight, disproportionately receives around 12% of the CVS output[13,14], 3) As with cells of other organ systems there also exists an IS between neurons and glia, which itself yields a capacity for metabolic waste retention[1,2]. Thus, we come to the glymphatic system and the reason for its existence. In the absence of lymphatic vessels to carry away waste from the brain IS, the glymphatic system has developed its own means to carry out this process[1,2]. To this end the glymphatic system facilitates the advective flow of CSF from perivascular spaces (PVS) through the neuropil, collecting waste as it filters between the cells, returning it to the CSF reservoir at which point it can be cleared from the CNS (*Figure 1*)[1,15]. Apart from the CSF another important player in glymphatic physiology is the aquaporin-4 (AQP4) water channel which is predominantly expressed on PVS-facing astrocytic endfeet (*Figure 1*)[1,15,16]. In preliminary summary the glymphatic system is a CNS-specific waste clearance system whose necessary development took place in the absence of brain lymphatics to help clear metabolic waste from the brain. Pivotal aspects of this system include CSF, PVS and AQP4.

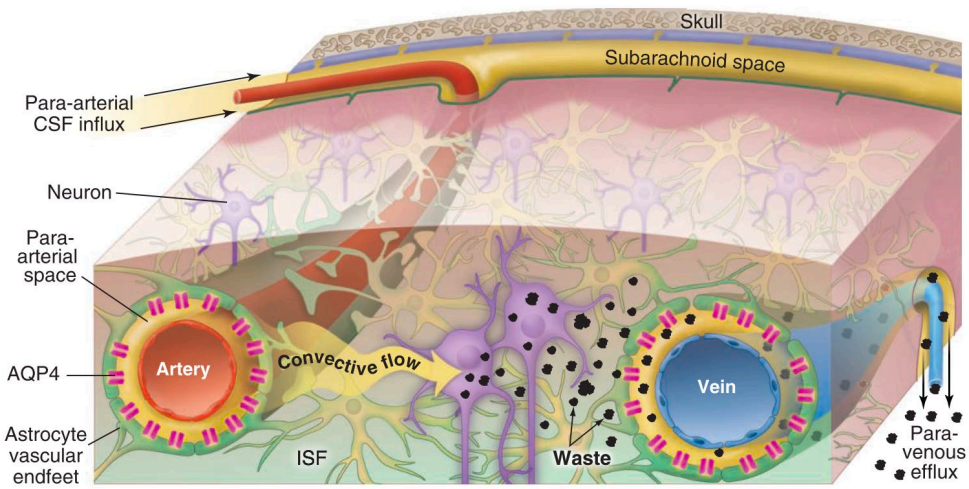

Figure 1 • The Glymphatic Model
Glymphatic function is based on the movement of CSF. From the SAS, CSF moves convectively within the neuropil along PVS surrounding penetrating arteries. From here, facilitated by AQP4 expressed on cerebrovascular-facing astrocytic endfeet, CSF advectively passes through the neuropil, acting to clear waste to PVS surrounding veins, upon which waste is returned to the CSF resevoir. Adapted from (Nedergaard, 2013).

Cerebrospinal Fluid

A Brief History

The first recognised substantiation eluding to the existence of fluid housed within in the human skull was uncovered in the Edwin Smith Papyrus, which dates back to approximately 1500 BC, and is thought to be a copy of an even older transcript from ancient Egypt (*Figure 2a*)[17–19]. This text is part of an important series of case reports, one such, case 6, pertaining to a man who had suffered a severe head wound[17–19]. Consequently this text also represents the first literature in human civilisation to ascribe a word for "brain".[17–19] At this time the nature of the fluid was not described and only after a series of hypotheses emerging through time from ancient Greece, the Roman Empire and renaissance Italy was the modern day term of cerebrospinal fluid (CSF), originally *liquide cérébro-spinal,* put forward by Francois Magendie in a publication from 1842[18–24]. Yet, credit for this identification and understanding should also be given to the Swedish theologist, Emmanuel Swedenborg, who made similar observations in work predating that of Magendie, written sometime between 1741-1744, but only published in 1887, as no editor of the time would publish his work as he was not qualified as a physician[19,25]. Once better understood, CSF removal was then explored as a potential treatment for conditions impacting the CNS[18]. Early lumbar puncture (LP) techniques, accessing CSF in the lumbar spine, were adopted as a means to reduce intracranial pressure (ICP) in conditions such as hydrocephalus, tubercular meningitis and in the case of cerebral tumours, however most of these interventions proved to be fatal[26]. The real value of CSF sampling as a diagnostic tool came later when low volume LP CSF samples were used for protein and glucose quantification after infection, pressure and cell constitutions, and microbial staining and cultivation[27,28]. Apart from its usefulness as a window into CNS pathology, various physiological roles of CSF have been elucidated in the past century: 1) CSF acts as a mechanical barrier around the brain and provides some degree cushioning in the instance of light head trauma, 2) CSF plays an important role in CNS homeostasis by maintaining a stable electrolyte environment and acid-base balance, as well as a delivery system for nutrients like glucose, 3) CSF acts as a delivery system for regionally produced substances like melatonin which require further cerebral distribution[29–31]. However, with the inception of glymphatics CSF has yet been ascribed a further critical role, that being the filtration and collection of metabolic waste from the brain, including by-products such as lactate and amyloid-beta (Aß), but before CSF can reach the glymphatic microarchitecture and serve its clearance role, it must first travel great distances from its site of production[15,32].

The Ventricular System

The journey of CSF begins in four hollow cavities distributed across the neuroaxis, called ventricles[18]. These intriguing structures were notably first conceptualised by Leonardo da Vinci as a series of bulbous cavities connected to the back of the eye

(*Figure 2b*)[18]. Only when da Vinci created wax casts by injecting molten wax into the fourth ventricle, and subsequently scraping away the brain, did the true nature of the ventricular structure come to light, as reflected in one of his later drawings (*Figure 2c*)[18,19]. These were most likely carried out in oxen brain owing the presence of the rete mirabile.

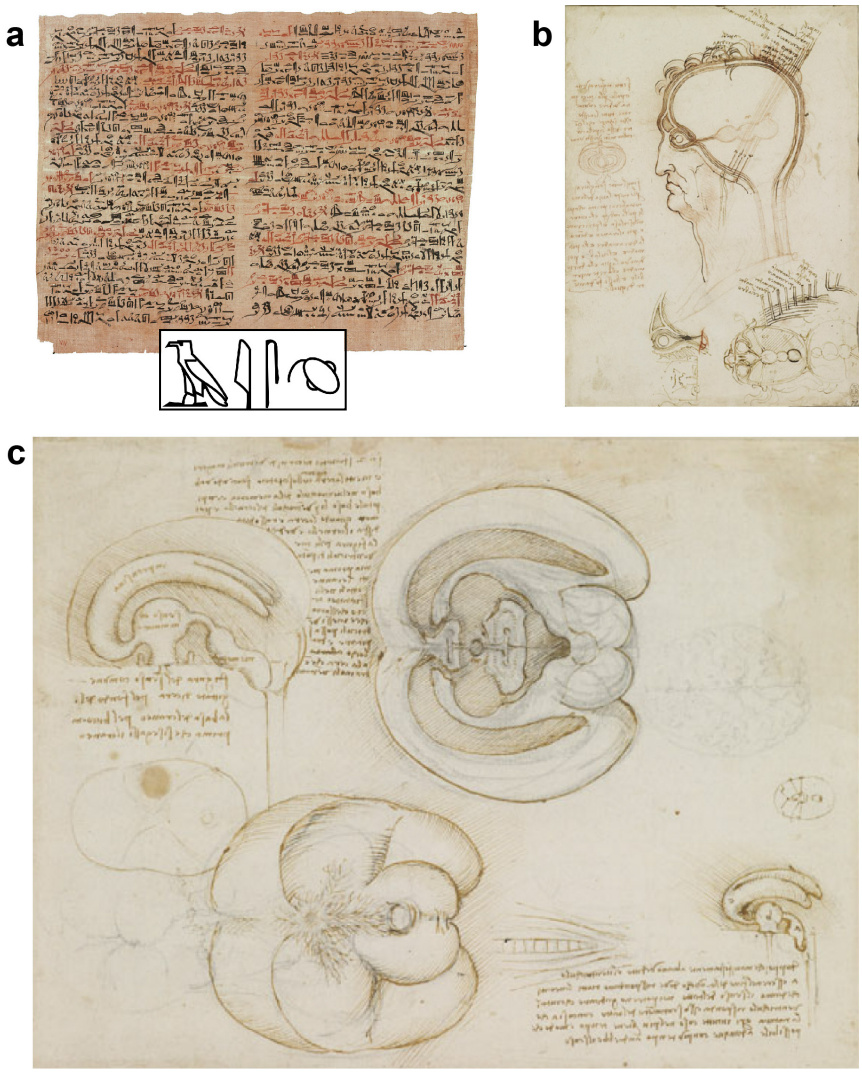

Figure 2 • The Origins of CSF and the Ventricular System
a) A photograph of the Edwin Smith Papyrus, currently housed at The New York Academy of Medicine library. This document dates back to 1500 BC and details a series of neuropathology case reports. Case 6 is thought to be the first reference in human history to CSF, while the text also contains the first symbology for the brain (see inset below image). **b-c**) Sketches by Leonardo da Vinci part of the Royal Collection Trust/© Her Majesty Queen Elizabeth II showing da Vinci's initial conception of the ventricular system (b) followed by a more detailed diagram after performing wax cast injections. Adapted from (Deisenhammer *et al.* 2015 and Tola Arribas, 2017).

The first sketches of the human ventricular system can be found in the iconic anatomy book, *De humani corporis fabrica,* which was the work of Andreas Vesalius[18,19]. The system begins with two lateral ventricles which are made up of a central body located in the parietal region, and three horns, frontal, temporal and occipital, each projecting to the respective, as named, brain regions[33,34]. The interventricular foramen of Monro connects the lateral ventricles to the third ventricle, which exists as a narrow passage in the diencephalon, bounded laterally by the medial aspect of each thalamus[18,19,35]. The aqueduct of Sylvius then connects the third ventricle to the fourth, which is located in the brainstem[18,19,36]. From the fourth ventricle CSF may then either continue travelling down the central canal of the spinal cord or move into the sub-arachnoid space (SAS) surrounding the brain, via either the medial (of Magendie) or lateral (of Luschka) apertures[18,19,34,37,38]. Once in the SAS CSF has access to the PVS, which are important initial conduits in glymphatic physiology[39]. Also worthy of mention here are the CSF cisterns, which are enlarged CSF-containing compartments that are continuous with the SAS[40,41]. The names of all the cisterns that exist are too numerous to list, but of note and necessary of remembrance in the context of the glymphatic system is the cisterna magna (CM). The largest of all the cisterns, the CM is positioned between the medulla anteriorly, and the cerebellum posteriorly, and is an important site for the introduction of tracers into the CSF in order to study the glymphatic system[42].

The Choroid Plexus

Something not yet alluded to is the fact that CSF is a fluid of unique properties, and found nowhere else in the body, and the production of such a unique fluid naturally requires a specialised tissue, the choroid plexus (CP). Described as a leaf like structure floating in the CSF, the epithelium of the CP is continuous with the ependymal epithelial lining of the ventricles[43,44]. Moreover, tufts of CP are located throughout each of the fours ventricles where they act to produce CSF[43]. On average the CP produces around 600ml of CSF a day, which amounts a 3-5 time turnover of the total circulating CSF volume over 24 hours[45,46]. Utilising a unique distribution of several ion transporters across the basolateral and apical cell surfaces, the choroid plexus produces CSF through an active secretory mechanism from an underlying fenestrated capillary network.[43–45] In keeping with the importance of CSF for glymphatic function so too is the CP recognised, yet for now largely unexplored, as an important part of glymphatic function. Despite the observation that the rate of CSF production does not relate to glymphatic function, CSF itself is required for normal glymphatic physiology to take place, and this may only come from the CP[47].

Efflux

As mentioned in the previous section, CSF is turned over several times throughout the course of the day. For this to be feasible it is only natural that CSF also has to have a route of exit from the CNS, hereafter, efflux. If the efflux of CSF is impaired in any way and normal CSF production persists, as is the case in non-communicating

hydrocephalus, the subsequent ICP elevations can result in mass effect of on adjacent brain tissue, brain herniation and death[48,49]. Although this represents pathological circumstances based on distinct pathology it echoes the fundamental credo of, *what goes in must come out*. In relation to glymphatic function, it is also of utmost importance that CSF is turned over frequently or else CSF containing waste already cleared from the brain could once again be re-circulated. This notion of waste re-circulation is a complex and as of yet poorly understood proposition, which will be expanded upon in a Paper IV. Returning to CSF efflux, there are several proposed mechanisms by which CSF exits the CNS. The classic theory, still taught in medical schools to this day, is that CSF is removed from the CNS through the arachnoid granulations, which are tube-like structures that project from the SAS into the superior sagittal sinus[12,50–53]. Despite being once described as one-way valves the arachnoid granulations possess a continuous layer of endothelial cells connected by tight junctions and to this day there exists little in vivo evidence to support their role in CSF efflux[54–57]. An alternate hypothesis brought to popularity by Schwalbe in 1869 highlighted both the cranial and spinal nerve sheaths as sites for CSF removal to systemic lymphatics, and since this time follow-up studies in numerous species have confirmed this observation, however the mechanism by which CSF reaches the lymphatics along these routes is still debated[58–62]. Shwalbe also described an efflux pattern across the cribriform plate, whereat the olfactory projections dive across the bone to the nasal mucosa[58]. The nasal efflux pathway has also been widely explored, in particular, by Miles Johnston, who performed in vivo injections of microfil in several species including rats, sheep, pigs and primates, where the silicon tracer could be mapped traversing the cribriform plate and entering lymphatic vessels in the nasal mucosa[53,63–69]. The most recent addition to the CSF efflux story comes with the re-discovery of the dural lymphatic vessels, first in the dorsal dura, and subsequently in the ventral dura[7,8,70–77]. First described in 1787 by Paolo Mascagni, and over the years by several other authors, the meningeal lymphatic vessels were again characterised in 2015 by two independent groups who both showed a network of lymphatic vessels running in close proximity to the superior sagittal sinus and middle meningeal artery[7,8]. Lymphatic vascular identity was confirmed in these studies by staining for specific lymphatic endothelial markers Lyve-1, Prox-1 and podoplanin[7,8]. Furthermore, tracers injected into the CSF space were identified in these vessels, which drained to the deep cervical lymph nodes, however other routes have also been found to drain to these nodes[8,72]. The identification of the skull marrow niche and its capacity to respond to CSF cues has shed interesting light on a potential role for the meningeal lymphatic vessels, however it remains unlikely that they represent a major efflux route based on the fact that ablation of these vessels, genetic, or otherwise, does not appear to alter ICP[7,11]. The culminating work on CSF efflux, at this juncture, by Steven Proulx, has utilised several advanced in vivo imaging techniques to capture real time CSF efflux in rodents. This body of work has shown that CSF reaches several regional lymph nodes including the cervical, mandibular and iliac lymph nodes and that this occurs

along several nerve routes including cranial, spinal and sacral nerves, as well as long the carotid sheath[12,59,78–80]. In summary CSF efflux, in a way, represents the final aspect of CNS waste clearance, and so it is a topic that is studied closely alongside that of glymphatic function, and so should be kept in mind.

Perivascular Spaces

In the context of the glymphatic system PVS represent low resistance conduits that permit the convective flow of CSF from the SAS to deeper sites within the neuropil[1,15,39]. Take note, that this is carefully defined as transport to *within* the neuropil, and not *into* the neuropil itself, the latter referring to the movement of CSF from the PVS space and to the neuropil, which is a distinct process. The observation of a potential space around cortical arteries penetrating the neuropil was initially described in 1842 by Durand-Fardel[81,82]. Despite this the spaces later became known as Virchow-Robin spaces, and early experiments in rodents suggested they could play a role in CSF-ISF exchange based on the penetration of CSF-injected tracers into PVS deep in the basal ganglia[81–86]. The existence of PVS, at least those around sufficiently large vessels, has also been confirmed in humans due to the advancement of magnetic resonance imaging (MRI) techniques (*Figure 3a-b*)[87–89]. While in pre-clinical glymphatic experiments the PVS are described as being present around both arteries and veins, the identification of peri-venous spaces in humans remains elusive[15,82].

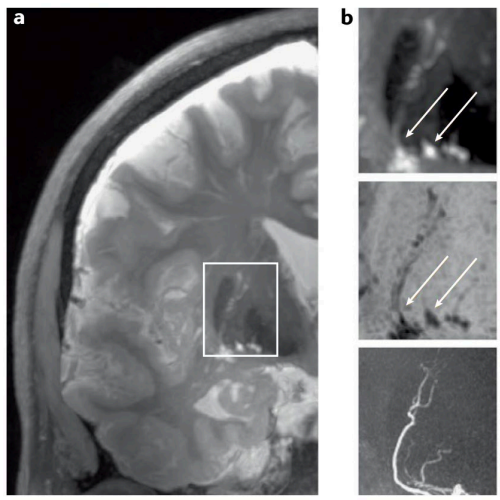

Figure 3 • Perivascular Spaces Visible using MRI
a-b) T1 and T2 weighted images from coronal MRI scan with 7T scanner showing PVS in basal ganglia along perforating vessels that correspond with arterioles imaged with magnetic resonance angiography. Arrows identify PVS inferior aspect in communication with basal CSF reservoir. Obtained from (Wardlaw *et al.* 2020), orginally adapted from (Bouvy *et al.* 2014).

A topic often debated with regards to PVS is the nature of the space itself, and if it is really a space at all. The Virchow-Robin spaces, which could be defined as so-called initial segments of penetrating vessels, as well as the large concentric PVS seen in the basal ganglia in humans under MRI, are less controversial and whereat an actual potential space can be observed with real time fluid flow[87,90]. However, where this notion of a true potential space becomes foggy is as vessels dive deeper into the brain and down to the capillary bed. There are two main challenges in unravelling this mystery: 1) At present no sufficient techniques exist to be able to measure or observe PVS flow in smaller, deeper vessels, 2) It has been found that the act of tissue fixation results in collapse of the PVS, such that what is observed ex vivo is not a fair representation of what might have occurred in vivo[91]. In keeping with this, what data we do have suggests that the potential space of the PVS does indeed end with the initial penetrating segment based on the fact that the pia mater, which forms the outer bound of the PVS in initial penetrating segments, eventually fuses and becomes a basal lamina at smaller arterioles and the capillary bed[41,85,92]. However, something worth considering in this context, and the context of PVS as conduits for CSF transport into the brain under the glymphatic hypothesis, is, what is the relevance of whether or not the object of discussion, i.e. the nature of what constitutes a PVS, is even relevant? Whether the space is potential or not, what is irrevocable is that tracers introduced into the CSF do penetrate deep within the neuropil along the vessels, observable all the way down to the capillary bed, acting as access points for CSF, whereat it may carry out the next step in glymphatic function, which is the movement of water in the CSF from around the vessels and through the neuropil to clear waste.

Aquaporin-4

First identified in 1994 by Agre and Verkman, it was found that the brain expressed an explicit aquaporin cDNA[93,94]. Initially termed mercury insensitive water channel (MIWC), it later came to be known as AQP4 and was highly expressed by astrocytes throughout the brain[95]. More specifically, AQP4 exhibited a polarised expression in astrocytes, favoured at astrocytic plasma membrane domains adjacent to cerebrovasculature and the brain surface[96,97]. Immunogold analyses have shown that endfoot expression is up to 10-fold greater than at non-endfoot membranes[98,99]. The discovery and characterisation of AQP4 coincided with the resolution of the identity of the mysterious orthogonal arrays of particles (OAP) that were discovered in freeze-fracture preparations of astrocytic endfeet (*Figure 4a*)[100–102]. The major protein component of these OAP's was undetermined until they were found absent on the astrocytic endfeet of AQP4 knockout (KO) animals[103,104]. As so named, AQP4 belongs to the aquaporin subfamily, which are selectively permeable to water[105]. Several isoforms of AQP4 have been described but the two most studied are M1 and M23, of which M1 is 22 amino acids longer and characterised by its inability to form OAP's[106–109]. Concerning structure, AQP4 is a tetramer, where

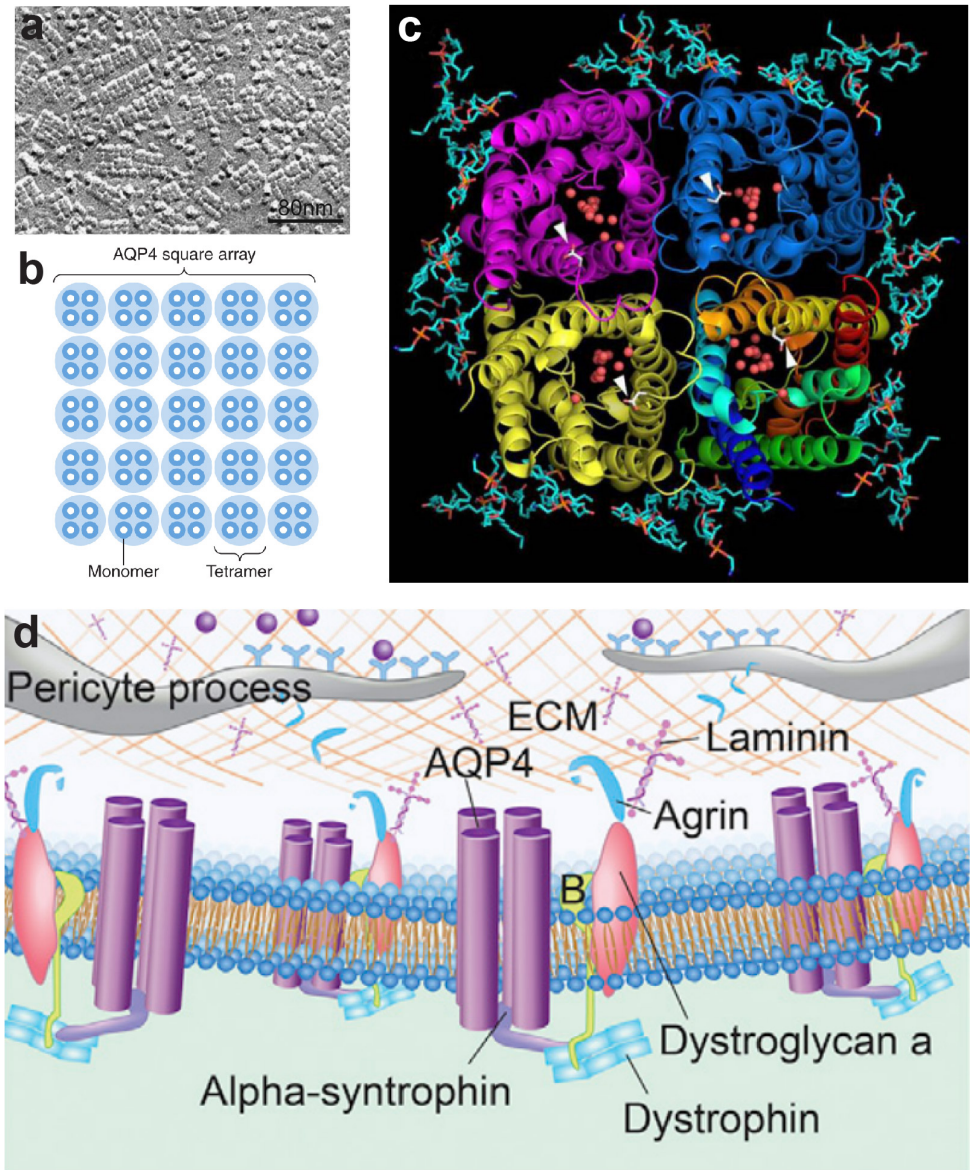

Figure 4 • Aquaporin-4 Structure and Anchorage

a) Electron micrograph of orthogonal array of particles (OAP) identified in early astrocyte foot process freeze fractures. **b**) Schematic showing proposed structure of OAP, made up of arrays of AQP4 tetramers. **c**) Ribbon diagram showing tetrameric organisation of AQP4, lipids represented with ball-and-sticks and water representsed by red spheres. **d**) Schematic of dystrophin-associated protein complex (DAPC) identified as important AQP4 anchorage unit. DAPC constituents include alpha-syntrophin, drystrophin and dystroglycan. Adapted from (Wolborg *et al.* 2011, Tani *et al.* 2009, Munk *et al.* 2019).

water may pass through a specialised pore within each monomer (*Figure 4b-c*)[110,111]. Subsequently the tetrameric structure also leads to the creation as a central pore which has been a subject of interest regarding the mediation of gas transport[112,113]. The interest in, and importance of, AQP4, with regards to the glymphatic system, lies in its polarised expression to cerebrovascular-facing astrocytic endfeet and its ability to permit the free passage of water. Once CSF has found its way within the neuropil along PVS, potential or otherwise, the next part of glymphatic physiology rests with the advective flux of water from the PVS and into the neuropil itself[1,15]. It is this movement of water that drives the clearance of metabolic waste from the neuropil back to the CSF reservoir[1,15]. Through the utilisation of AQP4 KO mice this important process has been shown to be dependent on the expression of AQP4 (*Figure 5a*)[15,16,114]. Some controversy does exist regarding the necessity of AQP4 for this process based on opposing findings from a single group that found AQP4 KO did not impair tracer movement from the CSF to the brain and had no impact on the clearance of intraparenchymally injected Aß[115]. However, a follow up study from several independent laboratories, using four different AQP4 KO mice reaffirmed that the absence of AQP4 did impair glymphatic influx, utilising both in vivo fluoroscopy and MRI as readout(*Figure 5b*)[16].

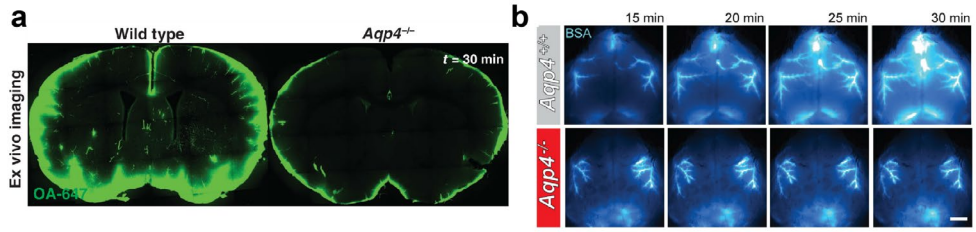

Figure 5 • Aquaporin 4 Knockout Mice Exhibit Impaired Glymphatic Function
a) Ex vivo coronal slices from wild type and AQP4 KO mice after CM injection of ovalbumin-647 (OA-647). **b**) In vivo dorsal cerebral images in wild type and AQP4 KO mice using transcranial fluorscopy over 30 minutes after CM injection with bovine serum albumin-647. Adapted from (Iliff *et al.* 2012, Mestre *et al.* 2018).

Meta-analysis revealed that the disparity in findings related in one instance to the choice of anaesthetic, tribromoethanol, and in another to the invasiveness of intraparenchymal injection, both of which impair glymphatic function limiting the possibility to tease out aberrations in normal physiology[16]. Furthermore, extensive work has been carried out in rodents surrounding the dysregulation of the dystroglycan associated protein complex (DAPC), whose components play a role in AQP4 membrane anchorage to astrocytic cytoskeletal elements (*Figure 4d*)[116–119]. DAPC components include dystroglycan, dystrophin, dystrobrevin and alpha-syntrophin[120]. Mice with alpha-syntrophin KO were found to exhibit reduced AQP4 polarisation and impaired glymphatic CSF-tracer influx[121,122]. Human transcriptome analysis revealed an association between dystroglycan, dystrobrevin and alpha-syntrophin gene products and dementia and AQP4 expression[123,124]. Additionally,

the knockdown of pericytes in *Pdgfb*$^{ret/ret}$ mice impairs the development of the glymphatic system including the polarised expression of AQP4, which is thought to relate to reduced agrin levels, a component produced by pericytes and important for dystroglycan binding[120]. Yet, despite the overwhelming volume of research into AQP4 in the context of glymphatics the precise mechanism through which it facilitates CSF movement into the neuropil is poorly understood. Strong criticism comes from the fact that the astrocytic endfoot layer is not a tight barrier and thus water from the PVS can simply enter the neuropil through endfoot gaps[125]. However, despite this observation and the lack of a mechanism, what is apparent is that the polarised expression of AQP4 to cerebrovascular endfeet is a necessary for glymphatic function and the absence of a mechanism does not change this fact.

Models to Study the Glymphatic System

As is the case with all scientific inquisition, a good model is required to test hypotheses and (hopefully) answer research questions, whether they be in silico, in vitro, in vivo or ex vivo. In the instance of glymphatics, since a complex brain-wide biological system is the research focus the superlative way to study it is in the brains of complete, living organisms. The way in which the glymphatic system is studied in rodents is by introducing tracers into the CSF[126,127]. Tracers used are typically either fluorescent, magnetic or radioactive, although in one case water isotypes have been utilised[15,114,128,129]. Tracers are introduced in vivo, either by CM injection (*Figure 6a-d*) or intraventricular injection and allowed to circulate for the desired amount of time. The CM route is typically preferred as it avoids any direct insult to the cortex, which has been shown to impair glymphatic function[16,115]. However, CM injection has also been criticised surrounding the consequence of infusion speeds and subsequent pressure elevations on glymphatic results. This criticism was recently put to rest in a publication that revealed, through dual cannulation, that if CSF is extracted at the same rate tracer is injected, the tracer distribution outcomes do not differ significantly from tracer injection alone[130]. Once tracers have been injected glymphatic pathways can be imaged in vivo using 2-photon, MRI or transcranial fluoroscopy to study real time system dynamics. Ex vivo processing can be used to make inferences on tracer penetration in vivo and glymphatic function as well as permits advanced microscopy readouts including confocal, electron and light sheet microscopy. In human studies gadolinium is typically injected into the intrathecal space in the lumbar spine where after MR imaging can be carried out over long time courses amounting days and even weeks[131,132].

Rodent Models

Developing a Glymphatic Archetype

Since the first paper describing the glymphatic system, which was published in 2012, the mainstay of work on, and thereby our understanding of the system, has

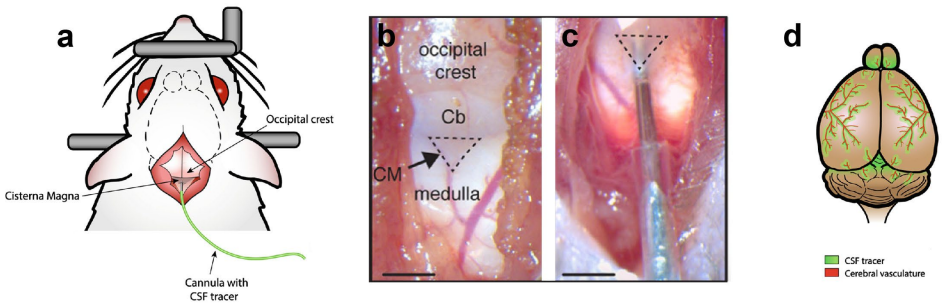

Figure 6 • Cisterna Magna Cannulation in Rodents
a) Schematic of the dorsal view of a rodent undergoing cisterna magna (CM) cannulation surgery. Head is fixed in place with ear bars. Skin and underlying neck muscles are parted revealing CM as grey inverted triangle. **b-c**) Magnified view of CM after parting overlying muscles and insertion of needle. **d**) Schematic of rodent brain showing CSF tracer distribution along cerebral vasculature. Adapted from (Ramos *et al.* 2019, Xavier *et al.* 2018).

come from rodent studies, and of these the majority represent mouse studies[15]. Although there exist knowledge gaps behind certain structures and mechanisms that constitute pivotal aspects of glymphatic physiology, much ground breaking work has been carried out in the last decade that has facilitated a more complete composition of the glymphatic model. As put forward in the seminal publication, the glymphatic system is based on the convective flow of CSF in PVS, both along pial and penetrating vessels, whereat CSF flux, facilitated by AQP4 water channels allows the CSF to move through the neuropil, clearing waste back to perivenous spaces and the CSF reservoir[15]. Although this work utilised 2-photon microscopy, only sufficient to image a small field of view, and ex vivo slice imaging, which lacked dynamic readout, similar findings validating this idea utilising MRI were later published[128,133]. This paper was also the first to show that the absence of AQP4 impairs this process, both with regards to the influx of CSF from the PVS to the neuropil, as well as the clearance of Aß from the neuropil[15]. The mechanism AQP4 mediated flux, as previously discussed, is not fully understood, but it is necessary for the process as a whole as has been demonstrated through countless independent studies[15,16,114,134].

Sleep and Anaesthetics

In addition to the necessity of AQP4, a subsequent step in better understanding the glymphatic system was made when it was revealed that glymphatic clearance is most efficient during sleep, approximately 95% more efficient than the awake state

to be exact (*Figure 7a-b*)[114]. Intriguingly, this enhanced effect was not only observed during sleep but also under the influence of ketamine-xylazine (KX) anaesthesia, which yields a similar electroencephalogram (EEG) power spectrum to natural sleep (*Figure 7c-f*)[114,135]. This effect could also be generated in awake mice under the administration of noradrenergic (NE) receptor antagonists. Utilising TMA^+ iontophoresis, the enhanced glymphatic function during sleep was attributed to a 60% increase in the IS. While KX appeared to mimic sleep, and thereby efficient glymphatic function, this was not the case for all anaesthetics and lead to the idea that it was not simply the act of being unconscious that drove glymphatic function but more so the brain state[114]. In keeping with this, isoflurane (ISO) alone inhibited glymphatic function by 32% when compared to ISO plus dexomedetomidine (dex)[136]. This difference in outcome between anaesthetic regimes was linked to the absence of spindle oscillations (9-15Hz) and suppression of NE release[136]. This idea was expanded further when five different anaesthetics, KX, ISO, ISO/dex, pentobarbital, tribromoethanol and alpha-chlorase, were utilised in a glymphatic study[137]. This data showed a strong correlation with glymphatic function and 4Hz

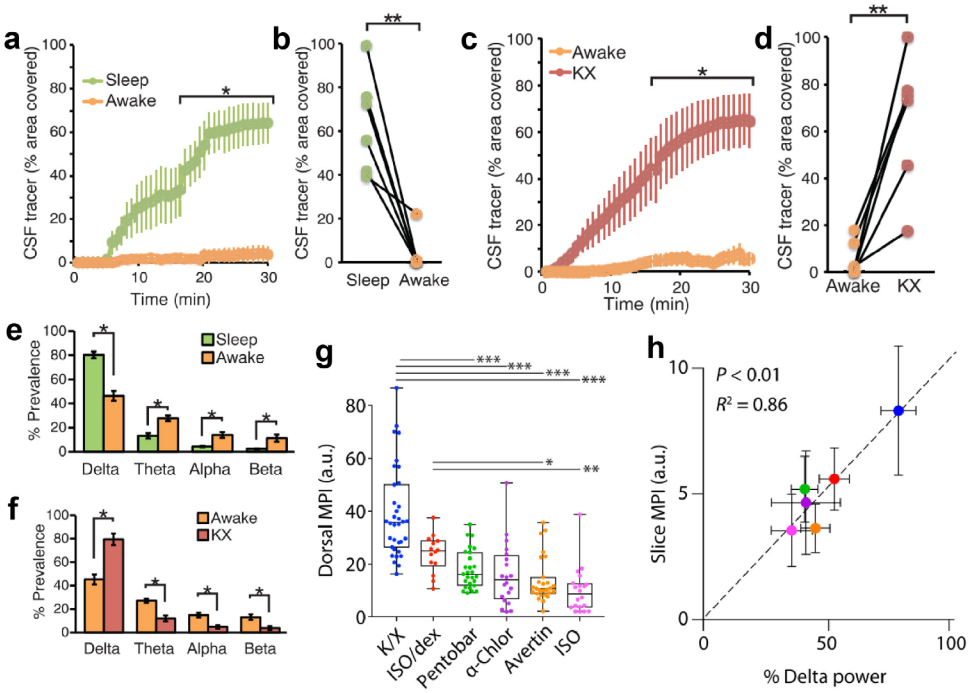

Figure 7 • Sleep but also Neuronal Oscillations Facilitate Glymphatic Function
a-b) CSF tracer percent area coverage in naturally sleeping and awake mice. **c-d**) CSF tracer percent area coverage in ketamine-xyaline anaethatised (KX) mice and awake mice. **e-f**) Percent prevalence of electroncephalogram (EEG) power spectra in natural sleeping, KX anaethatised and awake mice. **g**) Mean pixel intensity at dorsal cortex after CSF tracer injection in KX, isofluorane/ dexomedetomidine, pentobarbital, alpha-chlorase, avertin (tribromoethanol) and isofluorane anaethatised mice. **h**) Linear correlation between EEG delta power (4Hz) induced by anaesthetic and mean CSF tracer pixel intensity. Adapted from (Xie *et al.* 2013, Hablitz *et al.* 2018).

EEG activity arriving at the present view that deep sleep, characterised by high 4Hz power, is a key driver of the glymphatic system (*Figure 7g-h*)[137].

Glymphatic Drivers and Modulators

Apart from sleep, subsequent drivers, substances and states have been found to impact the glymphatic system. When CSF flow in the pial PVS was first identified using 2-photon it was suspected that arterial pulsations drove the flow and this was later confirmed with individual particle tracking in the PVS[91]. This process is termed perivascular pumping and is impaired in hypertension[91]. The consequences of alcohol consumption and alcoholism on the CNS and its development have long been studied and outlined consequences such as foetal alcohol syndrome and Wernicke-Korsakoff syndrome[138,139]. The effects of alcohol have also been studied in the context of glymphatics and show that while high doses of alcohol (1.5g/kg) impair the glymphatic system, low doses (0.5g/kg) in fact have the opposite result and increase glymphatic activity[140]. Two independent groups have studied the impact of exercise on glymphatics[141,142]. Voluntary wheel running in mice improved glymphatic function in the awake state, increased AQP4 expression and polarisation and enhanced the clearance of Aß[141,142]. Biological sex in young, adult and aged mice was found to incur no differences in glymphatic function[143]. MRI investigation of a mouse model of type-2 diabetes demonstrated a 3-fold reduction in the clearance of tracer from the hippocampus[144]. Animals injected with lipopolysaccharide exhibited significantly lower PVS flow and penetration into the neuropil[145]. Finally, advancing age generates a decline in the efficiency of exchange between the SAS and the neuropil, impairs Aß clearance up to 40%, and results in widespread loss of AQP4 polarisation[134].

Insights from Neurodegenerative Mouse Models

Along with strong genetic associations, one of the greatest risk factors for developing Alzheimer's disease (AD), is advanced age. In keeping with this, a consequence of time is degradation, it is an inevitability, but it might be possible that such degradation could be mitigated to some degree. Since the first glymphatic paper showed that the system is capable of clearing Aß, subsequent glymphatic studies in AD rodent models sought to understand this, if indeed possible[15]. The idea is simple, enhancing glymphatic function in early life, across the lifespan, to help reduce waste accumulation, in this case Aß and tau, and potentially extend the onset of dementia, akin to servicing a car pre-emptively instead of waiting for it to break down before seeking resolution. However, a therapeutic agent is yet to be developed to provide sustained glymphatic enhancement. Instead, studies have focused on understanding the relationship of AD, Aß, tau and the glymphatic system. The KO of AQP4, which has been established to impair glymphatic function, in APP/PS1 mice exacerbated cognitive deficits and lead to significantly worse performance on the Morris water maze paradigm[146]. In addition, mice experienced increases in Aß accumulation in both the cortex and hippocampus, as well as a higher density of

cerebral amyloid angiopathy (CAA) (*Figure 8a-b*). APP/PS1 mice without AQP4 KO exhibited significant reductions in AQP4 polarisation[146]. In keeping with this, pre-injection of Aß in the CM of healthy mice, followed by CSF tracer injection was

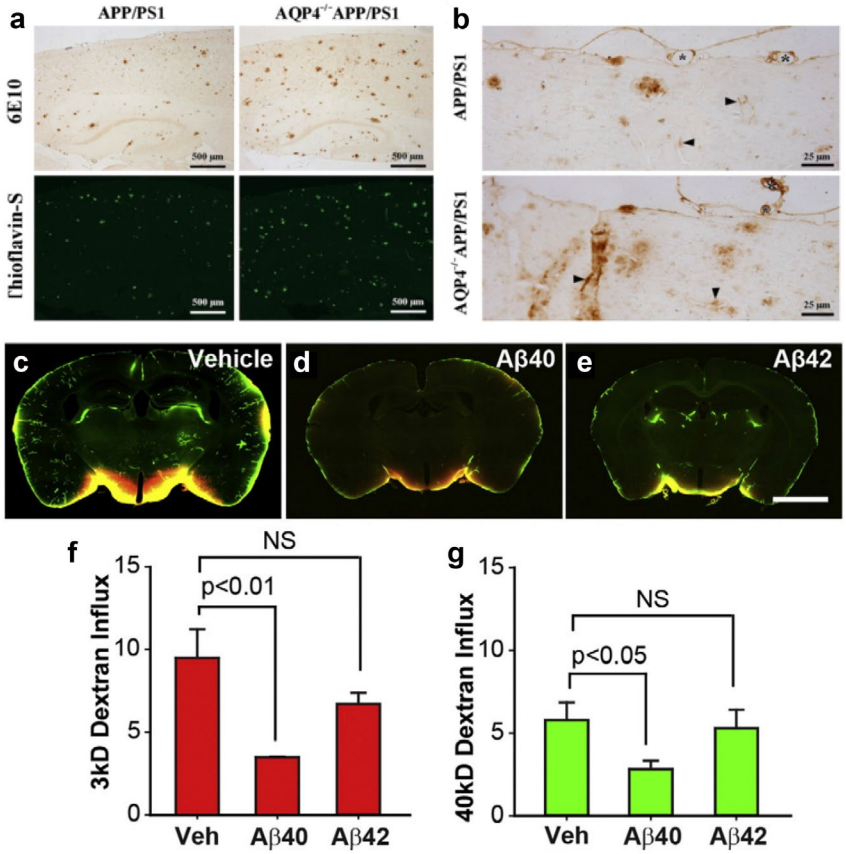

Figure 8 • Alzheimer's Mouse Models and Glymphatic Function
a) Representative images from APP/PS1 and APP/PS1 AQP4 KO mice showing enhanced amyloid plaque deposition in AQP4 KO, with 6E10 and Thioflavin-S stainings. **b**) Representative images from APP/PS1 and APP/PS1 AQP4 KO mice focused on penetrating vessels showing greater plaque deposition in walls of AQP4 KO. **c-e**) Coronal sections showing CSF tracer distribution in rodents pre-injected with vehicle, Aß1-40 or Aß1-42. **f-g**) Quantification of CSF tracer intensity in rodents pre-injected with vehicle, Aß1-40 or Aß1-42 where Aß1-40 exhibit significantly reduced tracer intensities. Adapted from (Xu *et al.* 2015, Peng *et al.* 2016).

sufficient to impair subsequent tracer distribution conveying that Aß acutely antagonises glymphatic function (*Figure 8c-g*)[147]. Interestingly, another study using the APP/PS1 AQP4 KO found that in the absence of AQP4, increased microglial activity helped to mitigate the impact of reduced glymphatic clearance, with subsequent microglial depletion adequate to severely enhance Aß deposition[148]. In 2015 it was affirmed that the glymphatic pathways could also clear tau, and that this clearance was impaired in a closed skull moderate TBI mouse model[149]. The impact

of tau has been studied in more detail in a mouse model that develops tau neurofibrillary tangle pathology, rTg4510[150]. Heterogenous deposition of tau was observed across the cerebrum and regions with the highest tau expression exhibited the greatest impairment in the clearance on intraparenchymally injected proteins[150]. Similar findings were observed concerning glymphatic tracer influx after gadolinium injection in the CM. This further correlated in significant reductions in AQP4 polarisation in brain regions most burdened with tau. Taken together these data illustrate that while impaired glymphatic function may aggravate cognitive decline and AD pathology, so too does the natural progression of the disease in these models aggravate glymphatic function and perturb the glymphatic microarchitecture.

Shortcomings of Rodent Models

The implication of the glymphatic system in the context of AD, and its idealisation as a future therapeutic target to ameliorate AD pathology convey that it is a system that is desired to be better understood in the context of the human brain, which some researchers have and are currently working on, and will be unpacked in the next section. However, the fact that it is seen as a candidate target for therapies means that all that has been learned from rodents should be put into context of the end goal, which is understanding these phenomena in humans. Although the existence of the glymphatic system is presumed to be the same in organisms of increasing complexity, and its macroscopic features have been demonstrated in humans using MRI, the remainder of everything we currently know from CSF dispersion mechanisms to glymphatic manipulators comes from rodents, which could potentially differ in larger mammals. The fact is, glymphatic microarchitecture has not been unpacked in other mammals nor have any of the manipulations or glymphatic drivers been corroborated. The primary reason why these aspects might differ in larger mammals, humans included, is based on the fact that while rodents have a smooth, lissencephalic cortical surface, large mammals have an intricate folded neuroarchitecture, termed gyrencephalic[151]. The sheer size of the human brain and those of larger mammals might also require more advanced gylmphatic microarchitecture to facilitate their cleaning, moreover they could be prone to the effects of other forms of regulation apart from the cardiac driven perivascular pumping. These notions echo the need to expand the story of glymphatics to humans and other large mammals.

Humans and Large Mammals

Human Data

Up until 2015 the existence of the glymphatic system had been confined to mice and rats, until Eide and Ringstad carried out the first known human glymphatic experiment[131]. Gadobutrol was injected intrathecally via lumbar puncture at L4/L5

in a 27-year-old woman with suspected intracranial hypotension due to CSF leakage[131]. The patient then underwent MR imaging in a 1.5T scanner at baseline as well as 1 and 4.5 hours after intrathecal injection and exhibited increases in gadobutrol signal units across the brain at both time points (*Figure 9a*)[131]. Although now only a small part of the human glymphatic story these data confirmed free transport of the tracer and widespread distribution across the brain, indicating a conservation of the glymphatic system from rodents to humans.

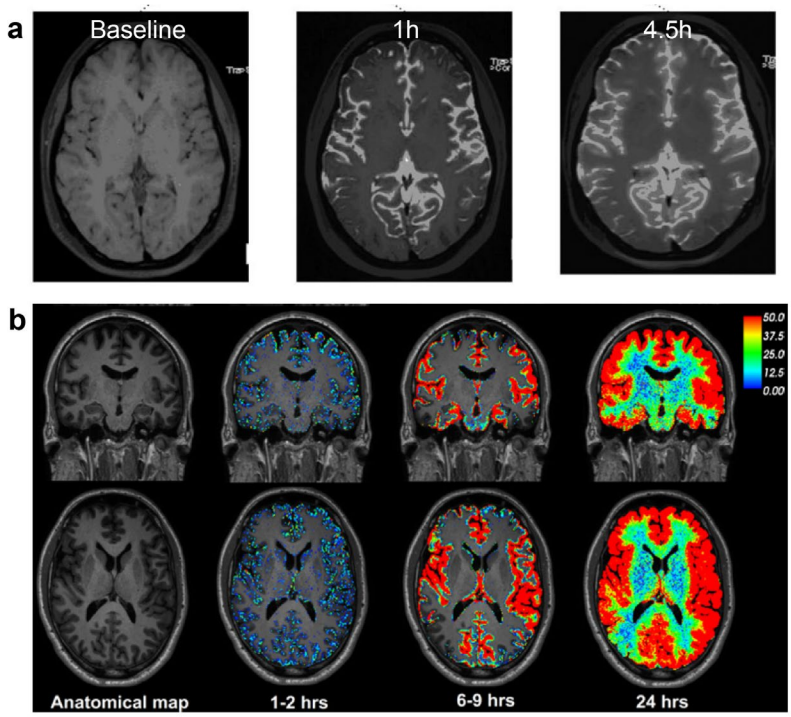

Figure 9 • Inception and Expansion of Human Glymphatic Model
a) Axial representative images of first human glymphatic experiment after intrathecal gadobutrol injection and MR imaging over 4.5h time course. **b**) Coronal and axial representative images in follow-up human glymphatic experiment with MR imaging over 24h time course highlighting the centripetal pattern of tracer penetration into the brain. Adapted from (Eide & Ringstad 2015, Eide *et al,* 2018).

This initial study in a single patient was followed up using a 3T scanner exploiting similar techniques in a large cohort of 15 normal pressure hydrocephalus patients and 7 reference subjects with suspected CSF leak[152]. Where the first patient was only imaged twice over 4.5 hours this experiment saw patients imaged several times over a 24 hour period. The extended imaging points from these data provided interesting insights in that brain tracer intensities appeared to peak overnight highlighting the role of sleep for glymphatic function and further validating the sleep-based data generated in rodents[152]. Tracer was also noted to propagate along

leptomeningeal arteries also linking back to the idea of perivascular pumping in rodents. Furthermore, in keeping with the notion that CSF efflux reaches cervical lymph nodes in rodents so too was this shown in humans, where tracer signal was found to peak in the lymph nodes after 24 hours, reflecting a more extended process[152]. Perhaps the most detailed description of human glymphatics came in 2018 when a cohort of patients with idiopathic intracranial hypertension and another cohort with idiopathic normal pressure hydrocephalus (iNPH) dementia received intrathecal tracer injections and were imaged at time points up to 4 weeks post-injection[132]. Results from this study are summarised as follows: 1) Primary tracer entry was identified in brain tissue adjacent to large artery trunks, reaffirming previous findings in humans and rodents, 2) Tracer enrichment in the human brain follows a centripetal pattern that occurs over the course of days, 3) iNPH dementia cohort experienced reduced tracer clearance which is proposed as a novel predictor to diagnose pre-clinical neurodegeneration (*Figure 9b*)[132]. Point 3 was also reaffirmed in a later study evaluating tracer clearance from the entorhinal cortex of iNPH patients[153]. Unfortunately the MR image resolution is limited to 1mm so details of perivascular contributions could not be assessed. Similar centripetal tracer distributions have been confirmed by other researchers also carrying out imaging at time points up to 79 hours after intrathecal injection[154]. In summary these data reaffirm that the glymphatic based influx and clearance of CSF that was described in rodents also exists in humans.

Shortcomings of Human Studies

Taken together, the aforementioned data represent the summary of our knowledge on the human glymphatic system, however it is also important to contextualise shortcomings and missing knowledge gaps. The first criticism of these human studies is that they are nearly exclusively carried out in subjects either suffering or suspected to suffer from a form of CNS pathology. Thereby, the results generated could be more representative of these pathological states than what would be seen in a healthy control. This is a difficult obstacle, at least for now, to overcome based on the need to carry out intrathecal tracer injections and the ethics concerning carrying these out in a healthy control. However, this should not detract from the notion that these data do in fact confirm the existence of glymphatic phenomena and reaffirm several of the observations seen in rodents. Secondly, although MRI in humans is sufficient to capture the macroscopic phenomena of glymphatic function, which arguably is the most important part, it still lacks the resolution to study the more detailed aspects of the system such as PVS flow and transfer of tracer from the PVS to the neuropil. In addition it is not possible to carry out detailed ex vivo investigations as in animal models as of course human brains cannot be extracted afterwards. This limits the validation of what is observed macroscopically with what might be occurring on the microscopic level such as AQP4 expression and distribution. Never the less, this ground breaking work continues to push the frontiers of the glymphatic field.

Findings from Primates

Although at the time not self-reported as a study of the glymphatic system, work in non-human primates (NHP) has emerged from a group in France investigating the consequences of sub-arachnoid haemorrhage (SAH) on CSF circulation[155]. This study was conducted using three adult *Macaca facicularis* and carried out in two parts. First, under physiological conditions, the animals received CM injection of DOTA-Gd and CSF circulation was evaluated. Follow up involved identical CM injection and CSF imaging, only in this instance the animals also underwent minimally invasive SAH through injection of autologous blood in the optic cistern. Under physiological conditions contrast agent was found to penetrate the neuropil as early as 20 minutes and reported after 2 hours to have penetrated most of the brain, save the deeper structures[155]. After SAH brain wide tracer penetration was reduced, most notably in anterior regions near to the SAH location. Interestingly, ex vivo processing and advanced light microscopy revealed a PVS localisation of fibrin, indicating autologous blood not only accrued at the surface but was also carried along PVS pathways within the neuropil[155]. The nature of CSF based penetration of the neuropil in this study is in keeping with both rodent and human findings and is itself a valuable addition to the field of glymphatics by confirming macroscopic glymphatic phenomena in an intermediate species. However, important ethical questions have arisen in recent years surrounding the use of NHP's for research. This makes an expansion of glymphatic work in NHP's less likely and echoes the need to establish a more ethically acceptable intermediate model to study the glymphatic system.

Pigs as a Model

Pigs have been widely used in research areas such as toxicology, diabetes and experimental surgery, attributable to their considerable semblance with human anatomy and physiology, but only recently have they emerged as a valuable model in the field of neuroscience[156–159]. Where before commercially produced pigs were exclusively utilised, the interest in pigs as a model has now led to the generation of standardised laboratory pigs, which are advantageous over primates both on ethical and economic levels[159]. This lead one group to generate a double transgenic AD pig model expressing both amyloid precursor protein (APP) and presinilin-1 (PS1) mutations in Gottingen mini pigs[160]. More recently a genetically modified pig was used as a donor for the first porcine-to-human heart transplant[161]. Despite the development of advanced genetic pig models, agricultural animals are still preferred due to their lower price point. However, when compared to rodents pigs are more costly to acquire and house as they need more space, and laboratory housing is generally limited. With the expansion of pig use in neuroscience several stereotaxic frames have been developed in conjunction with stereotactic atlases and as of now pigs have been used in a wide array of imaging studies investigating pathologies

such as TBI, stroke and Parkinson's disease[162–168]. A prime interest in the use of pigs in the field of glymphatics is based on their gyrencephalic brain structure, which more closely relates to human neuroanatomy than the lissencephalic rodent brain (*Figure 10*)[151]. Although the macroscopic dynamics of the glymphatic system have already been demonstrated in humans they have been unable to dive into more microscopic investigations that can only be achieved in animals. Thus, the pig could prove to be a valuable model in expanding our knowledge of the glymphatic system in an intermediate species.

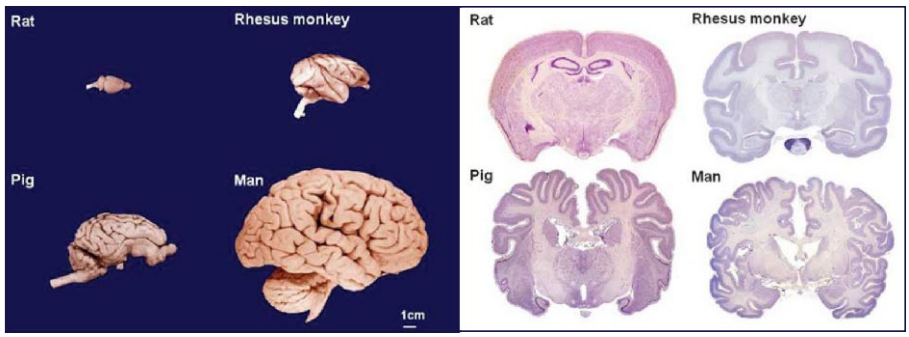

Figure 10 • Brain Size and Architecture Comparison Across Species

Lateral whole brain and coronal brain sections from rat, rhesus monkey, pig, and human, comparing size and cortical neuroarchitecture. Rat has smooth surfaced lissencephalic brain while rhesus monkey, pig and human have folded gyrencephalic brain. Adapted from (Howells *et al.* 2010).

The Glymphatic System and Neurodegeneration

By 2050, the elderly population is projected to double, and with this, increased incidences of neurodegenerative diseases (NDD) are expected, and of all NDD's, AD remains the most prevalent[169–171]. Although pathological processes are continually re-evaluated and effective therapies remain elusive the pathophysiology surrounding AD is fixed on aberrant APP processing and accumulation of Aß, in conjunction with the development of tau-based NFT's[172–175]. The ability of the glymphatic system to clear both Aß and tau from the rodent brain has highlighted the system as a potential therapeutic target to enhance the clearance of these metabolites to help prevent neurodegeneration[15,149,150]. Yet, these findings remain limited to rodents, who also exhibited great promise with several of the AD antibody trials, which subsequently failed to prove effective in humans[176,177]. Other factors resulting in links being made between the glymphatic system and neurodegeneration are sleep and the loss of AQP4 polarisation with age[134,178–180]. The importance of sleep for normal glymphatic physiology has been described previously in detail, but the link here is made based on the observation of a bidirectional relationship between sleep and neurodegeneration[181–184]. Reduced duration and poor quality of

sleep are frequently reported both in AD and PD patients[185,186]. What is difficult to disentangle is whether the pathophysiological consequences of neurodegeneration lead to these sleep impairments or whether the sleep impairments themselves contribute to the neuropathology. Simply based on the known facts about glymphatic function it would stand to reason that sustained impaired sleep would aggravate Aß aggregation in the brain and thus hasten the neurodegenerative process, however this is yet to be empirically demonstrated in humans and furthermore Aß loads and plaque deposition do not always correspond with disease severity[187–190]. Another link worth mentioning is that of AQP4, which is known to be a crucial piece of machinery for normal glymphatic function. While aged rodents have exhibited reduced AQP4 polarisation and glymphatic function, studies in humans have shown that AQP4 expression is altered after sleep deprivation and that certain AQP4 single nucleotide polymorphisms have been associated with poor sleep quality[134,191,192]. Neurodegeneration itself is a highly complex phenomenon that is currently studied from a vast array of viewpoints, of which brain clearance and glymphatics only represents one. The truth surrounding AD pathophysiology and its prevention is far more intricate than the proposed brain clearance preventative methods put forward in the glymphatic model. Yet, all this warrants is further exploration of the system in the context of neurodegeneration so we might reach a higher truth of how exactly the system may be involved in neurodegenerative physiology. A topic left all but unaddressed in this regard is that of "waste", i.e, Aß, recirculation. While it is accepted that the glymphatic system clears Aß from the neuropil back to the CSF reservoir, it remains unclear how this waste is segmented, if at all, to prevent recirculation. It seems unlikely that such segmentation would be possible, but at the same time it would not make sense for the brain to flush itself once more with waste that had just been cleared. As such, this idea is one of intrigue worth exploring in the glymphatic system in the context of AD, perhaps even in a large animal model.

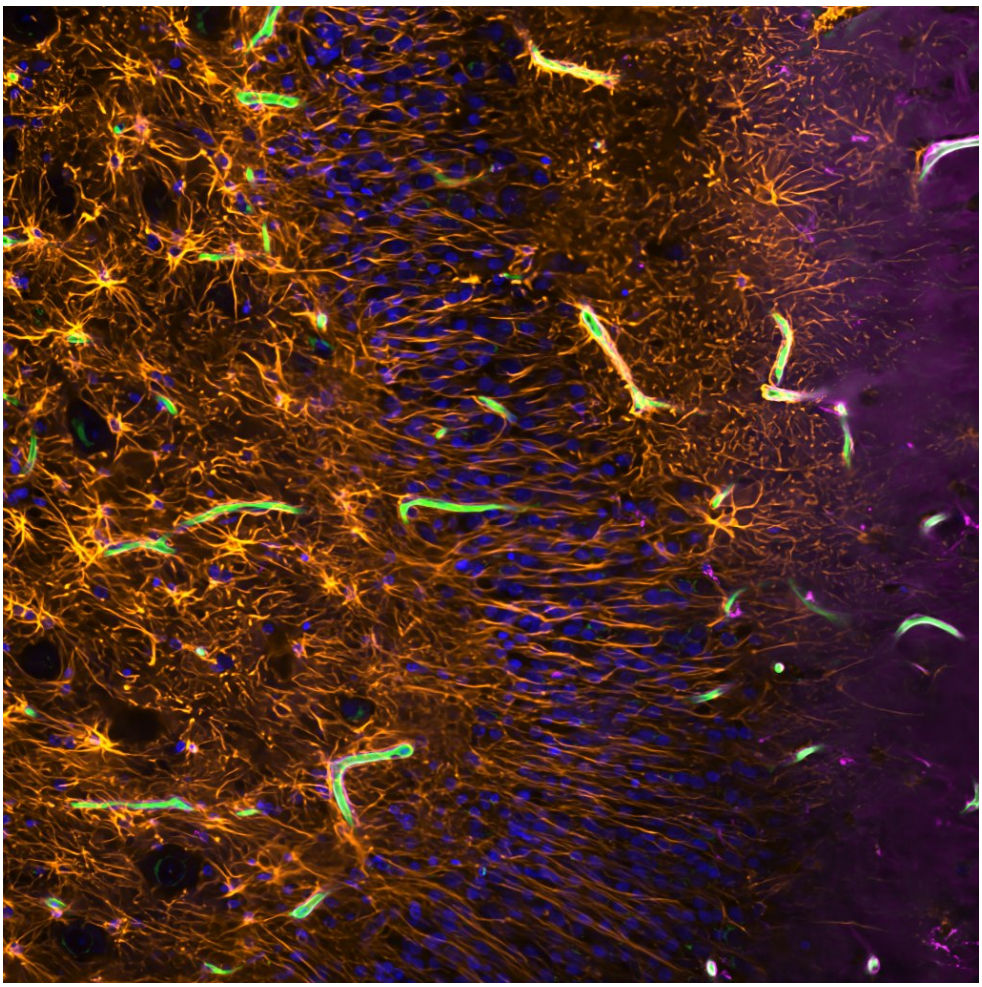

Aims of the Thesis

The primary focus of this thesis was to study the glymphatic system in a large animal model with a gyrencephalic brain. Ultimately, this began with translating the CM injection surgery from rodents to pigs, one of which presented with a subdural haematoma (SDH) and was explored as a case report. Once the porcine glymphatic system was characterised and the surgery proved repeatable it was then possible to explore the glymphatic system in the context of AD pathophysiology by introducing Aß in the CM. Finally, to study PVS transport in vivo an experimental porcine cranial window approach was adopted.

I. Develop a cisterna magna injection surgery for pigs.

II. Investigate how the glymphatic system described and characterised in rodents differs/is similar in the large gyrencephalic brain.

III. Explore of the consequences of a subdural haematoma on glymphatic function.

IV. Determine how amyloid-beta (re)-circulation in the CSF impacts the glymphatic system.

V. Develop a porcine cranial window technique to study perivascular transport in vivo in a large animal.

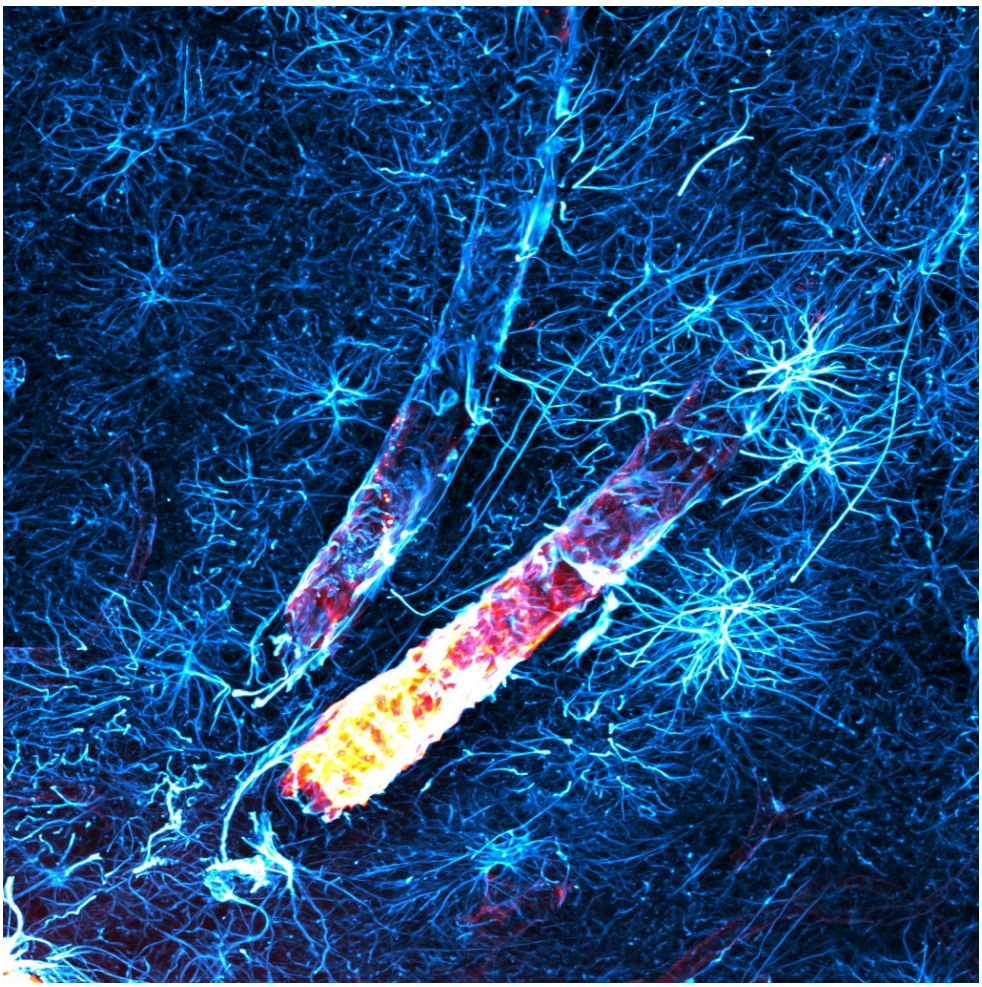

Summary of Results and Discussion

Paper I • Establishing a Porcine Cisterna Magna Injection Surgery

The glymphatic system is studied both in rodents and in humans by the introduction of a tracer in the CSF space. In the case of rodents this is achieved through CM cannulation, while in humans lumbar puncture is used[126,127,131]. Paper I of this thesis established a reliable protocol to introduce tracer into the CM of pigs in order to permit studies of the glymphatic system in this model organism[193]. The procedure itself is terminal with the animal euthanised upon completion in order to extract the whole brain intact and explore macroscopic and microscopic tracer distributions arbitrated by the glymphatic system.

The entire procedure is carried out under general anaesthesia using a cocktail of ketamine, fentanyl and midazolam. The animal is intubated and respiratory rate is maintained at 14 breaths per minute. Additional monitoring of vital signs is carried out including heart rate, blood pressure, temperature, partial pressure of oxygen and partial pressure of carbon dioxide. Anaesthesia is adjusted throughout the procedure according to fluctuations of the animals vitals.

Surgery begins with resection of the skin overlying the back of the head and neck. Each of the three muscle layers, trapezius, semispinalis capitus biventer and semispinalis capitus complexus are dissected in the midline and severed from origins along the occiput (*Figure 11a*). Muscles are retracted using two sets of self-retaining retractors (*Figure 11b*). The cisterna magna can then be palpated at the base of the skull while flexing the neck of the animal (*Figure 11c*). An 18G cannula is inserted approximately 3-5mm into the CM and fixed in place with superglue and/or dental cement (*Figure 11d*). Tracer can then be injected through the cannula, either by hand or with a micro-infusion pump, at desired rate to a desired volume. Tracer can be left to circulate for the desired amount of time, in this case two, four or six hours, after which the animal is euthanised by intravenous pentobarbital injection and the brain is then rapidly extracted and fixed in 4% formaldehyde. After overnight fixation whole intact brains can be imaged at dorsal, ventral and lateral aspects to investigate surface CSF distributions (*Figure 11e*). Following whole brain imaging, 10mm thick coronal sections are cut and left once more overnight in 4% formaldehyde for fixation, after which whole slices can also be imaged to

investigate macroscopic tracer penetration (*Figure 11g*). Higher magnification images help to identify periarterial and perivenous pathways (*Figure 11f*). To investigate microscopic aspects of the glymphatic system with confocal microscopy, immunohistochemical (IHC) staining can be carried out against AQP4 and glial-fibrillary acidic protein (GFAP) to identify PVS and tracer localisations (*Figure 11i-j*). To identify microscopic periarterial routes of CSF influx arteries can be identified using smooth muscle actin (SMA) (*Figure 11k*).

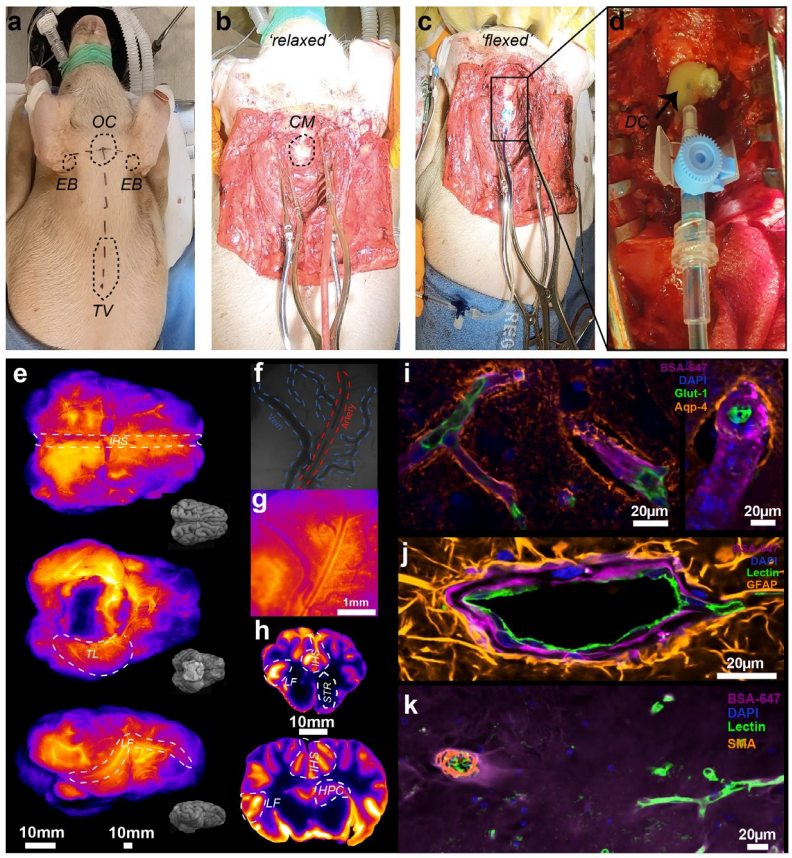

Figure 11 • Porcine CM surgery with macroscopic and microscopic glymphatic imaging readouts.
a) Pig prepared prior to surgery and marked where dermal incisions take place, starting from occipital crest (OC). **b**) Head in relaxed position with trapezius, semispinalis capitus biventer and semispinalis capitus complexus retracted exposing cisterna magna (CM). **c**) Head flexed manually to increase access to CM for cannulation and injection. **d**) Close up view of cannula inserted into CM after injection and fixed in place with dental cement (DC). **e**) Dorsal, ventral and lateral brain surfaces, respectively, after fluorescent imaging, inset with structural white light images. **f**) Structural white light image of artery and veins on brain surface. **g**)Fluorescent image of (f) showing tracer distribution along surface artery. **h**) Macroscopic slices from anterior and posterior cerebral regions show two-dimensional tracer dispersion and distribution. **i**) Confocal images showing tracer in the PVS, bounded by lectin-stained endothelial cells internally and AQP4 on astrocyte foot processes externally. **j**) Confocal image showing tracer in the PVS, bounded by lectin-stained endothelial cells internally with astrocyte foot processes stained with GFAP, visible projecting to form an outer boundary. **k**) Confocal image showing tracer in the PVS around an arteriole stained for smooth muscle actin (SMA) with tracer also visible in and around surrounding brain parenchyma. CM, cisterna magna; DC, dental cement; EB, ear base; OC, occipital crest; TV, thoracic vertebrae.

The advantage of injecting in the CM as opposed to the ventricle is that it avoids any direct damage to the brain, which has been found to be a strong inhibitor of the glymphatic system[16,115]. Questions in relation to CM injection are frequently posed around the topic of raised ICP. ICP measurement of the animals used for our glymphatic studies was not carried out and thus there is no empirical data to comment on this outcome. However, it is possible to make extrapolations from previous studies. First, in rats the elevation of ICP during CM injection was found only to be transient and returned to baseline soon after completion of the injection[128]. Thus, the mainstay of tracer circulation was under normal pressure conditions. Secondly, to investigate the consequences of raised ICP on subsequent tracer distribution work was carried out in mice with dual cannulation. Through one cannula tracer was injected into the CM and through the other an equal volume of CSF was withdrawn, maintaining a constant pressure. Consequently, when tracer distribution from this injection paradigm was compared to single cannulation and injection alone no significant differences is CSF tracer distribution were identified[130]. In keeping with this, in order to identify which tracer volumes could be used in pigs such as not generate pressure-related confounding, tracer injection volumes from mice were translated to pigs based of brain weight. The average weight of an adult mouse brain used in a glymphatic experiment is 0.5g, and these mice received 10uL of tracer at a rate of 1uL/min. Prior to carrying out our first CM cannulation and injection in pigs we established that the size of pigs we would use, weighing approximately 50kg, had a brain weight averaging 100g, thus 200 times larger than that of the mouse brain based on weight[39]. Using brain weights to translate tracer volumes an appropriate amount of tracer to inject would be 2ml at a rate of 200μL/min. Instead, we were even more conservative and injected only 500μL at a rate of 100μL/min to help mitigate elevations in ICP[39].

As a key technique carried out in all the other studies presented in this thesis this method set important foundations for future work to study the glymphatic system in pigs.

Paper II • Investigating Glymphatic Pathways in the Gyrencephalic Brain

As alluded to previously, all of the knowledge concerning the microscopic aspects of glymphatic physiology came from rodents. The purpose of this study was to investigate the extent of conservation of the microscopic glymphatic machinery in the brain of a large mammal, as well as to supplement previously described macroscopic distribution patterns in humans.

Sulci are Upstream Distributors of CSF

Sulci are the deep folds in the gyrencephalic brain that increase surface area without increasing brain size (*Figure 12a*), and our data show that they are also important structures for upstream CSF distribution, acting as reservoirs to navigate CSF to PVS influx sites housed within their depths. Interestingly, not all folds investigated in the porcine brain appeared to have the same capacity for CSF distribution. Both the interhemispheric fissure and rhinal fissure (Sylvian fissure in humans), which are more complex, branched folds, exhibited the highest tracer intensities both at the surface level and in macroscopic slices (*Figure 12b-e*).

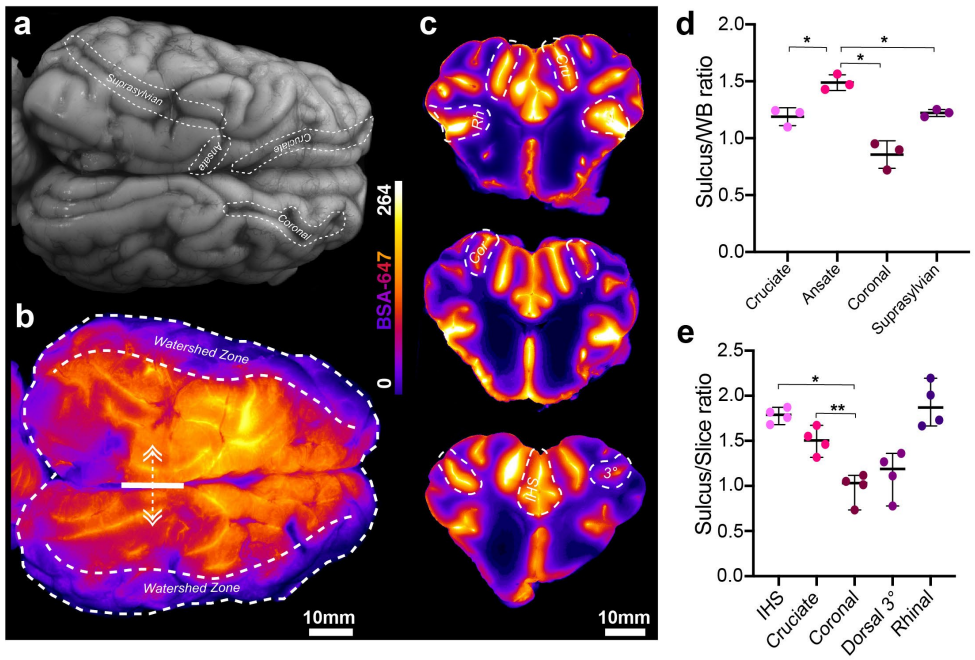

Figure 12 • Sulci Navigate CSF Distribution

a) Representative image of whole dorsal surface of pig brain under white light showing dorsal sulci. **b**) Representative image of whole dorsal surface of pig brain under fluorescent light showing tracer distribution and watershed areas. **c**) Representative images of macroscopic brain slices showing tracer distribution and sulci/fissures. **d**) Comparison of sulcus/whole brain intensity ratio amongst cruciate, ansate, coronal and suprasylvian sulci. **e**) Comparison of sulcus/whole slice intensity ratio amongst interhemispheric fissure, cruciate sulcus, coronal, 3° sulcus and rhinal fissure. N=3 or 4. *p<0.05, **p<0.01, ***p<0.001, ****p<0.0001 with ANOVA. Graphs represent mean ± SD. BSA-647, Alexa Fluor 647 conjugated to bovine serum albumin; Cor , Coronal; Cru , Cruciate; IHS, Interhemispheric; Rh, Rhinal; 3°, Tertiary.

Of the more simple folds, including the ansate, cruciate, coronal and suprasylvian sulci, tracer intensities decreased as a function of distance from the midline (*Figure 12d-e*). Since CSF distribution has been linked to the cardiac cycle this observation could be as a consequence of reduced arterial pulsations in regions located between large artery branches, so called watershed zones. In keeping with this, these regions

may be more vulnerable to waste accumulation as a consequence of reduced CSF supply and glymphatic function. High magnification epifluorescence and confocal imaging of 100μm thick cortical slices revealed the vast extent of the PVS network at the sulcul base. Notably, epifluorescence imaging only provided sufficient resolution to observe influx around primary penetrating arteries while a more complete extent of the network was identifiable under confocal (*Figure 13a-d*). Quantification of surface versus sulcul tracer intensities revealed consistently higher intensities in in the sulci (*Figure 13b*). Thus, taken together across a series of different imaging modalities, these data highlight the importance of the gyrencephalic brain folds for CSF distribution and emphasise how differences in neuroarchitecture may influence this outcome.

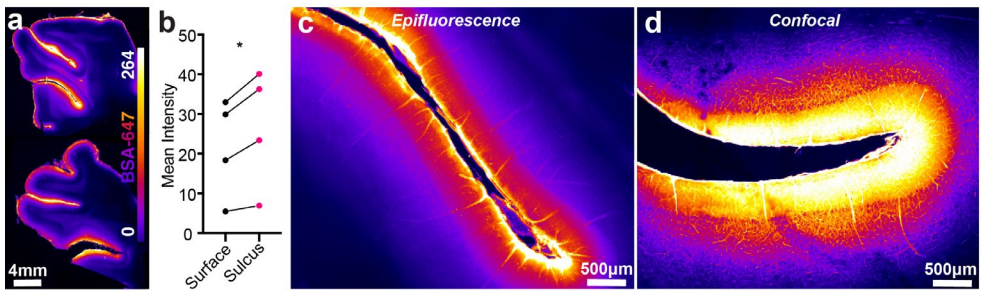

Figure 13 • Confocal Imaging Reveals Dense PVS Network
a) Representative images of vibratome brain slices demonstrating glymphatic influx. **b**) BSA-647 tracer intensity over exposed surface vs tracer intensity over of sulcul surface. **c**) Representative 20X magnification epiflourescent image of slice sulcus. **d**) Representative 20X magnification image of slice sulcus using confocal. N=4. *p<0.05 with paired t-test. BSA-647, Alexa Fluor 647 conjugated to bovine serum albumin.

PVS Architecture of the Porcine Brain

A pillar of glymphatic physiology rests in the transport of CSF to within the neuropil, through PVS, bound by astrocyte endfeet expressing AQP4. The patency of the PVS (network) itself has been a contentious issue owing to the fusion of the leptomeninges into a basement membrane at deeper sites. Whether the PVS are patent or not what is apparent is that they are important for CSF penetration to within the neuropil. Yet, in the context of glymphatics, PVS based CSF distribution and the PVS network have only been described in rodents. These structures were investigated in pig brain slices after in vivo CSF tracer injection and circulation. Pial arteries at the brain surface were identified with SMA IHC staining whereat CSF tracer could be seen around their borders (*Figure 14a*). One such large calibre pial and corresponding penetrating artery were imaged and showed CSF tracer penetration to within the neuropil, up to 160μm from the cortical surface, along the penetrating artery (*Figure 14b*). IHC staining for GFAP and AQP4 was used to

identify astrocytes and their endfeet, which form the outer boundary of the PVS (*Figure 14c-e*).

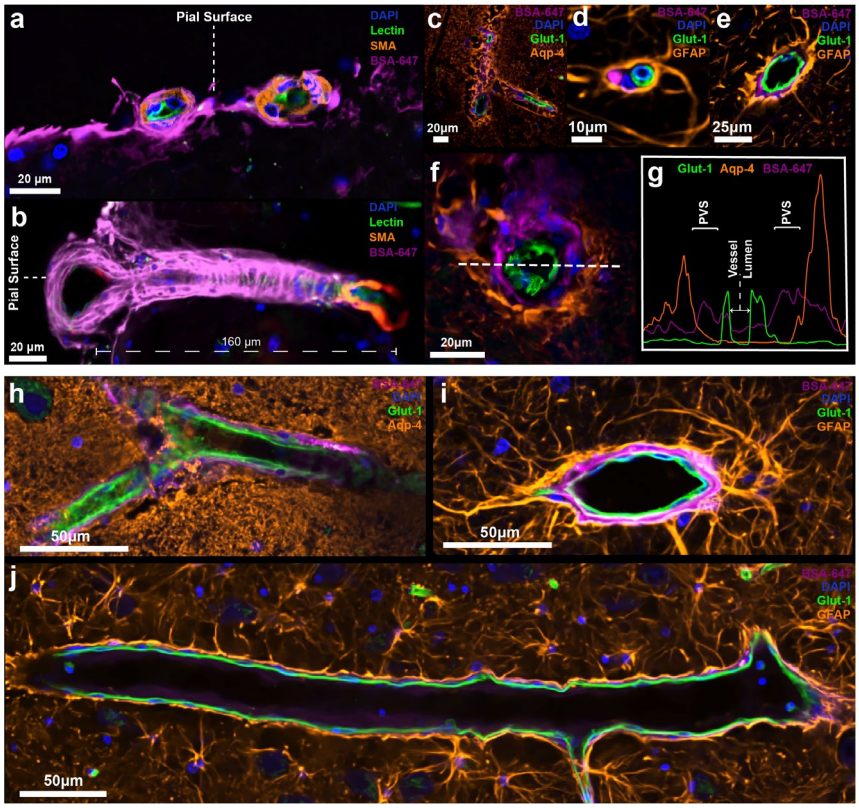

Figure 14 • Astrocyte Bound PVS is Maintained in Gyrencephalic Brain
a) Cross section through two pial arteries stained with SMA showing CSF-injected tracer surrounding vessels. **b**) Cross section through sulcul pial artery and and penetrating branch providing a pathway for CSF entry to within the neuropil. **c-e**) 20x magnification images of tracer in the PVS along vessels with AQP4 and GFAP stainings. **f-g**) Cross section through cortical vessel showing perivascular tracer ensheathed by AQP4 and corresponding intensity profiles of AQP4, BSA-647 and Glut-1 across the vessel cross-section. **h**) Representative image of PVS in hippocampus stained with AQP4, lectin and DAPI, with BSA-647 tracer. **i**) Representative image PVS cross section in hippocampus stained with GFAP, lectin and DAPI, with BSA-647 tracer. **j**) Representative image PVS longitudinal section in hippocampus stained with GFAP, lectin and DAPI with BSA-647 tracer.

High magnification confocal imaging within the cortex highlighted both longitudinal and coronal vessel sections, with CSF tracer visibly localised between the vessel wall and astrocytic endfeet (*Figure 14c-e*). This localisation can be appreciated through fluorophore line plots where three spatially distinct peaks are visible (*Figure 14f-g*). Apart from the cortex the hippocampus was also imaged at the same detail and there too were PVS carrying CSF tracer identified deep within the tissue (*Figure 14h-j*). These images show that the PVS identified in rodents also persist in pigs and that they provide a route of entry deep into the brain, even

subcortical structures. Thus, again, regardless of the patency or potential of the PVS, they do act as pathways for CSF to travel within the neuropil, in lissencephalic and gyrencephalic brains alike, and this is not just the case at the surface, but all the way down to a capillary level.

Glymphatic Microarchitecture: Pigs vs Mice

The unification of astrocyte bound PVS capable of CSF tracer distribution in rodents and pigs solidifies the idea of the conservation of the glymphatic system across species. However, what is of equal import is understanding what differences exist between these species, if any? To this end we carried out CM injections of the same CSF tracer in mice, at a comparable volume and identical concentration. Thereafter, whole mouse brains, and dorsal volumes of pig brain were optically cleared using the iDISCO+ tissue clearing protocol and imaged with a light sheet microscope[194]. Three-dimensional reconstructions from within the brain surface of each species showed a regular distribution of PVS across the surface, with those of the pig appearing more dense (*Figure 15a-b*). To quantify this, light sheet imaging data were reconstructed parallel to the brain surface such that the PVS would be coronally sectioned and appear under this low resolution as circles (*Figure 15c-d*). Analysis of both PVS density and area coverage revealed a 4-fold increase in pigs as compared to mice (*Figure 15e-f*). This emphasises that not only is the glymphatic microarchitecture present in the large gyrencephalic brain, but also appears to be more developed, lending insight into the likely architecture of the human glymphatic system.

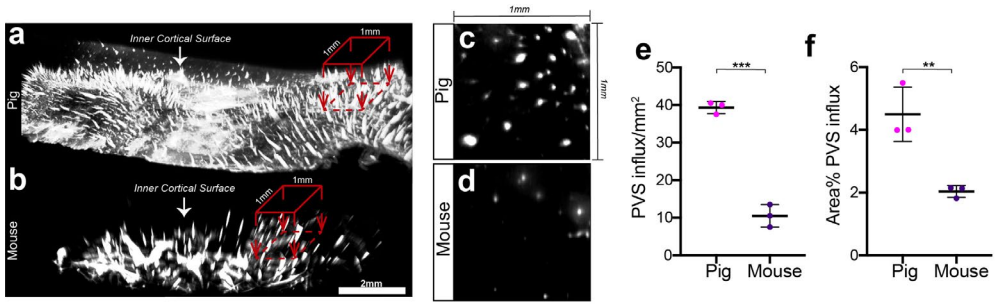

Figure 15 • PVS Network is more Developed in Pigs than Mice
a-b) 3D reconstruction of pig and mouse inner cortical surface highlighting perivascular influx sites. 1mm by 1mm region of interest is used to count perivascular influx sites projecting into the brain. **c-d**) Representative image of a cross section through perivascular channels parallel to cortical surface in pig brain (c) and mouse brain (d). **e-f**) Quantification of number of perivascular influx sites per mm^2 of cortical surface in pig and mouse brains (e) and percent of cortical surface area covered by perivascular influx in pig and mouse brains (f).

Paper III • Subdural Haematoma in Pig Leads to Global Impairments in Glymphatic Function: a case report

Subdural haematoma (SDH) is not something we readily sought to investigate in our glymphatic pig model, however, when animals repeatedly presented with this idiopathic pathology we felt it important that an investigation take place[195]. The first time we had seen an SDH was in one of the earliest pigs we had used, and it had been small haematoma, approximately 5mm × 5mm, that only amounted a localised CSF distribution impairment. Additionally, being the first presentation we thought nothing much of it. However, the animal of this case report was from much later study and presented with a large 15 × 35mm SDH overlying the fronto-parietal region (*Figure 16a-b*). We were unable to determine the timing of the SDH but from inspection it appeared sub-acute, and based on outcome must have been present prior to the injection of CSF tracer. Tracer delivery was deemed successful based on prior surgical experience and the observation of tracer in the hindbrain and spinal CSF space after brain extraction.

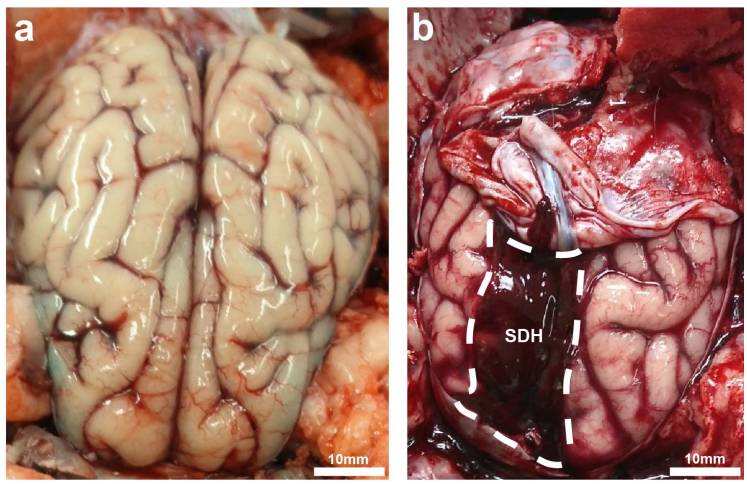

Figure 16 • Subdural Haematoma (SDH) in Pig Brain
a) Control versus **b**) idiopathic subdural hematoma (SDH) pig brains.

In this animal tracer was left to circulate for 3h and so we opted, once identifying the SDH, to carry out the normal tissue processing and imaging so as to be able to compare it to a unaffected animal that also underwent the same tracer CM injection and circulation time. Interestingly, when compared to the control animal the SDH pig exhibited adverse global impairments in CSF distribution rather than a local effect at the site of the lesion, as had been seen previously (*Figure 17a-d*). In order to better visualise the tracer distribution in the SDH animal, imaging exposure times

were increased by a factor of 4 and revealed that while overall tracer distribution was impaired the pattern across surfaces appeared unchanged (*Figure 17a-d*). In contrast, when comparing between surfaces, the dorsal surface was more affected than either the lateral or ventral (*Figure 17e-h*).

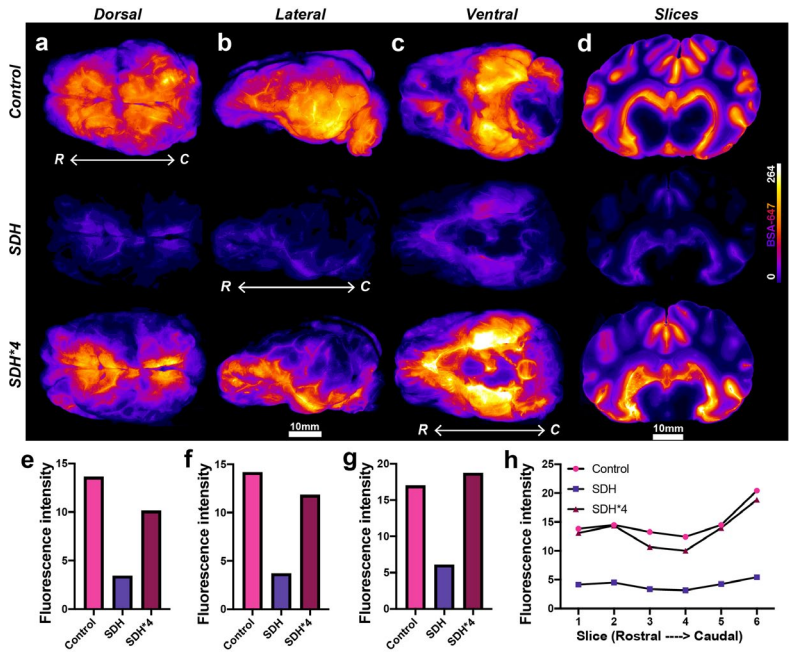

Figure 17 • SDH Generates Global Impairments in CSF Distribution
a-d) Fluorescent tracer (BSA-647) distribution along the dorsal (a), lateral (b) and (c) ventral surface of the brain and macroscopic slices (d) between control, SDH pig, and upon enhancing the signal exposure value by a factor of 4 (SDH*4) in relation to the control pig. **e-g**) Surface tracer intensities along (e) dorsal, (f) lateral, and (g) ventral surface of the brain between control, SDH and SDH*4 (normalized) conditions. **h**) Tracer intensity plots from 6 whole brain slices along the rostral-caudal axis. Intensity values are represented as arbitrary units. BSA-Alexa647, bovine serum albumin-Alexa647. SDH, subdural hematoma. R, rostral; C, caudal

Apart from macroscopic features we also wanted to investigate what had amounted on a microscopic level. Since astrocytes and AQP4 are important players in normal glymphatic physiology we carried out GFAP and AQP4 IHC stains to determine astrocyte integrity (*Figure 18a-f*). GFAP expression in tissue sections was reduced and further translated to a reduced AQP4 polarisation which has been shown to impair glymphatic function (*Figure 18g-h*). However, only having one of each animal means that this only has value in this case as an observation, not a quantification.

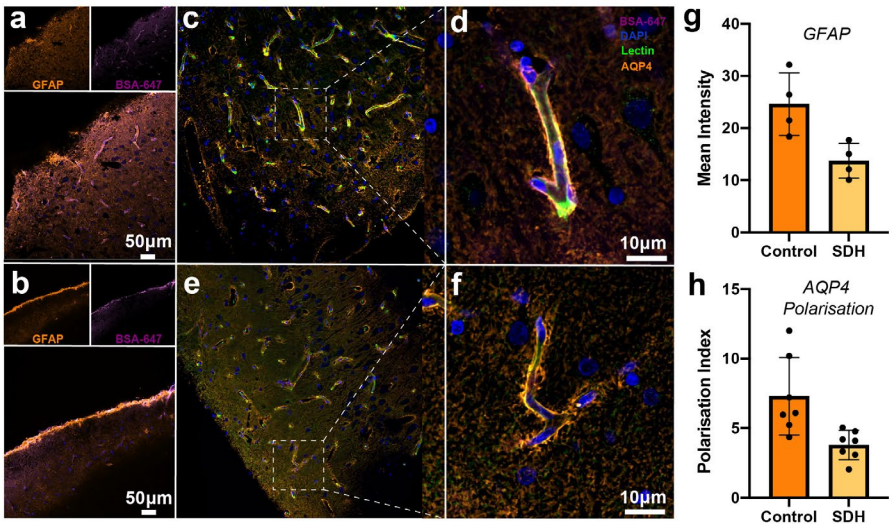

Figure 18 • Astrocyte Dysfunction in SDH
a-b) Representative images of GFAP immunostaining of control and SDH pigs respectively. **c-d**) Representative images of AQP4 immunostaining in control pig. **e-f**) Representative images of AQP4 immunostaining in SDH pig **g**) Quantification of mean GFAP intensity in control and SDH pig. **h**) Quantification of mean AQP4 polarisation in control and SDH pig.

Although opportunistic, this study held some interesting clinical relevance in that SDH is a common consequence of head trauma, which is itself a risk factor for AD[196,197]. Furthermore, undiagnosed SDH is frequent in the elderly population[198–200]. This case report shows that after SDH there is massive inhibition is CSF tracer distribution and glymphatic function, which itself may also prove to be a risk factor for AD due to a sustained period of impaired brain clearance. In terms of our research and animal welfare this raises important questions regarding the transport of large animals and injuries they may sustain while under transport. Although speculation, it stands to reason that if this animal was not braced correctly it would be prone to an acceleration-deceleration injury, a common cause of SDH due to rupture of bridging veins, in the case of a rapid change in velocity while under transport. Fortunately we work with the brain so we get to identify the SDH, its outcome and then exclude the animal from our study. However, this may be detrimental to those who work with other organ systems who might not be aware of an SDH which could potentially impact their data. In summary this case report poses important questions around large animal transport and questions what unknown glymphatic-based consequences might arise in patients impacted by undiagnosed SDH.

Paper IV • An arterial transmural entrapment system prevents amyloid recirculation into the brain.

Having successfully established a porcine model to study the glymphatic system the next step was to test it based on previous manipulations carried out in rodents, especially to make inferences on in clearance capacity in relation to Aß, which was established in the seminal paper[15]. While the glymphatic system has been found to clear a wide-array of metabolites from the neuropil including Aß, tau and lactate, research surrounding the recirculation of these metabolites once cleared to the CSF reservoir is lacking[15,32,149,150]. Effective waste management systems, like the CVS, are able to successfully segment waste. A prime example of this is the carrying of oxygen-rich blood by the arterial system, oxygen utilisation at tissues and subsequent carbon dioxide production, and finally clearance of carbon dioxide by the venous system. The linearity of the CVS makes this kind of clearance possible, but this form of waste segmentation in the CSF is not plausible. This being the case, the recirculation of waste once in the CSF appears an inevitability, the consequences of which would be of great interest to explore in the context of the glymphatic system, and more so if any CSF-based waste segmentation mechanisms might exist in the CNS to mitigate this.

To this end we carried out co-injections of CSF tracer (BSA-647), either with an artificial CSF (aCSF) vehicle or with amyloid-beta 1-42 HiLyte 555 (Aß1-42 555), in the CM of pigs and allowed for a 2 hour in vivo circulation time. Brains were then extracted, processed, and imaged using several advanced imaging techniques to examine the consequences of Aß recirculation for glymphatic function, and more specifically, Aß distribution pathways.

Acute Amyloid Exposure Globally Impairs CSF Distribution

After 2 hours of circulation of CSF tracer, BSA-647, with and without Aß1-42 555 whole brains were rapidly extracted and imaged at their dorsal, ventral and lateral surfaces. Quantification of surface BSA-647 revealed significantly lower values in the amyloid-injected cohort at all surfaces analysed, indicating that surface level influx of BSA-647 was impaired (*Figure 19a-e*). Imaging of macroscopic slices permitted analysis of BSA-647 values within the tissue and exposed significantly lower tracer intensities along the entire rostral-caudal plane (*Figure 19f-g*). Overall mean slice intensity was approximately 30% lower in the amyloid-injected cohort (*Figure 19h*). To further investigate the nature of this deficit tissue bounding sulci was sectioned and imaged at greater detail (*Figure 19i*). Not only were tissue tracer intensities significantly lower in the amyloid cohort, but it was also established that this cohort suffered from impaired transfer of tracer from the PVS to the neuropil

(*Figure 19j-k*). These data express that acute introduction of Aß1-42 555 significantly impaired glymphatic influx in the brain.

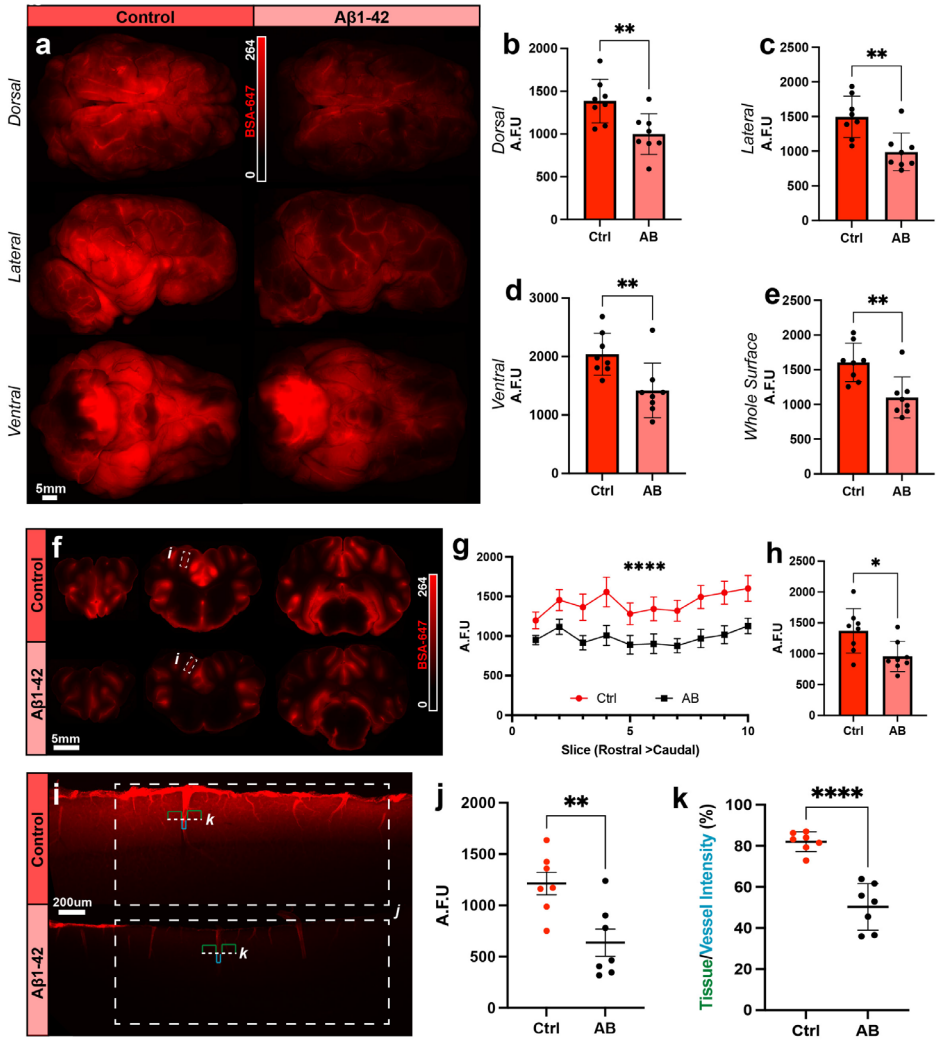

Figure 19 • Acute Amyloid Exposure Impairs Glymphatic Influx
a) Representative images of dorsal, lateral and ventral brain surfaces from control and Aß1-42 injected animals showing impaired BSA-647 distribution in amyloid group. **b-e**) Quantification of BSA intensity at dorsal, lateral, ventral and all brain surfaces between control and Aß1-42 injected animals. **f**) Representative cortical sections from control and Aß1-42 injected animals showing impaired BSA-647 glymphatic influx in amyloid group. **g**) Quantification of BSA-647 cortical section intensity in ten sections from rostral to caudal in control vs Aß1-42 injected animals. **h**) Quantification of total mean slice intensity between control and Aß1-42 injected animals. **i**) Representative high magnification images of the sulcul surface from control and Aß1-42 injected animals. **j**) Quantification of mean BSA-647 at surface and up to 1mm into the neuropil. **k**) Quantification of tracer transfer, i.e. glymphatic influx, from PVS to neuropil. N=8. *p<0.05, **p<0.01, ***p<0.001, ****p<0.0001. Graphs represent mean ± SD. Aß1-42 HiLyte-555, Amyloid beta 1-42 conjugated to Hilyte-555; A.F.U, Arbitrary fluorescent units; BSA-647, Alexa Fluor 647 conjugated to bovine serum albumin.

Aß1-42 Localises to Upper PVS Influx Sites

In order to better understand Aß distribution patterns, and how it contributes to reductions in glymphatic influx, this cohort was more closely examined.

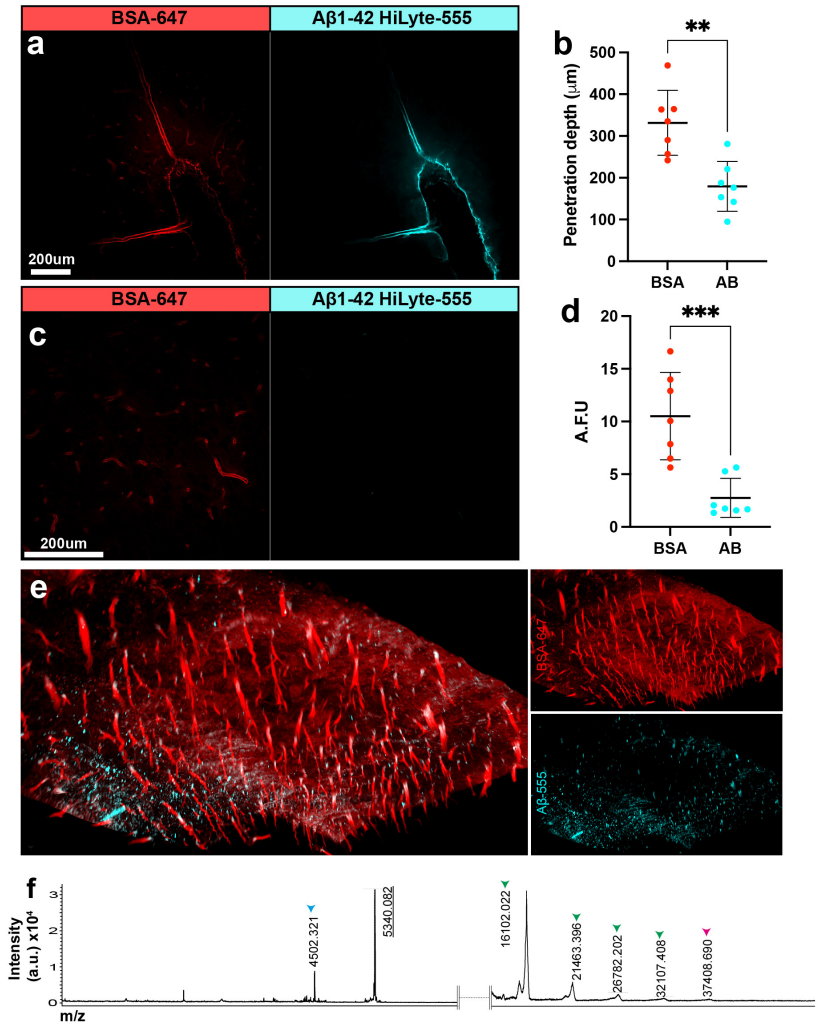

Figure 20 • Aß1-42 in the CSF aggregates at upstream PVS influx sites.
a) Representative images of a sulcus showing differential depth of penetration between BSA-647 vs Aß1-42. **b**) Quantification of tracer penetration depth along penetrating vessels for BSA-647 vs Aß1-42. **c**) Representative images approximately 1mm below surface showing BSA-647 in smaller PVS but absent of Aß1-42 **d**) Quantification of tracer intensities in deep region. **e**) Representative three dimensional reconstruction image from light sheet microscopy showing widespread Aß1-42 aggregation in upper PVS with consistent deeper BSA-647 penetration. **f**) Mass spectrometry readout of amyloid preparation showing single amyloid protein and fluorophore conjugate (5340.082), unconjugated amyloid (blue arrowhead) and amyloid oligomers (green arrowheads) up to amyloid septamer (red arrowhead). N=7. *p<0.05, **p<0.01, ***p<0.001, ****p<0.0001. Graphs represent mean ± SD. Aß1-42 HiLyte-555, Amyloid beta 1-42 conjugated to Hilyte-555; A.F.U, Arbitrary fluorescent units; BSA-647, Alexa Fluor 647 conjugated to bovine serum albumin.

Interestingly, inspection of the sulcul bases with confocal microscopy showed that BSA-647 moved significantly further along penetrating vessels than Aß1-42 555 (*Figure 20a-b*). In keeping with this, higher magnification images from approximately 1mm below the surface showed BSA-647 distributed in the smaller PVS network while Aß1-42 555 was absent at this depth (*Figure 20c-d*). In order to visualise this phenomenon in a larger volume of tissue, pieces of pig cortex were optically cleared and imaged with a next generation light sheet microscopy platform (*Figure 20e*). Similar observations were made across the volume where BSA-647 penetrated within the neuropil along PVS, while Aß1-42 555 appeared to aggregate at upper PVS influx sites (*Figure 20e*). The use of light sheet confirmed that this observation was not specific to individual vessels but was occurring on a much larger level across the brain tissue. The most curious aspect of this outcome is that Aß1-42 555 is approximately 13 times smaller than BSA-647, based on molecular weight, and that typically smaller tracers penetrate further into the neuropil. This could be explained, however, if Aß1-42 555 was aggregating prior to CM injection to form oligomers larger than BSA-647. Investigation of our co-injection preparation using mass spectrometry revealed that Aß1-42 555 was indeed oligomerising prior to introduction into the CSF, but was still at least half the size of BSA-647 (*Figure 20f*). This indicates that the accumulation of Aß in the upper PVS does not appear to be a consequence of protein size, but perhaps a more specific interaction.

Vessel Preparations Reveal an Elastin-based Amyloid Affinity

In early explorations of the amyloid-injected cohort a strong amyloid signal was observed at the large calibre vessels on the ventral aspect of the brain that form part of the circle of Willis. While BSA-647 was more evident at vessel borders, Aß appeared to be more dispersed across the vessel wall. Since these vessels are large enough to be seen comfortably with the eye we were inspired to perform circle of Willis isolations in order to image the vessels in greater detail. This began with imaging the whole structure, intact, on a stereoscope at higher magnifications than with the whole brain imaging, but this did not generate any greater insight (*Figure 21a*). To really explore these vessels in detail they were coronally sectioned into 50μm slices and stained for various structural markers including SMA and elastin. Initial images from confocal revealed distinct localisations between BSA-647, which adhered more to the outer aspect of the vessel, at presumed collapsed PVS, and Aß1-42 555, which appeared to localise to the inner elastic lamina (*Figure 21b-c*), each protein either side of the SMA dense tunica media (*Figure 21d-f*). Closer inspection of Aß1-42 555 also exposed a string-like distribution across the vessel wall (*Figure 21e*). These string-like structures were identified as elastin fibres and the inner lumen localisation of Aß1-42 555 was thus at the inner elastic lamina of the vessel, connected from outer aspects by elastic fibres running through the vessel

(*Figure 21g-h*). In this way it appears as if elastin forms a network from the outer part of the vessel, in contact with CSF, to the internal elastic lamina, which is in close contact with the endothelial cells. This is interesting in the context of amyloid clearance as it is well established that amyloid transporters in the form of lipoprotein related receptor protein-1 (LRP1) is expressed at vascular endothelial cells and is able to removed Aß from the brain. Thus, this pathway could in fact represent a transport mechanism by which to guide Aß in the PVS CSF to sites of clearance. To test whether this elastin-based distribution was specific to Aß1-42 555, or was

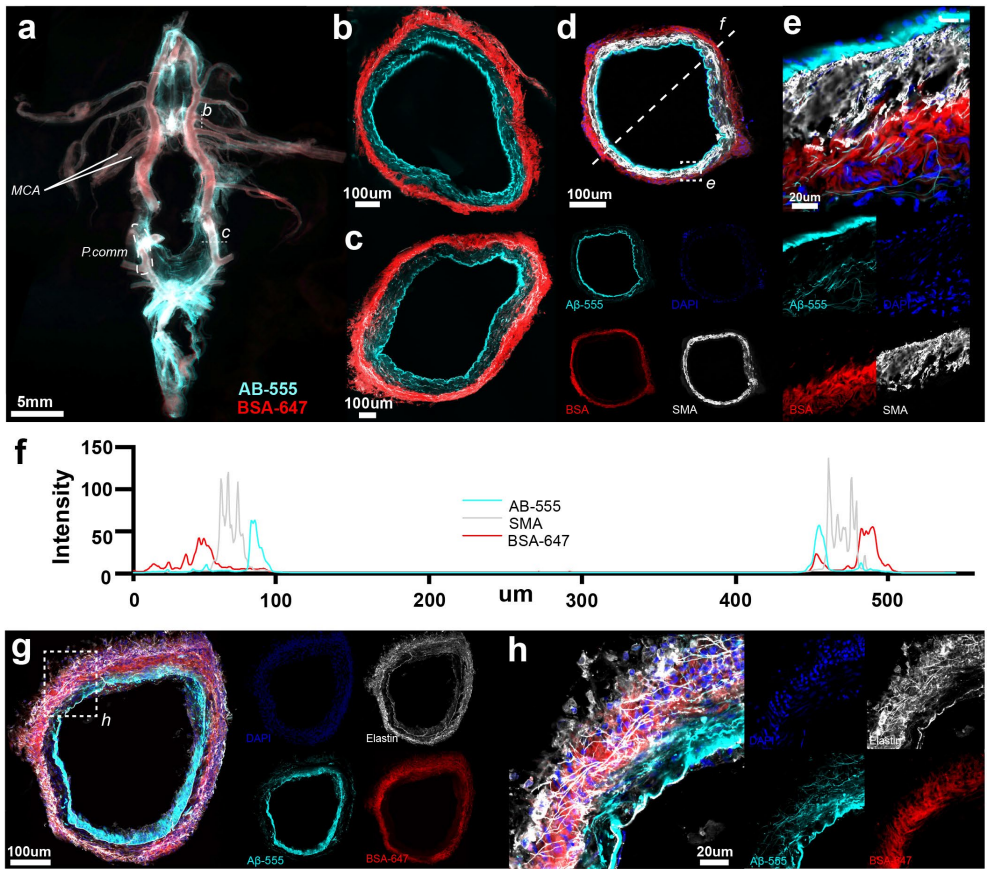

Figure 21 • Aß1-42 but not BSA-647 Localises to Vascular Elastin Elements

a) Representative macroscope image of whole dissected circle of Willis from Aß1-42 injected animal. **b-c**) Representative confocal images of 50um MCA and P.comm vessel sections from Aß1-42 injected animal showing BSA-647 and Aß1-42 HiLyte-555 localisations.). **d**) Representative image of MCA from Aß1-42 injected animal with immunohistochemical stain against smooth muscle actin (SMA) and dotted line along which fluorophore intensity is plotted. **e**) Higher magnification image from (d) of vessel wall where SMA (white) denotes tunica media of vessel with BSA-647 (red) towards the adventitia, and Aß1-42 towards the intima. **f**) Intensity plot from MCA of Aß1-42 injected animal showing differential peaks for fluorophore localisation across vessel wall. **g**) Representative image of MCA from Aß1-42 injected animal with immunohistochemical stain against elastin (white). **h**) Higher magnification image from (g) of vessel wall showing co-localisation of Aß1-42 (cyan) and elastin (white) at internal elastic lamina elastin fibres throughout vessel wall.

merely based on protein size, further co-injections were carried out with either Aß1-40 555 or 10, 000 MW dextran-555. The Aß1-40 yielded identical distributions to the Aß1-42, while dextran remain localised to the outer vessel wall, along with BSA-647 (*Figure 22a-c*), giving rise to the idea that this pathway from the outer vessel wall to the internal elastic lamina and endothelial cells may be specific for biologically relevant proteins, but further work would be needed to affirm this. Finally, to establish that the amyloid distributions were not an artefact of fixation further co-injection experiments were carried out with Aß1-42 555. After brain extraction vessels were freshly isolated, sectioned absent of fixation and imaged within 2 hours of the termination of the experiment. These preparations also revealed the same string-like amyloid distribution leading down to the internal elastic lamina (*Figure 22d-e*). To view this potential pathway in even greater detail vessels were processed, then imaged on a transmission electron microscopy platform. This imaging provided structural insight on this pathway which could be tracked running from the adventitia, between smooth muscle cells of the media, finally amounting connecting tributaries at the internal elastic lamina (*Figure 22f-k*).

Although these data only represent snapshots of a proposed dynamic process, what they do confirm is that there is a potential pathway running from the vessel adventitia down to the internal elastic lamina, confirmed with electron microscopy. Furthermore, Aß1-42 and Aß1-40, which were introduced into the CSF, robustly localised to elastin elements along this pathway, culminating at the internal elastic lamina. While we propose that this pathway could act as a funnel to help with amyloid clearance, we did not detect fluorescence signal from the endothelial cells. In order to confirm this transport, future experiments would benefit from CM injections utilising either Aß-gold conjugates that could be imaged at greater detail with electron microscopy or isotopes that could be quantified in the blood. While these facets require further work what does appear to be evident is that this pathway mitigates the recirculation of amyloid from the CSF into the neuropil. Thus, while the CSF may not be able to segment waste like the CVS, it appears that the large cerebral vasculature, in the form of pial and penetrating arteries, contribute to the entrapment of Aß through an elastin pathway in their wall, which all but prevents Aß moving along the PVS of smaller vessels and into the neuropil. In this way the brain may have indeed developed a means to overcome waste recirculation through this pathway. If this is indeed the case it would help to better understand the pathophysiology of CAA, which amounts nearly exclusively in arteries, and as such may amount in instances of increased Aß production whereby this pathway could be overwhelmed, leading to Aß deposition in the vessel wall.

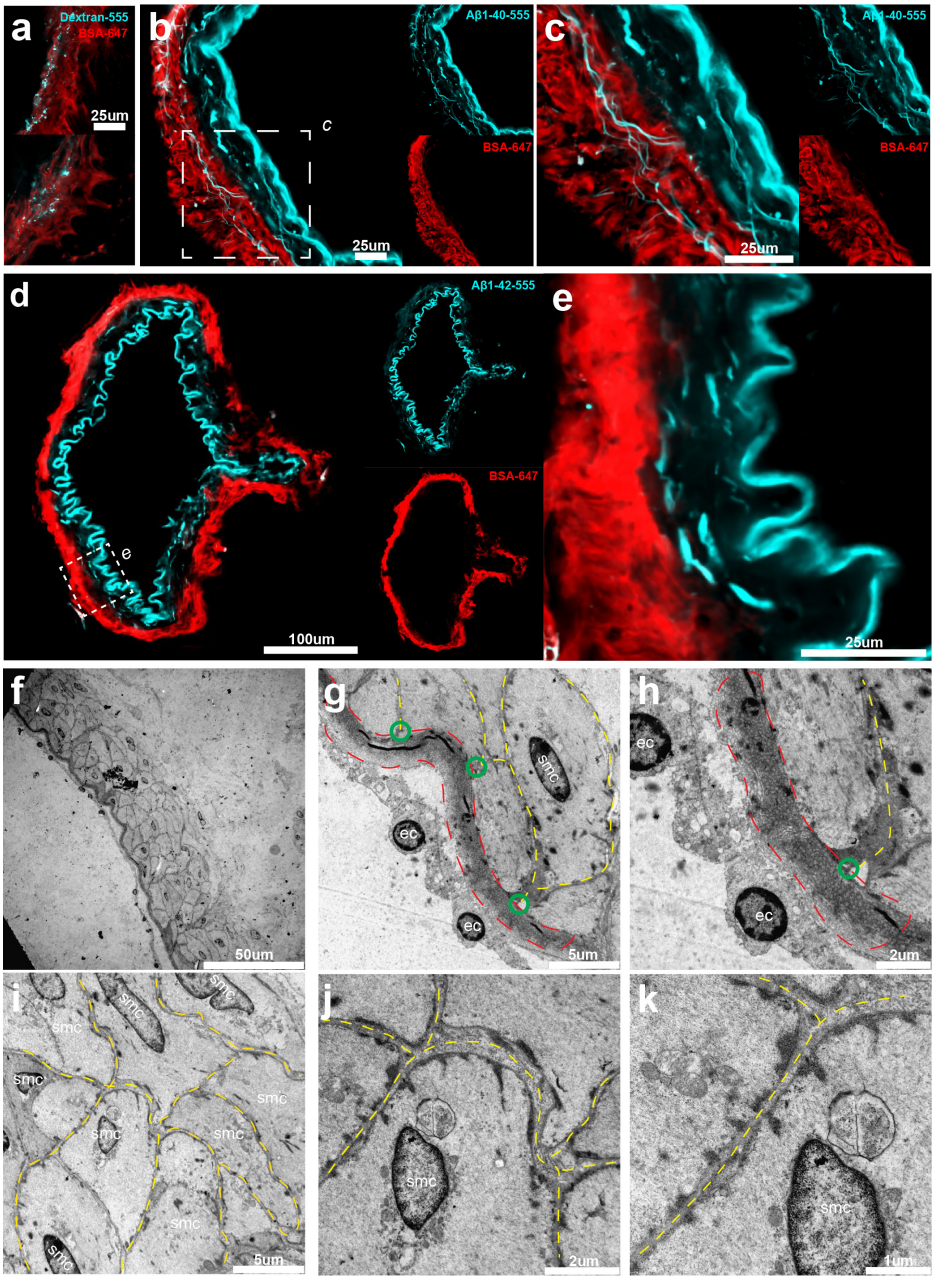

Figure 22 • Elastin Localisation Pathways are Specific for Aß
a) Images of MCA wall from dextran-555 co-injected animal showing dextran localises to outer wall with BSA-647. **b**) Image of MCA wall from Aß1-40 and BSA-647 co-injected animal. **c**) High magnification image from (b) showing BSA-647 and Aß1-40 distributions in wall. **d-e**) Images of MCA wall from fresh vessel preparations after Aß1-42 and BSA-647 co-injection. **f-k**) TEM images showing architecture of vessel wall with. Basement membrane pathways (yellow lines) from adventitia to internal elastic membrane (red ROI) with convergence sites (green circles). ec, endothelial cell; smc, smooth muscle cell.

Paper V • Live Imaging of Perivascular Transport through a Porcine Cranial Window

Although ex vivo tissue examinations permit detailed insights into the microscopic glymphatic machinery, they in fact represent only temporally isolated snap shots of a dynamic system. It is because of the system dynamics that it becomes important to study it in vivo. One of the challenges, identified early on, with using a large animal model like a pig, was that it would be difficult to move to in vivo brain imaging studies at a later stage. Where the mouse has a thin skull that lends itself to transcranial imaging, in the pig one is confronted with more than 10mm of cortical bone. Where MR scanners and coils have been specially designed for use with rodents there exist no such platforms for larger mammals, barring those designed for use for humans. Finally, where countless advanced light imaging platforms have been created for in vivo imaging in rodents, the development of similar platforms to use with large mammals has fallen behind.

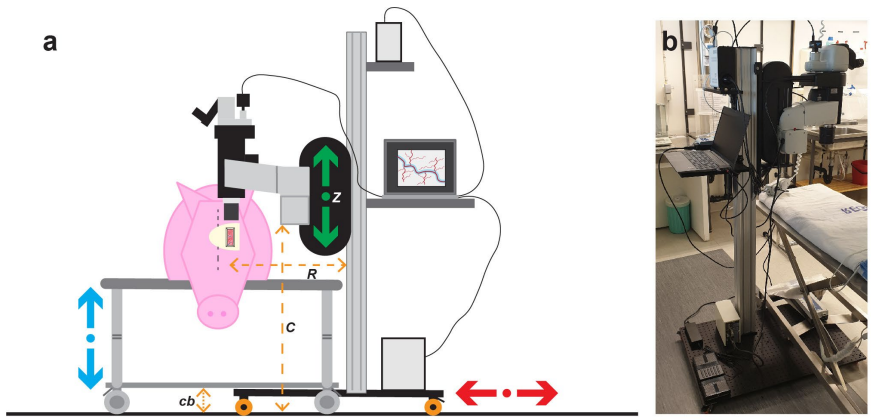

Figure 23 • Microscope Design for use with Large Animals
a) Schematic of design and setup of macroscope platform for live imaging in large animal based on variables including clearance (*C*), reach (*R*), clearance under surgical table (*cb*) and z-drive (*Z*). **b**) Real image of macroscope platform.

Thus, in order to carry out any in vivo imaging of CSF transport in the pig brain it was necessary to construct our own imaging platform. For this we chose to utilise the stereoscope with which we had carried out all whole pig brain ex vivo imaging, and also employed for in vivo imaging in rodents. The crucial factor needed for the microscope to be compatible with imaging in a live pig was its clearance (*C*), defined as the space, or z-dimension, between the stage and objective lens. On a factory bought platform this is approximately 30cm, and for our experiments we needed it to be in the 1.5m range to be able to fit a 50kg pig on a surgical table beneath. To achieve this, and still maintain a capacity for fine z-focus (*Z*), both the

microscope body and z-drive were mounted on a 2m high aluminium pole, itself bolted down to a heavy stage on wheels (*Figure 23a-b*). Other critical factors were that the body abutted far enough out to be able to reach the center of the surgical table on which the pig would be placed (*R*), and that the clearance of the base (*cb*) was low enough to be able to slide under the surgical table (*Figure 23a-b*).

For the surgical aspect, CSF tracers are injected into the CM as described in Paper I. To then generate the cranial window, first the midline of the dorsal skull, and C-shaped incision site are marked, after which the skin is reflected and the underlying periosteum is cleared (*Figure 24a-b*). A cranial window, approximately 10mm X 20mm is cut using a *Piezosurgery Flex* device, 4-5mm lateral of the midline, exposing the underlying dura (*Figure 24c-d*).

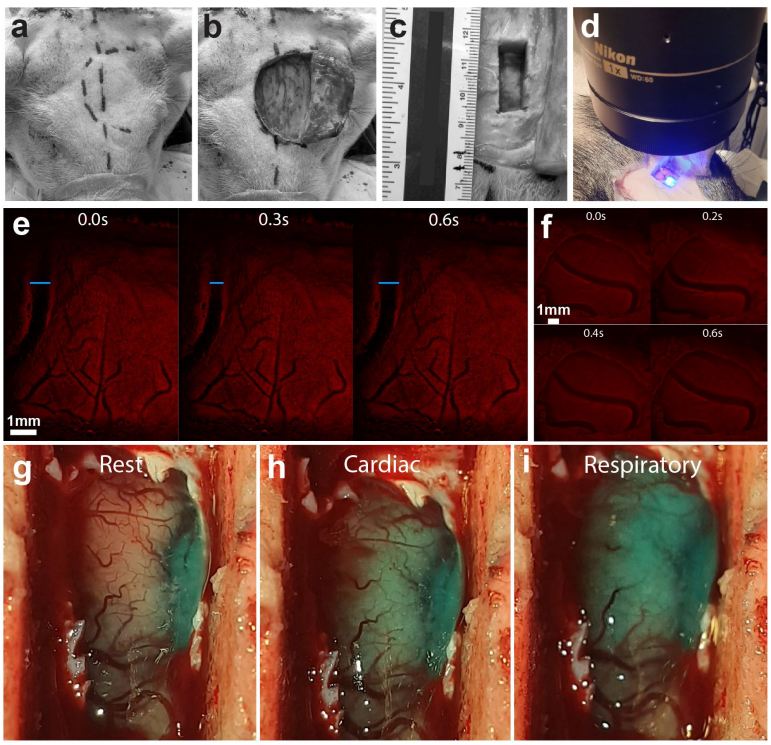

Figure 24 • Live Imaging through Porcine Cranial Window
a-d) Images showing process of cranial window generation and imaging. **e**) Live imaging of vessels through intact dura with 300ms temporal resolution. **f**) Live imaging of perivascular transport after dural excision at 200ms temporal resolution. **g-i**) Images of sub-arachnoid membrane expansion at rest, during systole, and during respiration.

Imaging can commence both through the dura, and after removal of the dura. Imaging through the dura at a temporal resolution of 300ms made it possible to capture perivascular transport in a large vessel, but limited dynamic resolution in smaller vessels due to dural thickness and opacity (*Figure 24e*). Excision of the dura

permitted better spatial resolution with a series of images acquired at a 200ms temporal resolution (5Hz) showing the motion of a single vessel in space and the CSF tracer in its PVS (*Figure 24f*). However, the cost of better spatial resolution after dural excision also led to increased brain motion which made imaging more challenging. Real time video recording of the cranial window highlighted substantial motion of the intact subarachnoid membrane, given rise by both cardiac and respiratory effects, of which respiration generated the greatest motion and CSF flux (*Figure 24g-i*). Interestingly, while cranial window generation in rodents impairs glymphatic function this was not the case in this study, leading to the idea that it may in fact be sub-arachnoid compromise that mediates these effects rather than skull or dura (*Figure 25*). While still few in number, what was observed here was that the cranial window animals appeared to have better CSF distribution than those with a closed skull. This could relate to an increased capacity for sub-arachnoid expansion and thereby generation of stronger CSF wave pulses, which could in turn lead to improved glymphatic function by increasing the upstream fluid driver, but more quantitative work will be required to explore this. In summary, although the imaging data acquired in these experiments was only rudimentary, and not yet quantifiable, it represents a proof of principle that we hope can be expanded upon in the future to study PVS CSF transport in a large animal in vivo. Furthermore, it has raised new questions concerning the role of the sub-arachnoid membrane and its rebounding capacity for translating respiratory and cardiac effects to CSF propagation.

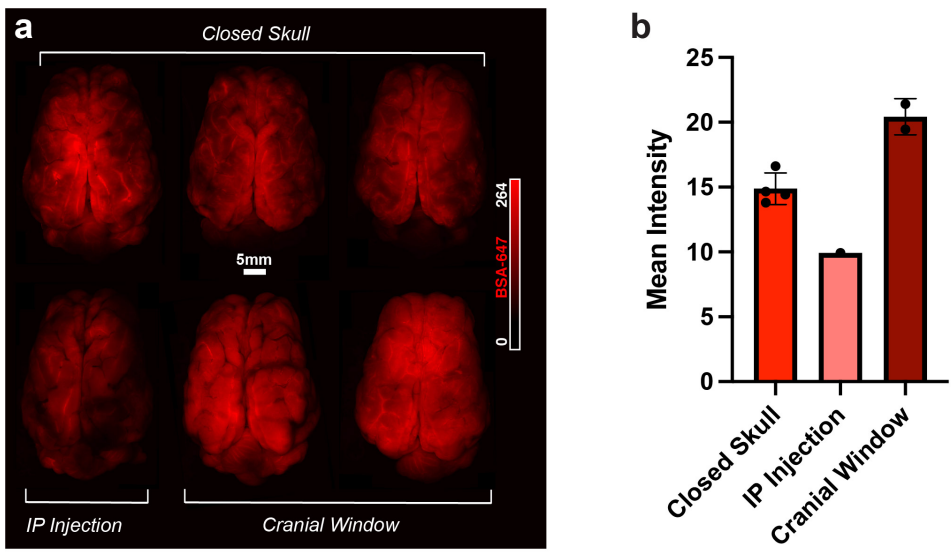

Figure 25 • Dural Compromise does not Impair CSF Distribution
a) Representative images of the dorsal cortex showing BSA-647 tracer distribution in three control animals, one animal that underwent an intraparenchymal injection, and two animals that underwent cranial window surgery.**b**) Quantification of BSA-647 intensity across dorsal cortex in closed skull, IP injection and cranial window animals.

black hole

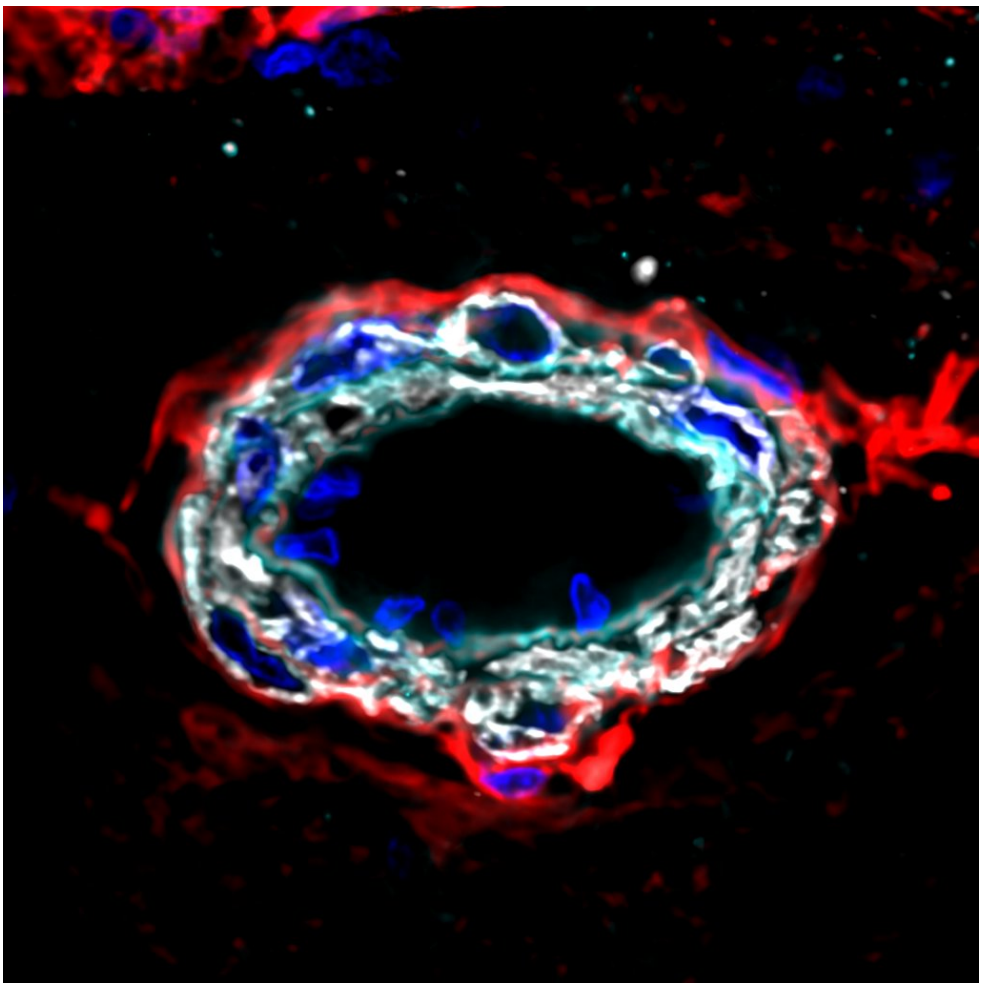

Concluding Remarks and Future Perspective

The focus of this thesis was to build knowledge on brain wide clearance system, which, at this point in time, has only received 10 years of foundational work. The main step the work contained herein took for the glymphatic field, was to generate a large animal model to study the system, such that we might gain greater insight into the evolution of this system from rodents to a large mammal, and thereby make inferences on the likely architecture of human glymphatics.

This began with the adaptation of the CM injection surgery (Paper I) employed in rodent models to our model of choice, the pig. From a standpoint considering brain size, brain structure, sleeping behaviour, ethical considerations and cost, the pig was deemed an suitable intermediate model to bridge the translation of glymphatics from rodents to humans[39,151,159,201]. However, when looking back and considering practical lessons learned from the translation of the CM injection surgery, the pig anatomy does deliver some challenges. As a rooting animal that readily digs into the ground with its snout while foraging, it has developed, thick, strong neck muscles. Moreover it lacks a conventional neck, where instead the head and thorax lie on the same plane perpendicular to the ground. This anatomy, coupled to the long, flat occiput result in the CM sitting very deep from the surface, approximately 15cm. In keeping with this, when the animal lies in the prone position, as is the case during surgery, the CM lies hidden between the base of the skull and the atlas. Only when the neck is flexed and space is generated between these structures can the CM be palpated and cannulated. For those who possess a porcine stereotactic frame this can be easily overcome, but in our case it required one person continually flexing the neck while another would both cannulate and inject. Despite this, after some years, the procedure itself has proved easily repeatable and permitted an expansion of our work in studying the glymphatic system in a porcine model. A means by which this procedure could be advanced would be to reduce the invasiveness of intrathecal tracer injection. This would permit longer time point tracer circulations as well as investigating glymphatic function in awake animals. This could be possible through placing the animals in a lateral recumbency position and attempting to pass a spinal needle through the soft tissue and into the CM. Due to the minimal invasiveness of this approach animals could be awoken after tracer injection and euthanised after tracer circulation whilst awake. However, the CM is

a relatively small target to hit from such a great distance making this a challenge, but this could be overcome with imaging guidance. Alternately a lumbar puncture approach could be adopted, but the ossification of the lumbar spinal ligaments in the pig also make this difficult.

The first characterisation of the glymphatic microarchitecture in pigs (Paper II), and any large mammal for that matter, was carried out after the translation of the CM injection surgery, and successful CSF-tracer injections in our two first pigs, *Harry* and *Charles.* Not only did these animals allow for the subsequent advanced imaging investigations that took place, but also the setting up of a whole new tissue processing pipeline in our lab. Aspects like tissue fixation and which antibodies would be compatible with pigs was an unknown, and with this tissue we were able to pilot these factors. The best way to fix a pig brain is the submerge the whole brain overnight in 4% PFA, cut macroscopic sections, and then fix them once more overnight. This is without forgetting that one may still image the surface aspects of the intact brain on a stereoscope before slicing commences. In terms of compatible antibodies, these are all listed with suppliers in the methods section. Along with tissue processing, these animals were also used to set up an imaging pipeline that served as a basis for everything that followed. Apart from these key foundational aspects the findings from these pigs lead to several important knowledge points concerning glymphatic physiology in a large mammal: 1) Brain gyrification plays a role in upstream CSF distribution with sulci acting as a highway for CSF dispersion, 2) CSF penetrates within the neuropil along PVS, patent or otherwise, and is traceable down to a capillary level, 3) Pigs have a 4-fold increase in PVS density as compared to rodents suggesting a significantly greater propensity for glymphatic CSF transport. With this research we have characterised the microscopic glymphatic pathways in the gyrencephalic brain and helped shed light on the likely architecture of human glymphatic structure, helping to bridge the glymphatic gap between rodents and humans.

The write up of a SDH in the context of porcine CSF distribution (Paper III) was an opportunistic find, but did itself raise some important ideas. Although we only wrote about one animal there have in fact over the years been three that presented with a SDH. While it is all but impossible to identify an aetiology behind these pathology it has stirred thought regarding large animal transport and whether these injuries may have mounted at this stage. The findings themselves however are also of merit in their own right as they give some insight into the consequence of SDH on glymphatic function, a model that would be difficult to setup in pigs. Although only a n=1 study what we found was that the presence of a large SDH was associated with global impairments in glymphatic function. This observation is of interest with regards to human SDH, especially undiagnosed SDH in the elderly which could further predispose them to compromised glymphatic function and brain clearance.

The interaction of AD, Aß and the glymphatic system was studied in the early glymphatic years (2012-2016) in rodents, but has not been a focus in recent years.

Moreover, the consequence of Aß recirculation by the glymphatic system was a topic not readily addressed. Thus, we sought to study the impact of Aß1-42 on the glymphatic system (Paper IV) in order to assess outcomes of waste recirculation and if waste segmentation in the CSF was possible, all in our porcine model. Acute exposure to Aß1-42 was sufficient to significantly impair the glymphatic system across the brain. Follow up experiments found that Aß1-40 was also able to elicit this outcome hinting at a general amyloid-based effect. Closer inspection of amyloid distribution revealed an aggregation in upper PVS. While initially considered a potential mechanical blockade, detailed vessel inspection revealed a distinct elastin based pathway from outer vessel borders to the internal elastic lamina, along which Aß was localised. Inert proteins of a similar size were not found along this pathway, highlighting either an amyloid specific, or biologically relevant protein transport function. Although an intramural periarterial drainage system has been described around vessels, it posits that waste is carried retrograde to blood flow in the basement membrane of arteries out of the brain, and examination of carotids at the base of the skull revealed no Aß[92]. Yet, on the basis of waste segmentation, we propose that this transmural pathway, clearly running from vessel outer borders to the lumen, may act as an amyloid-ensnarement system in large pial and penetrating vessels. In this way, Aß cleared from the neuropil to the CSF is in part prevented to recirculate into the brain by this ensnarement system, which may yet also act as a mediator to transport CSF-based Aß to endothelial cell transporters that can remove it from the CNS[202,203]. The potential physiology of this ensnarement system may also generate new ideas concerning the pathophysiology of CAA. While what is highlighted above are observations and hypotheses, further detailed examination of this system is required before any physiological claims can be made. Future work would benefit exploring the idea of this pathway for biologically relevant proteins to determine if this is Aß specific or could perhaps assist with the entrapment and clearance of other metabolites. To investigate the role of elastin in this process hemizygous elastin mice could undergo similar co-injections with amyloid to assess whether Aß entrapment still mounts or if in the reduction of this machinery Aß recirculates into the brain. Furthermore, these hemizygous elastin mice could be crossed with APP/PS1 mice, a mouse model of AD utilised in previous glymphatic experiments, to determine if the absence of elastin aggravates AD pathology. To determine if Aß in the internal elastic lamina is removed via endothelial cell-mediated transport a possible approach would be to carry out Aß-gold conjugate injections in conjunction with EM. Finally, to supplement this, mice with a knockout or knockdown of LRP1, a vessel wall transporter associated with Aß transport into the bloodstream, could be used to assess if, in the absence of LRP1, Aß aggregates in the vessel wall.

In an attempt to study PVS transport in vivo in a large animal we setup a porcine cranial window model (Paper V). This ties together the CM injection surgery with the generation of a cranial window in the dorsal skull. While the surgery itself was a success and we were able to generate the window without incurring any damage

to the underlying dura and sub-arachnoid membranes, the imaging is what proved a true challenge. While brain motion is minimal with the dura intact, the opacity of the tissue prevents quality image acquisition. When the dura is removed to enhance clarity brain motion becomes substantial through respiratory and cardiac effects, which also restricts image quality. In keeping with this, we were able to capture image sequences highlighting perivascular transport of CSF tracer in vivo, although the repeatability of this is questionable and the value in terms of quantification remains to be seen. The vision of these experiments is to one day be able to image PVS transport of tracer and Aß in order to garner information on the in vivo process relating to observed Aß vessel distributions, identified in Paper IV. For this to be possible we would need to image at higher magnifications with longer exposure times on our large animal stereoscope, and to achieve this we would have to limit brain motion after dural excision. This may be possible using agarose to fill the window and apply a counter pressure to limit motion, which will be the subject of future experiments. If it is possible to limit brain motion and the current imaging platform is not sufficient to capture these microscopic processes it may warrant the use of a new generation 2-photon compatible with large mammals. Using this setup it could then be possible to gather in vivo data surrounding the Aß-ensnarement system in dorsal pial vials, as described in the ventral pial vessels in Paper IV.

In summary, it is now possible to study the glymphatic system in a pig model and it has been shown that the glymphatic microarchitecture described in rodents also persists in the large gyrencephalic brain, and seems to be even more developed. SDH appears to be an global inhibitor of glymphatic function, which may predispose those affected with it to impaired brain clearance. Brain clearance itself, primarily waste segmentation and recirculation, is a complex and poorly understood topic, but what has mounted is that there may indeed exist a system to prevent waste recirculation into the brain through an elastin-based transmural ensnarement pathway. The end goal will be to study this ensnarement pathway in vivo in the large mammalian brain which will hopefully someday be made possible through a porcine cranial window model.

a starry night reborn

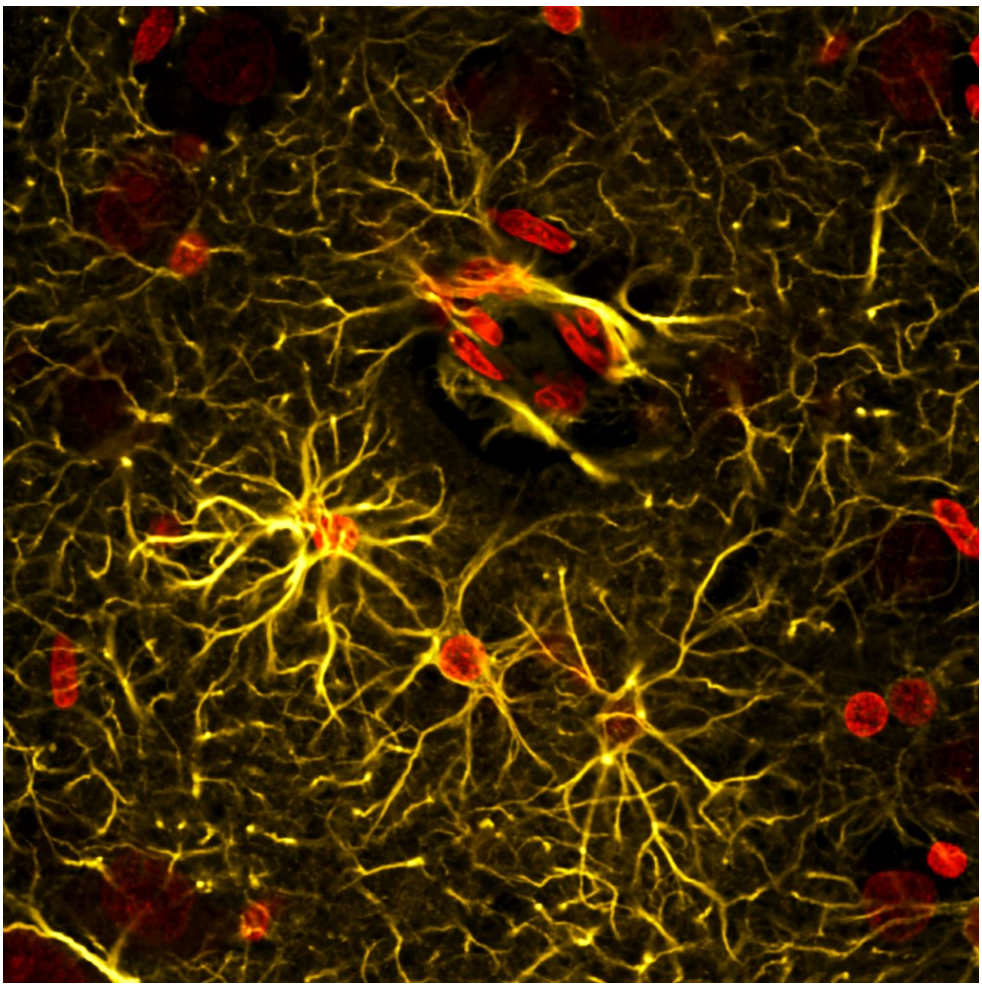

Key Methods

Animals

Mice

Adult male C57BL/6 mice were used for the all experiments. Mice were housed in standard laboratory conditions with a 12h dark-light cycle, ad libitum access to food and water. All experimental procedures were performed according to ethical approval by the Malmö-Lund ethical Committee on Animal Research (Dnr 5.8.18-08269/2019) and conducted according to the CODEX guidelines by the Swedish Research Council, Directive 2010/63/EU of the European Parliament on the protection of animals used for scientific purposes and Regulation (EU) 2019/1010 on the alignment of reporting obligations.

Pigs

Adult male pigs, Sus scrofa domesticus, weighing 45-55 kg, were used for all experiments. Pigs were housed in two's in pens with a 12h light-dark cycle, ad libitum access to water. All experimental procedures were performed according to ethical approval by the Malmö-Lund ethical Committee on Animal Research (Dnr 5.8.18-05527/2019) and conducted according to the CODEX guidelines by the Swedish Research Council, Directive 2010/63/EU of the European Parliament on the protection of animals used for scientific purposes and Regulation (EU) 2019/1010 on the alignment of reporting obligations.

Surgery

Rodent Cisterna Magna Cannulation

Mice received a single intraperitoneal injection of ketamine (100 mg/kg)/xylazine (20 mg/kg) (KX). After anaesthesia induction, an incision was made and muscles overlying the back of the skull were reflected laterally to reveal the cisterna magna

(CM), as previously described. The core temperature was kept at 37 °C using a heat pad connected to a rectal feedback probe. CM injection was carried out with a 30G dental needle (Carpule, Sopira) connected to a 100 µL Hamilton syringe via PE10 tubing. 10µL of AlexaFluor647-conjugated bovine serum albumin (BSA-647, Invitrogen) tracer (Paper II) OR 5µL BSA-647 + 3 µL Aß1-42 HiLyte-555/aCSF (Paper IV) were injected into the CM at 1µL/min using an KDS Legato 100 single infusion syringe pump. After injection, tracers were left to circulate for 30 minutes.

Porcine Cisterna Magna Cannulation

Pigs were first tranquilised/premedicated with an intramuscular injection of Zoletil (tiletamine 3.75 mg/kg + zolazepam 3.75 mg/kg) and Dexdomitor (dexmedetomidine 37.5 µg/kg). Once unconscious, animals were intubated and a 20G cannula was inserted into the ear vein. For maintenance anaesthesia a triple-drip (100 ml ketamine 100 mg/ml (5 mg/kg/min), 200ml fentanyl 50 µg/ml (2.5 µg/kg/min), 100 ml midazolam 5mg/ml (0.25 mg/kg/min) was applied through the ear vein until effect (± 0.5ml/10kg/min). Detailed CM injection surgery is described in Paper I. Briefly, the skin overlying the back of the head and neck was resected. The underlying muscle layers were severed at their respective origins and retracted. Any excess tissue overlying the skull base and atlas was removed. For CM injection while the neck of the animal was flexed an 18G cannula was introduced approximately 5mm into the cisterna magna and fixed in place with glue. 500µL BSA-647 (Paper II/III) OR 500µL BSA-647 + 300µL Aß1-42 HiLyte-555/ Aß1-40 HiLyte-555/ Aß1-42/ 10, 000 MW dextran 555/ aCSF (Paper IV) was injected using a 1 ml syringe connected to a 10 cm I.V line at a rate of 100 µL per minute. After injection, BSA-647 was allowed to circulate for 2, 4 or 6 hours (Paper II) or 2 hours (Paper I, III, IV, V).

Porcine Cranial Window

Detailed cranial window surgery is described in Paper V. Briefly, skin over the dorsal skull was reflected and periosteum cleared. A 10mm × 20mm cranial window was cut using a *Piezosurgery Flex* device, approximately 5mm lateral of the midline.

Tissue processing

Fixation

For optical tissue clearing in mice, mice were transcardially perfused with 4% PFA and brains were immersion post-fixed overnight in PFA (Paper II). For standard ex vivo imaging in mice, brains were extracted fresh and immersion post-fixed overnight in PFA (Paper IV). In pigs whole brains were immersion post-fixed overnight in 4% formaldehyde. After macroscopic sectioning, slices were further immersion post-fixed overnight in 4% formaldehyde. For electron microscopy processing pig cortical tissues (1 mm x 2 mm) were pre-fixed in a solution containing 1 % PFA and 1.5 % glutaraldehyde in 0.1 M phosphate buffered saline for 3 h at room temperature and then rinsed several times prior to fixation with 1 % osmium tetroxide. This was followed by dehydration with acetone (30-100 %), impregnation and embedding in pure Epon for sectioning (60 nm).

Sectioning

In mice, 100µm coronal sections were cut with a vibratome (Leica VT1200S). In pigs, macroscopic sections, approximately 10mm thick, were cut with a salmon knife. For microscopic sections, tissue bounding the IHS and rhinal fissure was sectioned using a vibratome (Leica VT1200S). For vessel sectioning, segments of the middle cerebral artery and posterior communicating artery were immersed in 20% sucrose solution for 48h before being embedded in OCT. 50µm coronal vessel sections were cut using a cryotome.

Immunohistochemistry

Free-floating brain sections, or vessel sections mounted on slides, were permeabilized and blocked for 45 min at 4 °C in a solution of 1 % BSA, 0.5 % Triton X-100 and 5 % normal donkey serum in PBS. Primary antibodies (rabbit anti-AQP4, 1:500, MerckMillipore; rabbit anti-GFAP, 1:500, Agilent Technologies; mouse anti-GLUT1, 1:250, Abcam, rabbit anti-SMA, 1:500, AbCam, rabbit anti-elastin, 1:250, AbCam) were added in PBS and incubated overnight at 4 °C on a rocking table. After 3x10 min washes in PBS at room temperature secondary antibodies (Alexa-Fluor 488- and 568-conjugated secondary antibodies, 1:1000) in PBS were added for 90 minutes at 4°C on a rocking table. Slices were then washed in PBS with DAPI (1:1000) and/or tomato lectin (Lycoperiscon esculentum, 1:100, SigmaAldrich) for 20 minutes, washed again and mounted.

Immunogold

Immunostaining was performed using primary antibody against BSA (1:1000, Sigma Aldrich) and secondary antibody conjugated to 10 nm gold nanospheres (1:20, Abcam). Sections were stained with 4 % uranyl acetate for 20 mins followed by 0.5 % lead citrate for 2 minutes to increase the contrast of the tissue.

Tissue Clearing

The iDISCO+ protocol was carried out as explained by Renier *et al* (2016). Pig brain pieces and whole mouse brains were dehydrated in increasing methanol/H_2O series (20%, 40%, 60%, 80%, 100%, 100%, 1 hour each), delipidated with methanol/dichloromethane (33%/66% for 3 hours) and pure dichloromethane (2 x 15 min), and optically cleared by impregnation dibenzyl ether (DBE) for at least 14 days prior to imaging.

Imaging

Advanced Light Microscopy

In vivo

For in vivo imaging through cranial window Nikon SMZ25 stereomicroscope with a Plan Apo 0.5x objective equipped with an Moment sCMOS camera was used.

Ex vivo

Whole brains and macroscopic slices were imaged using a Nikon SMZ25 stereomicroscope with a Plan Apo 0.5x objective equipped with an Andor Zyla 4.2 Plus sCMOS camera. The excitation wavelength was 635 nm using a CoolLED pE4000 LED illumination and the emission filter used was a quadruple bandpass filter. Vibratome slices were imaged with both Nikon Ti2 Eclipse and Nikon A1RHD confocal microscopes. Cleared pig brain tissue and whole cleared mouse brains were imaged using an Ultramicroscope II light-sheet microscope (LaVision Biotech) or an Ultramicroscope Blaze (Miltenyi). Brain pieces were imaged immersed in DBE.

Electron Microscopy

Sections were examined using FEI Tecnai Biotwin 120kv transmission electron microscope (TEM) and photographed using Olympus Veleta 2x2k camera at magnifications ranging from 2000-30,000×.

Statistical Analyses

All statistical analyses in this thesis were carried out in GraphPad Prism. Data were all tested for normality. When normally distributed, a parametric test of either a paired t-test, unpaired t-test, one way-ANOVA or two way-ANOVA were used. For data not normally distributed a non-parametric test was applied of either a Mann-Whitney test or Wilcoxon matched pairs signed rank test. All values are expressed as mean/mean difference $\pm$ SD. P-values ≤ 0.05 were considered statistically significant.

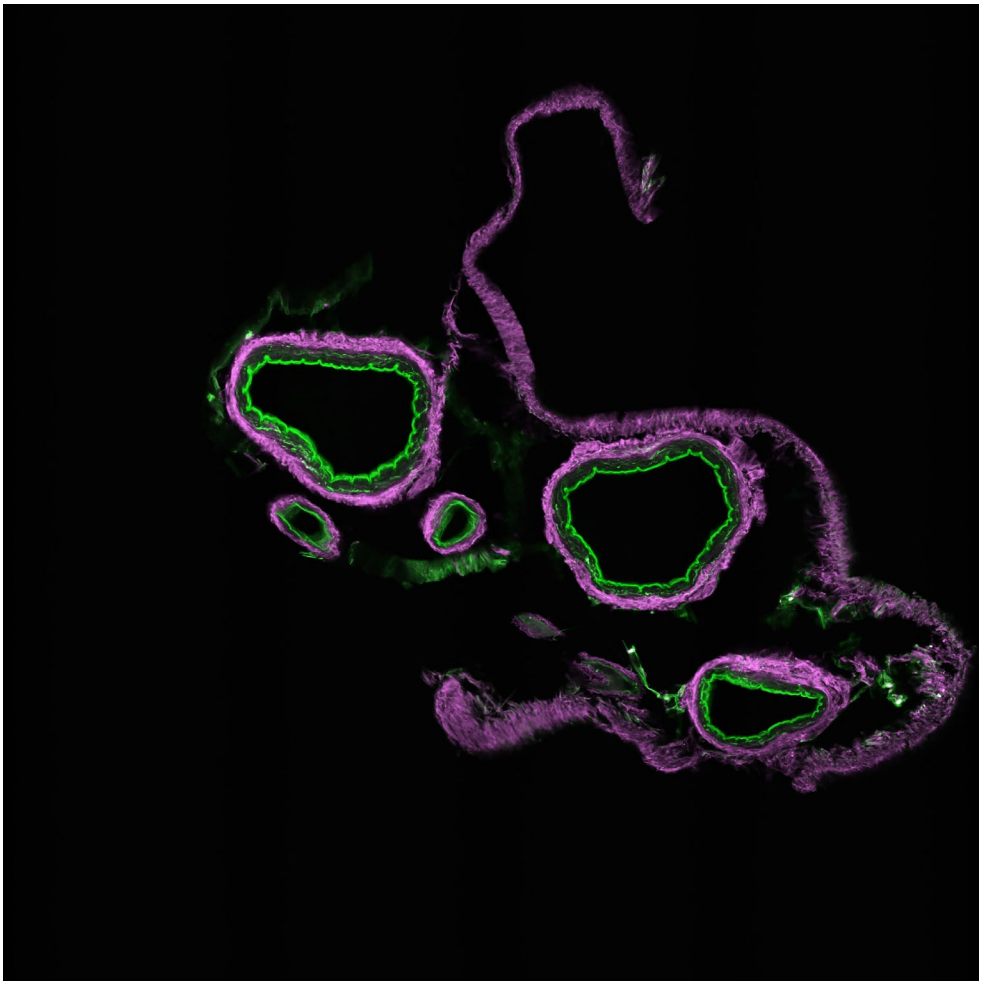

References

1. Nedergaard, M. Garbage truck of the brain. *Science (80-.).* **340**, 1529–1530 (2013).
2. Jessen, N. A., Munk, A. S. F., Lundgaard, I. & Nedergaard, M. The Glymphatic System: A Beginner's Guide. *Neurochem. Res.* **40**, 2583–2599 (2015).
3. Liao, S. & Padera, T. P. Lymphatic Function and Immune Regulation in Health and Disease. *Lymphat. Res. Biol.* **11**, 136–143 (2013).
4. Swartz, M. A. The physiology of the lymphatic system. *Adv. Drug Deliv. Rev.* **50**, 3–20 (2001).
5. Randolph, G. J., Ivanov, S., Zinselmeyer, B. H. & Scallan, J. P. The lymphatic system: integral roles in immunity. *Annu. Rev. Immunol.* **35**, 31–52 (2017).
6. Brotons, M. L., Bolca, C., Fréchette, É. & Deslauriers, J. Anatomy and physiology of the thoracic lymphatic system. *Thorac. Surg. Clin.* **22**, 139–153 (2012).
7. Aspelund, A. *et al.* A dural lymphatic vascular system that drains brain interstitial fluid and macromolecules. *J. Exp. Med.* **212**, 991–999 (2015).
8. Louveau, A. *et al.* Structural and functional features of central nervous system lymphatic vessels. *Nature* **523**, 337–341 (2015).
9. Shrestha, R., Millington, O., Brewer, J. & Bushell, T. Is central nervous system an immune-privileged site? *Kathmandu Univ. Med. J.* **11**, 102–107 (2013).
10. Suter, T. *et al.* The brain as an immune privileged site: dendritic cells of the central nervous system inhibit T cell activation. *Eur. J. Immunol.* **33**, 2998–3006 (2003).
11. Mazzitelli, J. A. *et al.* Cerebrospinal fluid regulates skull bone marrow niches via direct access through dural channels. *Nat. Neurosci.* (2022). doi:10.1038/s41593-022-01029-1
12. Proulx, S. T. Cerebrospinal fluid outflow: a review of the historical and contemporary evidence for arachnoid villi, perineural routes, and dural lymphatics. *Cell. Mol. Life Sci.* **78**, 2429–2457 (2021).
13. Meng, L., Hou, W., Chui, J., Han, R. & Gelb, A. W. Cardiac output and cerebral blood flow: the integrated regulation of brain perfusion in adult humans. *Anesthesiology* **123**, 1198–1208 (2015).
14. Williams, L. R. & Leggett, R. W. Reference values for resting blood flow to organs of man. *Clin. Phys. Physiol. Meas.* **10**, 187 (1989).
15. Iliff, J. J. *et al.* A Paravascular Pathway Facilitates CSF Flow Through the Brain Parenchyma and the Clearance of Interstitial Solutes , Including Amyloid b. **111**, (2012).
16. Mestre, H. *et al.* Aquaporin-4-dependent glymphatic solute transport in the rodent

brain. *Elife* **7**, 1–31 (2018).

17. Breasted, J. H. The Edwin Smith Surgical Papyrus: published in facsimile and hieroglyphic transliteration with translation and commentary in two volumes. (1930).
18. Deisenhammer, F., Sellebjerg, F., Teunissen, C. E. & Tumani, H. *Cerebrospinal fluid in clinical neurology*. *Cerebrospinal Fluid in Clinical Neurology* (2015). doi:10.1007/978-3-319-01225-4
19. Ángel, M., Arribas, T. & Arribas, M. A. T. The history of cerebrospinal fluid: from Classical Antiquity to the late modern period. *Neurosci. Hist.* **5**, 105–113 (2017).
20. Rocca, J. Galen and the ventricular system. *J. Hist. Neurosci.* **6**, 227–239 (1997).
21. Varolio, C. *De nervis opticis nonnullisq: aliis praeter communem opinionem in humano capite obseruatis*. (Culture et Civilisation, 1969).
22. Herbowski, L. The maze of the cerebrospinal fluid discovery. *Anat. Res. Int.* **2013**, (2013).
23. Di Ieva, A. & Yaşargil, M. G. Liquor cotunnii: the history of cerebrospinal fluid in Domenico Cotugno's work. *Neurosurgery* **63**, 352–358 (2008).
24. Magendie, F. *Recherches physiologiques et cliniques sur le liquide céphalo-rachidien ou cérébro-spinal*. (Méquignon-Marvis fils, 1842).
25. Hajdu, S. I. Discovery of the cerebrospinal fluid. *Ann. Clin. Lab. Sci.* **33**, 334–336 (2003).
26. Wynter, W. E. Four cases of tubercular meningitis in which paracentesis of the theca vertebralis was performed for the relief of fluid pressure. *Lancet* **137**, 981–982 (1891).
27. Lichtheim, L. Re: the proposal of Quincke to withdraw cerebrospinal fluid by lumbar puncture in cases of brain disease. *Dtsch Med Wochenschr* **19**, 1234 (1893).
28. Mestrezat, W. Le liquide céphalo-rachidien normal et pathologique. in *Le liquide cephalo-rachidien normal et pathologique* xvi–680 (1912).
29. Wood, J. H. Physiology, pharmacology, and dynamics of cerebrospinal fluid. *Neurobiol. cerebrospinal fluid 1* 1–16 (1980).
30. Noback, C. R., Ruggiero, D. A., Strominger, N. L. & Demarest, R. J. *The human nervous system: structure and function*. (Springer Science & Business Media, 2005).
31. Wright, B. L. C., Lai, J. T. F. & Sinclair, A. J. Cerebrospinal fluid and lumbar puncture: a practical review. *J. Neurol.* **259**, 1530–1545 (2012).
32. Lundgaard, I. *et al.* Glymphatic clearance controls state-dependent changes in brain lactate concentration. *J. Cereb. Blood Flow Metab.* **37**, 2112–2124 (2017).
33. Sakka, L., Coll, G. & Chazal, J. Anatomy and physiology of cerebrospinal fluid. *Eur. Ann. Otorhinolaryngol. Head Neck Dis.* **128**, 309–316 (2011).
34. Mortazavi, M. M. *et al.* The ventricular system of the brain: a comprehensive review of its history, anatomy, histology, embryology, and surgical considerations. *Child's Nerv. Syst.* **30**, 19–35 (2014).
35. Monro, A. Observations on the Structure and Functions of the Nervous. *Syst. Edinburgh Creech* (1783).

36. Baker, F. *The Two Sylviuses: An Historical Study...* (1909).
37. Key, A. & Retzius, G. Studien in der Anatomie des Nervensystems und des Bindegewebes. *Erste Hälfte. Stock.* (1875).
38. Oliveira, J. P. S., Mendes, N. T., Martins, Á. R. & Sanvito, W. L. Cerebrospinal fluid: history, collection techniques, indications, contraindications and complications. *J. Bras. Patol. e Med. Lab.* **56**, (2020).
39. Bèchet, N. B., Shanbhag, N. C. & Lundgaard, I. Glymphatic pathways in the gyrencephalic brain. *J. Cereb. Blood Flow Metab.* **41**, 2264–2279 (2021).
40. Brodbelt, A. & Stoodley, M. CSF pathways: a review. *Br. J. Neurosurg.* **21**, 510–520 (2007).
41. Barshes, N., Demopoulos, A. & Engelhard, H. H. Anatomy and physiology of the leptomeninges and CSF space. *Leptomeningeal Metastases* 1–16 (2005).
42. Whitney, N., Sun, H., Pollock, J. M. & Ross, D. A. The human foramen magnum—Normal anatomy of the cisterna magna in adults. *Neuroradiology* **55**, 1333–1339 (2013).
43. Redzic, Z. B. & Segal, M. B. The structure of the choroid plexus and the physiology of the choroid plexus epithelium. *Adv. Drug Deliv. Rev.* **56**, 1695–1716 (2004).
44. Cserr, H. Physiology of the choroid plexus. *Physiol. Rev.* **51**, 273–311 (1971).
45. Marques, F. *et al.* The choroid plexus in health and in disease: dialogues into and out of the brain. *Neurobiol. Dis.* **107**, 32–40 (2017).
46. Spector, R., Keep, R. F., Snodgrass, S. R., Smith, Q. R. & Johanson, C. E. A balanced view of choroid plexus structure and function: focus on adult humans. *Exp. Neurol.* **267**, 78–86 (2015).
47. Liu, G. *et al.* Direct measurement of cerebrospinal fluid production in mice. *Cell Rep.* **33**, 108524 (2020).
48. Maller, V. V. & Gray, R. I. Noncommunicating Hydrocephalus. *Semin. Ultrasound, CT MRI* **37**, 109–119 (2016).
49. Nishiyama, K., Mori, H. & Tanaka, R. Changes in cerebrospinal fluid hydrodynamics following endoscopic third ventriculostomy for shunt-dependent noncommunicating hydrocephalus. *J. Neurosurg.* **98**, 1027–1031 (2003).
50. Kido, D. K., Gomez, D. G., Pavese, A. M. & Potts, D. G. Human spinal arachnoid villi and granulations. *Neuroradiology* **11**, 221–228 (1976).
51. Upton, M. L. & Weller, R. O. The morphology of cerebrospinal fluid drainage pathways in human arachnoid granulations. *J. Neurosurg.* **63**, 867–875 (1985).
52. McComb, J. G. Recent research into the nature of cerebrospinal fluid formation and absorption. *J. Neurosurg.* **59**, 369–383 (1983).
53. Zakharov, A. *et al.* Integrating the roles of extracranial lymphatics and intracranial veins in cerebrospinal fluid absorption in sheep. *Microvasc. Res.* **67**, 96–104 (2004).
54. Welch, K. & Friedman, V. The cerebrospinal fluid valves. *Brain* **83**, 454–469 (1960).
55. Welch, K. & Pollay, M. The spinal arachnoid villi of the monkeys Cercopithecus aethiops sabaeus and Macaca irus. *Anat. Rec.* **145**, 43–48 (1963).

56. Alksne, J. F. & White, L. E. Electron-microscope study of the effect of increased intracranial pressure on the arachnoid villus. *J. Neurosurg.* **22**, 481–488 (1965).

57. Shabo, A. L. & Maxwell, D. S. The morphology of the arachnoid villi: a light and electron microscopic study in the monkey. *J. Neurosurg.* **29**, 451–463 (1968).

58. SCHWALBE & G. Der Arachnoidalraum, ein Lymphraum und sein Zusammenhang mit dem Perichorioidalraum. *Zentralbl. Med. Wiss.* **7**, 465–467 (1869).

59. Ma, Q., Ineichen, B. V., Detmar, M. & Proulx, S. T. Outflow of cerebrospinal fluid is predominantly through lymphatic vessels and is reduced in aged mice. *Nat. Commun.* **8**, (2017).

60. Földi, M. *et al.* New contributions to the anatomical connections of the brain and the lymphatic system. *Acta Anat. (Basel).* **64**, 498–505 (1966).

61. Bradbury, M. W. & Cole, D. F. The role of the lymphatic system in drainage of cerebrospinal fluid and aqueous humour. *J. Physiol.* **299**, 353–365 (1980).

62. Boulton, M., Flessner, M., Armstrong, D., Hay, J. & Johnston, M. Determination of volumetric cerebrospinal fluid absorption into extracranial lymphatics in sheep. *Am. J. Physiol. Integr. Comp. Physiol.* **274**, R88–R96 (1998).

63. Johnston, M. G. *Experimental biology of the lymphatic circulation*. (Elsevier, 1985).

64. Johnston, M. & Papaiconomou, C. Cerebrospinal fluid transport: a lymphatic perspective. *News Physiol. Sci.* **17**, 227–30 (2002).

65. Papaiconomou, C., Bozanovic-Sosic, R., Zakharov, A. & Johnston, M. Does neonatal cerebrospinal fluid absorption occur via arachnoid projections or extracranial lymphatics? *Am. J. Physiol. - Regul. Integr. Comp. Physiol.* **283**, 869–876 (2002).

66. Zakharov, A., Papaiconomou, C., Djenic, J., Midha, R. & Johnston, M. Lymphatic cerebrospinal fluid absorption pathways in neonatal sheep revealed by subarachnoid injection of Microfil. *Neuropathol. Appl. Neurobiol.* **29**, 563–573 (2003).

67. Johnston, M., Zakharov, A., Papaiconomou, C., Salmasi, G. & Armstrong, D. Evidence of connections between cerebrospinal fluid and nasal lymphatic vessels in humans, non-human primates and other mammalian species. *Cerebrospinal Fluid Res.* **1**, 1–13 (2004).

68. Papaiconomou, C., Zakharov, A., Azizi, N., Djenic, J. & Johnston, M. Reassessment of the pathways responsible for cerebrospinal fluid absorption in the neonate. *Child's Nerv. Syst.* **20**, 29–36 (2004).

69. Koh, L., Zakharov, A. & Johnston, M. Integration of the subarachnoid space and lymphatics: Is it time to embrace a new concept of cerebrospinal fluid absorption? *Cerebrospinal Fluid Res.* **2**, 1–11 (2005).

70. Louveau, A. *et al.* Understanding the functions and relationships of the glymphatic system and meningeal lymphatics. *J. Clin. Invest.* **127**, 3210–3219 (2017).

71. Absinta, M. *et al.* Human and nonhuman primate meninges harbor lymphatic vessels that can be visualized noninvasively by MRI. *Elife* **6**, 1–15 (2017).

72. Da Mesquita, S. *et al.* Functional aspects of meningeal lymphatics in ageing and Alzheimer's disease. *Nature* **560**, 185–191 (2018).

73. Da Mesquita, S. *et al.* Functional aspects of meningeal lymphatics in ageing and

Alzheimer's disease. *Nature* (2018). doi:10.1038/s41586-018-0368-8

74. Louveau, A. *et al.* CNS lymphatic drainage and neuroinflammation are regulated by meningeal lymphatic vasculature. *Nat. Neurosci.* **21**, 1380–1391 (2018).

75. Bolte, A. C. *et al.* Meningeal lymphatic dysfunction exacerbates traumatic brain injury pathogenesis. *Nat. Commun.* **11**, 1–18 (2020).

76. Antila, S. *et al.* Development and plasticity of meningeal lymphatic vessels. *J. Exp. Med.* **214**, 3645–3667 (2017).

77. Patel, T. K. *et al.* Dural lymphatics regulate clearance of extracellular tau from the CNS. *Mol. Neurodegener.* **14**, 1–9 (2019).

78. Ma, Q., Decker, Y., Müller, A., Ineichen, B. V. & Proulx, S. T. Clearance of cerebrospinal fluid from the sacral spine through lymphatic vessels. *J. Exp. Med.* jem.20190351 (2019). doi:10.1084/jem.20190351

79. Ma, Q. *et al.* Rapid lymphatic efflux limits cerebrospinal fluid flow to the brain. *Acta Neuropathol.* **137**, 151–165 (2019).

80. Decker, Y. *et al.* Magnetic resonance imaging of cerebrospinal fluid outflow after low-rate lateral ventricle infusion in mice. *JCI insight* **7**, (2022).

81. Woollam, D. H. M. & Millen, J. W. The perivascular spaces of the mammalian central nervous system and their relation to the perineuronal and subarachnoid spaces. *J. Anat.* **89**, 193 (1955).

82. Wardlaw, J. M. *et al.* Perivascular spaces in the brain: anatomy, physiology and pathology. *Nat. Rev. Neurol.* **16**, 137–153 (2020).

83. Weed, L. H. Studies on cerebro-spinal fluid. No. II: the theories of drainage of cerebro-spinal fluid with an analysis of the methods of investigation. *J. Med. Res.* **31**, 21 (1914).

84. Weed, L. H. Studies on Cerebro-Spinal Fluid. No. III: The pathways of escape from the Subarachnoid Spaces with particular reference to the Arachnoid Villi. *J. Med. Res.* **31**, 51 (1914).

85. Tarasoff-Conway, J. M. *et al.* Clearance systems in the brain - Implications for Alzheimer disease. *Nat. Rev. Neurol.* **11**, 457–470 (2015).

86. Weed, L. H. The absorption of cerebrospinal fluid into the venous system. *Am. J. Anat.* **31**, 191–221 (1923).

87. Bouvy, W. H. *et al.* Visualization of perivascular spaces and perforating arteries with 7 T magnetic resonance imaging. *Invest. Radiol.* **49**, 307–313 (2014).

88. Potter, G. M., Chappell, F. M., Morris, Z. & Wardlaw, J. M. Cerebral perivascular spaces visible on magnetic resonance imaging: development of a qualitative rating scale and its observer reliability. *Cerebrovasc. Dis.* **39**, 224–231 (2015).

89. Zhu, Y.-C. *et al.* High degree of dilated Virchow-Robin spaces on MRI is associated with increased risk of dementia. *J. Alzheimer's Dis.* **22**, 663–672 (2010).

90. Doubal, F. N., MacLullich, A. M. J., Ferguson, K. J., Dennis, M. S. & Wardlaw, J. M. Enlarged perivascular spaces on MRI are a feature of cerebral small vessel disease. *Stroke* **41**, 450–454 (2010).

91. Mestre, H. *et al.* Flow of cerebrospinal fluid is driven by arterial pulsations and is reduced in hypertension. *Nat. Commun.* **9**, 4878 (2018).

92. Morris, A. W. J. *et al.* Vascular basement membranes as pathways for the passage of fluid into and out of the brain. *Acta Neuropathol.* **131**, 725–736 (2016).

93. Jung, J. S. *et al.* Molecular characterization of an aquaporin cDNA from brain: candidate osmoreceptor and regulator of water balance. *Proc. Natl. Acad. Sci.* **91**, 13052–13056 (1994).

94. Hasegawa, H., Ma, T., Skach, W., Matthay, M. A. & Verkman, A. S. Molecular cloning of a mercurial-insensitive water channel expressed in selected water-transporting tissues. *J. Biol. Chem.* **269**, 5497–5500 (1994).

95. Nagelhus, E. A. & Ottersen, O. P. Physiological Roles of Aquaporin-4 in Brain. *Physiol. Rev.* **93**, 1543–1562 (2013).

96. Nielsen, S. *et al.* Specialized membrane domains for water transport in glial cells: high-resolution immunogold cytochemistry of aquaporin-4 in rat brain. *J. Neurosci.* **17**, 171–180 (1997).

97. Frigeri, A. *et al.* Localization of MIWC and GLIP water channel homologs in neuromuscular, epithelial and glandular tissues. *J. Cell Sci.* **108**, 2993–3002 (1995).

98. Nagelhus, E. A. *et al.* Aquaporin-4 water channel protein in the rat retina and optic nerve: polarized expression in Müller cells and fibrous astrocytes. *J. Neurosci.* **18**, 2506–2519 (1998).

99. Nagelhus, E. A. *et al.* Immunogold evidence suggests that coupling of K+ siphoning and water transport in rat retinal Müller cells is mediated by a coenrichment of Kir4. 1 and AQP4 in specific membrane domains. *Glia* **26**, 47–54 (1999).

100. Dermietzel, R. Visualization by freeze-fracturing of regular structures in glial cell membranes. *Naturwissenschaften* **60**, 208 (1973).

101. Wolburg, H. Orthogonal arrays of intramembranous particles: a review with special reference to astrocytes. *J. Hirnforsch.* **36**, 239–258 (1995).

102. Wolburg, H., Wolburg-Buchholz, K., Fallier-Becker, P., Noell, S. & Mack, A. F. Structure and functions of aquaporin-4-based orthogonal arrays of particles. *Int. Rev. Cell Mol. Biol.* **287**, 1–41 (2011).

103. Verbavatz, J.-M., Ma, T., Gobin, R. & Verkman, A. S. Absence of orthogonal arrays in kidney, brain and muscle from transgenic knockout mice lacking water channel aquaporin-4. *J. Cell Sci.* **110**, 2855–2860 (1997).

104. Yang, B., Brown, D. & Verkman, A. S. The Mercurial Insensitive Water Channel (AQP-4) Forms Orthogonal Arrays in Stably Transfected Chinese Hamster Ovary Cells (∗). *J. Biol. Chem.* **271**, 4577–4580 (1996).

105. King, L. S., Kozono, D. & Agre, P. From structure to disease: the evolving tale of aquaporin biology. *Nat. Rev. Mol. cell Biol.* **5**, 687–698 (2004).

106. Suzuki, H., Nishikawa, K., Hiroaki, Y. & Fujiyoshi, Y. Formation of aquaporin-4 arrays is inhibited by palmitoylation of N-terminal cysteine residues. *Biochim. Biophys. Acta (BBA)-Biomembranes* **1778**, 1181–1189 (2008).

107. Strand, L., Moe, S. E., Solbu, T. T., Vaadal, M. & Holen, T. Roles of aquaporin-4 isoforms and amino acids in square array assembly. *Biochemistry* **48**, 5785–5793 (2009).

108. Furman, C. S. *et al.* Aquaporin-4 square array assembly: opposing actions of M1

and M23 isoforms. *Proc. Natl. Acad. Sci.* **100**, 13609–13614 (2003).

109. Crane, J. M., Bennett, J. L. & Verkman, A. S. Live Cell Analysis of Aquaporin-4 M1/M23 Interactions and Regulated Orthogonal Array Assembly in Glial Cells*♦. *J. Biol. Chem.* **284**, 35850–35860 (2009).

110. Neely, J. D., Christensen, B. M., Nielsen, S. & Agre, P. Heterotetrameric composition of aquaporin-4 water channels. *Biochemistry* **38**, 11156–11163 (1999).

111. Nicchia, G. P. *et al.* Higher order structure of aquaporin-4. *Neuroscience* **168**, 903–914 (2010).

112. Wang, Y. & Tajkhorshid, E. Nitric oxide conduction by the brain aquaporin AQP4. *Proteins Struct. Funct. Bioinforma.* **78**, 661–670 (2010).

113. Musa-Aziz, R., Chen, L.-M., Pelletier, M. F. & Boron, W. F. Relative CO2/NH3 selectivities of Aqp1, Aqp4, Aqp5, Amtb, and Rhag. *Proc. Natl. Acad. Sci.* **106**, 5406–5411 (2009).

114. Xie, L. *et al.* Sleep drives metabolite clearance from the Adult Brain. **373**, 373–378 (2013).

115. Smith, A. J., Yao, X., Dix, J. A., Jin, B. J. & Verkman, A. S. Test of the 'glymphatic' hypothesis demonstrates diffusive and aquaporin-4-independent solute transport in rodent brain parenchyma. *Elife* **6**, 1–16 (2017).

116. Frigeri, A., Nicchia, G. P., Verbavatz, J. M., Valenti, G. & Svelto, M. Expression of aquaporin-4 in fast-twitch fibers of mammalian skeletal muscle. *J. Clin. Invest.* **102**, 695–703 (1998).

117. FRIGERI, A. *et al.* Aquaporin-4 deficiency in skeletal muscle and brain of dystrophic mdx mice. *FASEB J.* **15**, 90–98 (2001).

118. Liu, J. W. *et al.* Immunocytochemical studies of aquaporin 4 in the skeletal muscle of mdx mouse. *J. Neurol. Sci.* **164**, 24–28 (1999).

119. Yang, B. *et al.* Skeletal muscle function and water permeability in aquaporin-4 deficient mice. *Am. J. Physiol. Physiol.* **278**, C1108–C1115 (2000).

120. Munk, A. S. *et al.* PDGF-B Is Required for Development of the Glymphatic System. *Cell Rep.* **26**, 2955-2969.e3 (2019).

121. Neely, J. D. *et al.* Syntrophin-dependent expression and localization of Aquaporin-4 water channel protein. *Proc. Natl. Acad. Sci.* **98**, 14108–14113 (2001).

122. Amiry-Moghaddam, M. *et al.* An α-syntrophin-dependent pool of AQP4 in astroglial end-feet confers bidirectional water flow between blood and brain. *Proc. Natl. Acad. Sci.* **100**, 2106–2111 (2003).

123. Simon, M. J. *et al.* Transcriptional network analysis of human astrocytic endfoot genes reveals region-specific associations with dementia status and tau pathology. *Sci. Rep.* **8**, 1–16 (2018).

124. Simon, M. J., Murchison, C. & Iliff, J. J. A transcriptome-based assessment of the astrocytic dystrophin-associated complex in the developing human brain. *J. Neurosci. Res.* **96**, 180–193 (2018).

125. Hladky, S. B. & Barrand, M. A. *The glymphatic hypothesis: the theory and the evidence*. *Fluids and Barriers of the CNS* **19**, (BioMed Central, 2022).

126. Ramos, M. *et al.* Cisterna Magna Injection in Rats to Study Glymphatic Function.

Methods Mol. Biol. **1938**, (2019).

127. Xavier, A. L. R. *et al.* Cannula Implantation into the Cisterna Magna of Rodents. *J. Vis. Exp.* (2018). doi:10.3791/57378

128. Yang, L. *et al.* Evaluating glymphatic pathway function utilizing clinically relevant intrathecal infusion of CSF tracer. *J. Transl. Med.* **11**, 1 (2013).

129. Alshuhri, M. S., Gallagher, L., Work, L. M. & Holmes, W. M. Direct imaging of glymphatic transport using H217O MRI. *JCI Insight* (2021). doi:10.1172/jci.insight.141159

130. Raghunandan, A. *et al.* Bulk flow of cerebrospinal fluid observed in periarterial spaces is not an artifact of injection. *bioRxiv* 2020.11.09.374512 (2020). doi:10.1101/2020.11.09.374512

131. Eide, P. K. & Ringstad, G. MRI with intrathecal MRI gadolinium contrast medium administration: a possible method to assess glymphatic function in human brain. *Acta Radiol. Open* **4**, 205846011560963 (2015).

132. Ringstad, G. *et al.* Brain-wide glymphatic enhancement and clearance in humans assessed with MRI. *JCI Insight* **3**, (2018).

133. Iliff, J. J. *et al.* Brain-wide pathway for waste clearance captured by contrast-enhanced MRI. *J. Clin. Invest.* **123**, 1299–1309 (2013).

134. Kress, B. T. *et al.* Impairment of paravascular clearance pathways in the aging brain. *Ann. Neurol.* **76**, 845–861 (2014).

135. Bèchet, N. B. *et al.* Light sheet fluorescence microscopy of optically cleared brains for studying the glymphatic system. *J. Cereb. Blood Flow Metab.* **40**, 1975–1986 (2020).

136. Benveniste, H. *et al.* Anesthesia with Dexmedetomidine and Low-dose Isoflurane Increases Solute Transport via the Glymphatic Pathway in Rat Brain When Compared with High-dose Isoflurane. *Anesthesiology* **127**, 976–988 (2017).

137. Hablitz, L. M. *et al.* Increased glymphatic influx is correlated with high EEG delta power and low heart rate in mice under anesthesia. *Sci. Adv.* **5**, eaav5447 (2019).

138. Zubaran, C., Fernandes, J. G. & Rodnight, R. Wernicke-Korsakoff syndrome. *Postgrad. Med. J.* **73**, 27–31 (1997).

139. Clarren, S. K. & Smith, D. W. The fetal alcohol syndrome. *N. Engl. J. Med.* **298**, 1063–1067 (1978).

140. Lundgaard, I., Wang, W., Eberhardt, A., Vinitsky, H. S. & Cameron, B. Beneficial effects of low alcohol exposure , but adverse effects of high alcohol intake on glymphatic function. *Sci. Rep.* 1–16 (2018). doi:10.1038/s41598-018-20424-y

141. Holstein-rathlou, S. Von, Caesar, N. & Nedergaard, M. Neuroscience Letters Voluntary running enhances glymphatic in fl ux in awake behaving , young mice. *Neurosci. Lett.* **662**, 253–258 (2018).

142. He, X. F. *et al.* Voluntary exercise promotes glymphatic clearance of amyloid beta and reduces the activation of astrocytes and microglia in aged mice. *Front. Mol. Neurosci.* **10**, 1–14 (2017).

143. Giannetto, M. *et al.* Biological sex does not predict glymphatic influx in healthy young, middle aged or old mice. *Sci. Rep.* **10**, 1–8 (2020).

144. Jiang, Q. *et al.* Impairment of the glymphatic system after diabetes. *J. Cereb. Blood Flow Metab.* **37**, 1326–1337 (2017).

145. Manouchehrian, O., Ramos, M., Bachiller, S., Lundgaard, I. & Deierborg, T. Acute systemic LPS-exposure impairs perivascular CSF distribution in mice. *J. Neuroinflammation* **18**, 1–13 (2021).

146. Xu, Z. *et al.* Deletion of aquaporin-4 in APP/PS1 mice exacerbates brain Aβ accumulation and memory deficits. *Mol. Neurodegener.* **10**, 1–16 (2015).

147. Peng, W. *et al.* Suppression of glymphatic fluid transport in a mouse model of Alzheimer's disease. *Neurobiol. Dis.* **93**, 215–225 (2016).

148. Feng, W. *et al.* Microglia prevent beta-amyloid plaque formation in the early stage of an Alzheimer's disease mouse model with suppression of glymphatic clearance. **1**, 1–15 (2019).

149. Iliff, J. J. *et al.* Impairment of glymphatic pathway function promotes tau pathology after traumatic brain injury. *J. Neurosci.* **34**, 16180–16193 (2014).

150. Harrison, I. F. *et al.* Impaired glymphatic function and clearance of tau in an Alzheimer's disease model. *Brain* 1–18 (2020). doi:10.1093/brain/awaa179

151. Howells, D. W. *et al.* Different strokes for different folks: The rich diversity of animal models of focal cerebral ischemia. *J. Cereb. Blood Flow Metab.* **30**, 1412–1431 (2010).

152. Ringstad, G., Vatnehol, S. A. S. & Eide, P. K. Glymphatic MRI in idiopathic normal pressure hydrocephalus. *Brain* **140**, 2691–2705 (2017).

153. Eide, P. K. & Ringstad, G. Delayed clearance of cerebrospinal fluid tracer from entorhinal cortex in idiopathic normal pressure hydrocephalus: A glymphatic magnetic resonance imaging study. *J. Cereb. Blood Flow Metab.* **39**, 1355–1368 (2019).

154. Watts, R. *et al.* Measuring Glymphatic Flow in Man Using Quantitative. *Am. J. Neuroradiol.* **40**, (2019).

155. Goulay, R. *et al.* Subarachnoid Hemorrhage Severely Impairs Brain Parenchymal Cerebrospinal Fluid Circulation in Nonhuman Primate. *Stroke* **48**, 2301–2305 (2017).

156. Lehmann, H. The minipig in general toxicology. *Scand. J. Lab. Anim. Sci.* **25**, 59–62 (1998).

157. Larsen, M. O. & Rolin, B. Use of the Göttingen minipig as a model of diabetes, with special focus on type 1 diabetes research. *ILAR J.* **45**, 303–313 (2004).

158. Richer, J. P. *et al.* Sacrococcygeal and transsacral epidural anesthesia in the laboratory pig: a model for experimental surgery. *Surg. Radiol. Anat.* **20**, 431–435 (1998).

159. Lind, N. M. *et al.* The use of pigs in neuroscience: Modeling brain disorders. *Neurosci. Biobehav. Rev.* **31**, 728–751 (2007).

160. Jakobsen, J. E. *et al.* Expression of the Alzheimer's Disease Mutations AβPP695sw and PSEN1M146I in Double-Transgenic Göttingen Minipigs. *J. Alzheimer's Dis.* **53**, 1617–1630 (2016).

161. Sade, R. M. & Mukherjee, R. Ethical issues in xenotransplantation: the first pig-to-

human heart transplant. *Ann. Thorac. Surg.* **113**, 712–714 (2022).

162. Marcilloux, J.-C., Rampin, O., Felix, M.-B., Laplace, J.-P. & Albe-Fessard, D. A stereotaxic apparatus for the study of the central nervous structures in the pig. *Brain Res. Bull.* **22**, 591–597 (1989).

163. Poceta, J. S., Hamlin, M. N., Haack, D. W. & Bohr, D. F. Stereotaxic placement of cannulae in cerebral ventricles of the pig. *Anat. Rec.* **200**, 349–356 (1981).

164. Saito, T., Bjarkam, C. R., Nakamura, M. & Nemoto, T. Determination of stereotaxic coordinates for the hippocampus in the domestic pig. *J. Neurosci. Methods* **80**, 29–36 (1998).

165. Grate, L. L., Golden, J. A., Hoopes, P. J., Hunter, J. V & Duhaime, A.-C. Traumatic brain injury in piglets of different ages: techniques for lesion analysis using histology and magnetic resonance imaging. *J. Neurosci. Methods* **123**, 201–206 (2003).

166. Duhaime, A.-C. *et al.* Magnetic resonance imaging studies of age-dependent responses to scaled focal brain injury in the piglet. *J. Neurosurg.* **99**, 542–548 (2003).

167. Dall, A. M. *et al.* Quantitative [18F] fluorodopa/PET and histology of fetal mesencephalic dopaminergic grafts to the striatum of MPTP-poisoned minipigs. *Cell Transplant.* **11**, 733–746 (2002).

168. Sakoh, M., Røhl, L., Gyldensted, C., Gjedde, A. & Østergaard, L. Cerebral blood flow and blood volume measured by magnetic resonance imaging bolus tracking after acute stroke in pigs: comparison with [15O] H2O positron emission tomography. *Stroke* **31**, 1958–1964 (2000).

169. Mayeux, R. & Yaakov, S. Epidemiology of Alzheimer Disease. *Cold Spring Harb. Perspect. Med.* **2**, (2012).

170. Mullane, K. & Williams, M. Alzheimer's therapeutics: Continued clinical failures question the validity of the amyloid hypothesis - But what lies beyond? *Biochem. Pharmacol.* **85**, 289–305 (2013).

171. Kung, H. C., Hoyert, D. L., Xu, J. Q. & Murphy, S. L. Deaths: final data for 2005. National vital statistics reports; vol 56 no. 10. *Hyattsville, MD Natl. Cent. Heal. Stat.* (2008).

172. Hardy, J. & Higgins, G. Alzheimer's disease: the amyloid cascade hypothesis. *Science (80-.).* **256**, 184–186 (1992).

173. Hardy, J. & Selkoe, D. The amyloid hypothesis of Alzheimer's disease: Progress and problems on the road to therapeutics. *Science (80-.).* **297**, 353–356 (2002).

174. Hardy, J. The relationship between amyloid and tau. *J. Mol. Neurosci.* **20**, 203–206 (2003).

175. Stancu, I.-C., Vasconcelos, B., Terwel, D. & Dewachter, I. Models of β-amyloid induced Tau-pathology: the long and "folded" road to understand the mechanism. *Mol. Neurodegener.* **9**, 1–14 (2014).

176. van Dyck, C. H. Anti-Amyloid-β Monoclonal Antibodies for Alzheimer's Disease: Pitfalls and Promise. *Biol. Psychiatry* **83**, 311–319 (2018).

177. Robinson, S. R., Bishop, G. M., Lee, H. G. & Münch, G. Lessons from the AN 1792

Alzheimer vaccine: Lest we forget. *Neurobiol. Aging* **25**, 609–615 (2004).

178. Spira, A. P. *et al.* Self-reported sleep and β-amyloid deposition in community-dwelling older adults. *JAMA Neurol.* **70**, 1537–1543 (2013).

179. Mendelsohn, A. R. & Larrick, J. W. Sleep Facilitates Clearance of Metabolites from the Brain: Glymphatic Function in Aging and Neurodegenerative Diseases. *Rejuvenation Res.* **16**, 518–523 (2013).

180. Ju, Y. E. S. *et al.* Obstructive sleep apnea decreases central nervous system–derived proteins in the cerebrospinal fluid. *Ann. Neurol.* **80**, 154–159 (2016).

181. Wulff, K., Gatti, S., Wettstein, J. G. & Foster, R. G. Sleep and circadian rhythm disruption in psychiatric and neurodegenerative disease. *Nat. Rev. Neurosci.* **11**, 589–599 (2010).

182. Raggi, A. & Ferri, R. Sleep disorders in neurodegenerative diseases. *Eur. J. Neurol.* **17**, 1326–1338 (2010).

183. Bhatt, M. H., Podder, N. & Chokroverty, S. Sleep and neurodegenerative diseases. in *Seminars in neurology* **25**, 39–51 (Copyright© 2005 by Thieme Medical Publishers, Inc., 333 Seventh Avenue, New …, 2005).

184. Iranzo, A. & Santamaria, J. Sleep in neurodegenerative diseases. *Sleep Med.* 271–283 (2015).

185. Kylkilahti, T. M. *et al.* Achieving brain clearance and preventing neurodegenerative diseases—A glymphatic perspective. *J. Cereb. Blood Flow Metab.* (2021). doi:10.1177/0271678X20982388

186. Abbott, S. M., Malkani, R. G. & Zee, P. C. Circadian disruption and human health: A bidirectional relationship. *Eur. J. Neurosci.* **51**, 567–583 (2020).

187. Nelson, P. T. *et al.* Clinicopathologic correlations in a large Alzheimer disease center autopsy cohort: neuritic plaques and neurofibrillary tangles" do count" when staging disease severity. *J. Neuropathol. Exp. Neurol.* **66**, 1136–1146 (2007).

188. Castellani, R. J. *et al.* Neuropathology of Alzheimer disease: pathognomonic but not pathogenic. *Acta Neuropathol.* **111**, 503–509 (2006).

189. Lee, H. *et al.* Amyloid-β in Alzheimer disease: the null versus the alternate hypotheses. *J. Pharmacol. Exp. Ther.* **321**, 823–829 (2007).

190. Marchesi, V. T. An alternative interpretation of the amyloid Aβ hypothesis with regard to the pathogenesis of Alzheimer's disease. *Proc. Natl. Acad. Sci.* **102**, 9093–9098 (2005).

191. Zhang, R. *et al.* Aquaporin 4 deletion exacerbates brain impairments in a mouse model of chronic sleep disruption. *CNS Neurosci. Ther.* **26**, 228–239 (2020).

192. Rainey-Smith, S. R. *et al.* Genetic variation in Aquaporin-4 moderates the relationship between sleep and brain Aβ-amyloid burden. *Transl. Psychiatry* **8**, 1–11 (2018).

193. Bèchet, N. B., Shanbhag, N. C. & Lundgaard, I. Direct Cannula Implantation in the Cisterna Magna of Pigs. *J. Vis. Exp.* 1–12 (2021). doi:10.3791/62641

194. Renier, N. *et al.* Mapping of Brain Activity by Automated Volume Analysis of Immediate Early Genes. *Cell* **165**, 1789–1802 (2016).

195. Shanbhag, N. C., Bèchet, N. B., Kritsilis, M. & Lundgaard, I. Impaired cerebrospinal

fluid transport due to idiopathic subdural hematoma in pig: an unusual case. *BMC Vet. Res.* **17**, 1–8 (2021).

196. Smith, D. H., Johnson, V. E. & Stewart, W. Chronic neuropathologies of single and repetitive TBI: Substrates of dementia? *Nat. Rev. Neurol.* **9**, 211–221 (2013).

197. Johnson, V. E., Stewart, W., Arena, J. D. & Smith, D. H. Traumatic Brain Injury as a Trigger of Neurodegeneration BT - Neurodegenerative Diseases: Pathology, Mechanisms, and Potential Therapeutic Targets. in (eds. Beart, P., Robinson, M., Rattray, M. & Maragakis, N. J.) 383–400 (Springer International Publishing, 2017). doi:10.1007/978-3-319-57193-5_15

198. Adhiyaman, V., Asghar, M., Ganeshram, K. N. & Bhowmick, B. K. Chronic subdural haematoma in the elderly. *Postgrad. Med. J.* **78**, 71–75 (2002).

199. Adhiyaman, V., Chattopadhyay, I., Irshad, F., Curran, D. & Abraham, S. Increasing incidence of chronic subdural haematoma in the elderly. *Qjm* **110**, 375–378 (2017).

200. Rauhala, M. *et al.* Chronic subdural hematoma—incidence, complications, and financial impact. *Acta Neurochir. (Wien).* **162**, 2033–2043 (2020).

201. Campbell, S. S. & Tobler, I. Animal sleep: A review of sleep duration across phylogeny. *Neurosci. Biobehav. Rev.* **8**, 269–300 (1984).

202. Pascale, C. L. *et al.* Amyloid-beta transporter expression at the blood-CSF barrier is age-dependent. *Fluids Barriers CNS* **8**, 1–11 (2011).

203. Deane, R., Wu, Z. & Zlokovic, B. V. RAGE (Yin) versus LRP (Yang) balance regulates Alzheimer amyloid β-peptide clearance through transport across the blood-brain barrier. *Stroke* **35**, 2628–2631 (2004).

a flaming nova 2

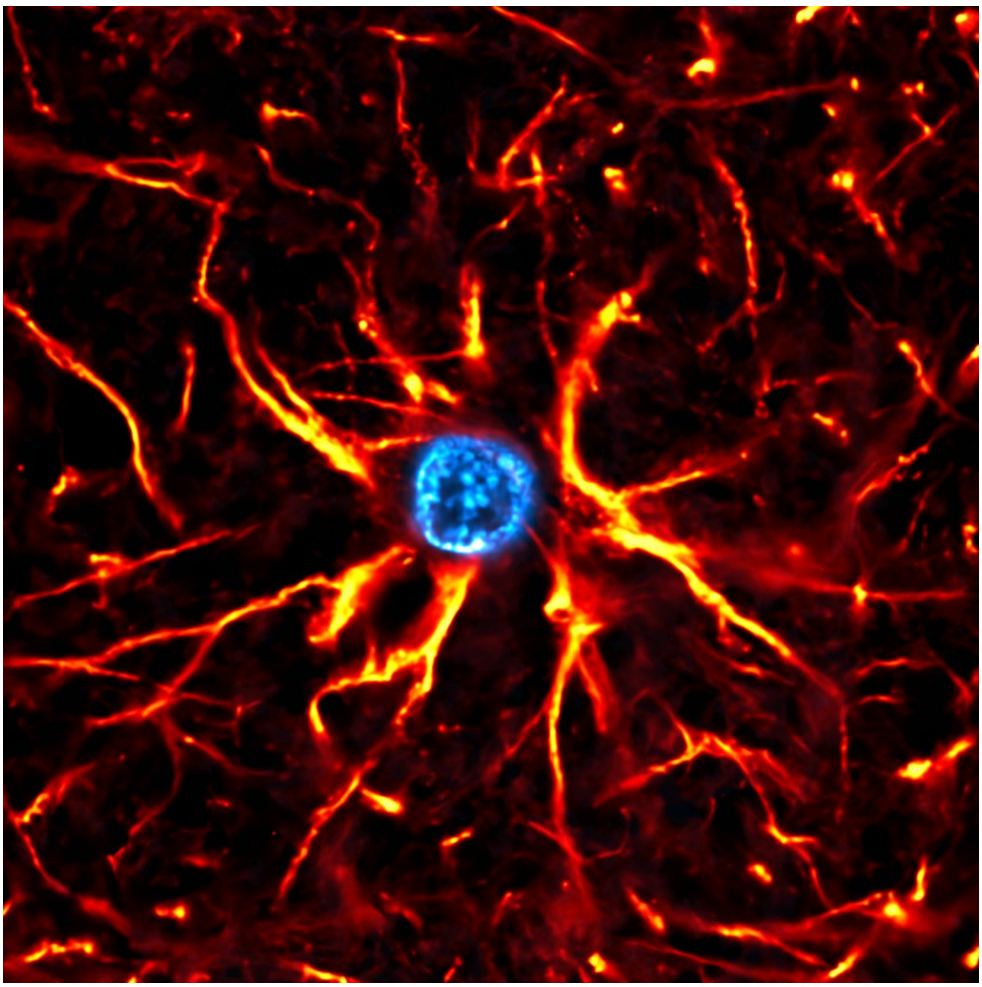

Acknowledgements

Congratulations! You made it to the end of this thesis, or, more likely, you just skipped to this page, I don't blame you, but at least go back and look at some of the pretty pictures when you have a moment. From my small understanding of things, two aspects of life are certain, you are born alone, and you die alone, not so dissimilar to the beginning and end of the PhD, but as for all that other stuff in between, well that is filled with interactions, good, bad, and neutral, that all contribute to who you are and where you have come, in any given moment. As I sit now and reflect on what to write here I realise that I have come a very long way from home, like literally 14, 451 km (Google Maps Malmö to Pietermaritzburg), and it has been 7 long years since I left the sun-scathed shores of my beautiful homeland. More so, I have reached the end of this long academic road, neither of which would have been possible without several people who afforded me their support, wisdom, and friendship in completing this arduous journey. That being said, I would like to take this opportunity to thank all these people, and it makes the most sense to do this chronologically.

At one point in time I was going to be a medical doctor, eventually a surgeon. The tragedy herein is that this road would have kept me all but trapped in South Africa for a good 20 more years. I love my country, I loved growing up there, and now more than ever appreciate the differential perspective and way of thinking it has given me, but my heart always longed to see more of the world. Life is short, and having already experienced the first 22 years of my life in South Africa the opportunity cost of staying on that path was too great, at least for me, and so I left medical school in search of something more. This is probably the most difficult decision I have had to make, and ultimately the first falling domino that lead me to where I am now. Yet this pivotal moment was not something carried out alone. So firstly, I would like to thank my friend, and Anatomy Professor at the time, **Graham**, for your wise council and support, for it was you who helped guide me to this path and figure out what steps to take, something I will never forget. To my friends **Suhail, David, Murray** and **Andrew**, they say you are a product of the company you keep, and if this is true I know that I can certainly hold my head up high having you lot as friends. I will forever carry the memories of our early years in Cape Town together, from bunking histology lectures to go play billiards to early hour obstetrics deliveries in New Somerset Hospital, these were some of the best years of my life, and although we don't see each other as much as before I hope we

never lose contact. Nor can I forget my oldest friend, **Dirk**, keep tearing up that South African finance market so you can bank roll whatever crazy ideas I conceive in the future.

To my parents **Cathy** and **Mike**, it goes without saying that I would never have started or maintained this journey without your support. I can't imagine how difficult it must have been for you when I left medical school for the unknown, but your strength and unconditional love, then, before, and now, has always given me the necessary tools to excel. I know life has never been the most easy for our family, but I wouldn't change a thing and am proud to have you as parents. To my brothers, **Marc** and **James**, sadly I don't think you will ever understand this, but who and how each of you are, make me who I am, and I love you. To **Uncle Tony** and **Uncle Brian,** the two wise old men in my life, I have learned so much from the both of you and am grateful for the moments we have shared.

The start of my PhD was not the easiest one. Thanks to the impeccable hard work and proficiency of the Swedish Migration Agency I had to be voluntarily "deported" from Sweden, not once, but twice, before I could start my PhD. Not that anyone of import in Sweden will likely ever read this, but the migration aspect of this country is a true disappointment. The sad thing is, like many others, all I wanted was to come here and do my research, not cause any problems, but be a functional, tax-paying member of Swedish society. The fact that I had to fight so hard to do this is a disgrace. The saddest part of all is that had I known then what I know now I would never have come to Sweden, and it is this exact way of thinking that will discourage the future immigration of other highly educated people into Sweden, which will only serve to lessen value for the country across the board, but perhaps that is what they want. To my supervisor, **Iben**, thank you for supporting me through this difficult time, it was a first for us both. More so, thank you for the openness and flexibility you have shown over the years to let me explore these projects. I still remember sitting in your office in F-Hus discussing what new models we could use to study the glymphatic system. It was certainly no easy feat but look how far we have come in such a short time. I hope in the years that follow we can maintain a close collaboration to take what we have built even further. To my fellow lab mates **Marta, Roberta, Tekla, Marios, Sam, ChenChen, Na, Max** and **Xuanhui**, thank you for making the lab such a pleasant working environment and all our fun gossip and after work activities. To my friend **Nagesh**, we have achieved a lot together over the years, your calm support and focused attitude played a big role in the quality of work we have put out. Although we both will soon go our separate ways I hope we stay in contact, I will miss having you around. Thank you to all the BMC in vivo staff who have been with us through the surgeries over the years and helped make our work a success, **Rebecca, Tina, Maria, Anna, Caroline, Jeanette**. To **Sebastian** and **Bengt**, thank you for taking the time to train me on each of your respective imaging platforms, for they have all been a huge part of this body of work.

Nothing stays the same forever, I don't know who said that, but it is an inevitable truth, and aptly reflects the nature of my time and friendships over the years at the BMC. Friendships come and go, like the ebbing tide, but the memories remain, and those are what I hold on to, despite whatever may or may not have happened. The interactions we have each shared have made me who I am, and I like who I am, so thank you for that my friends, **Mert, Martino, Matilde, Alex, Marta S, Ana, Isak, Marija, Julie, Laura D, Kat, Marcus, Jess, Andreas, Eliska, Oscar, Tiago, Emile, Dima, Laura A, Chang, Edoardo, Alba, Maria, David, Veronica, Lavanya.** To number one Portuguese bro, **Fabio**, although we don't see each other as much you'll always have a friend here in Malmö, and since your company is doing so well and you too will be here for the next years I hope we can see each other more often like the old days. To the one who used to copy me in maths in high school and then ended up in the same city in Sweden, all by chance, and my now house mate, **Scott,** thank you for your friendship. It's funny how life has kept us together all these years, must be for a reason. I know I can always count on you when I need a friend and I look back fondly at all the wild times we've had being the South Africans in Sweden. Life here definitely would not have been the same without you, beers are on you next Thursday.

Lastly, to my partner **Ugne**, we met in the most unlikely of ways, but isn't that how all the great romances start? Your pure friendship and support in our years together has been the greatest blessing. You are my ride-or-die homie and it brings me great peace to know that I have you to lean on when times are rough, and times do always seem to be rough for a third world immigrant in Sweden so this is all the more important. I am looking forward to all that life has in store for us and can't wait to be there when it is your time to defend.

Finally, to anyone I have forgotten, and you the reader, thank you.

The biggest milestone of this work was successfully being able to carry out the cisterna magna injection in pigs. While to those trained in human surgical practice this may seem trivial, to those of us without empirical surgical training, it was a formidable accomplishment. Below, is a cortical slice from one of the first porcine cisterna magna injections, imaged at BMC F-hus, 18 December 2019. May it also serve as a reminder that animals' lives were expended for the generation of these ideas, to whom we are grateful for their sacrifice, and without whom none of this would have been possible.

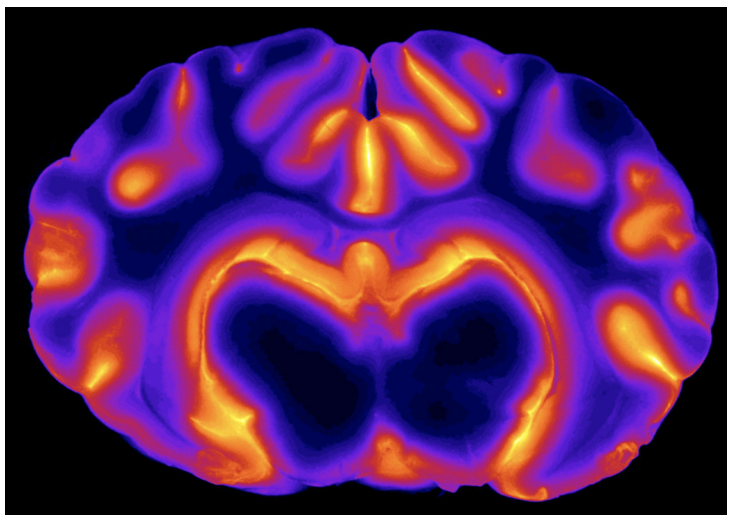

Printed by Media-Tryck, Lund 2022 NORDIC SWAN ECOLABEL 3041 0903

LUND UNIVERSITY

FACULTY OF MEDICINE

Department of Experimental Medical Science

Lund University, Faculty of Medicine
Doctoral Dissertation Series 2022:100
ISBN 978-91-8021-261-8
ISSN 1652-8220